Interaction of Ships and Ocean Structures With Ice Loads and Stochastic Ocean Waves

R. A. Ibrahim

N. G. Chalhoub

Department of Mechanical Engineering,
Wayne State University,
Detroit, MI 48202

Jeffery Falzarano
School of Naval Architecture,
University of New Orleans,
New Orleans, LA 70148

The influence of floating ice on the dynamic behavior of ships and offshore structures depends on many factors such as ice thickness and its relative speed with respect to the floating structure. The ice resistance to ship motion forms an essential problem in ship design and navigation. Furthermore, local or global ice loads acting on ocean systems are random and nonsmooth when impact interaction takes place. Impact loads on the bow of a ship navigating in solid ice may be modeled by a Poisson law. The measured stress amplitudes on the ship frame at the bow follow an exponential distribution. The nonhomogeneity and difference in ice microstructure, as well as the influence of salt and temperature, result in a great uncertainty in the ice strength. Therefore, the current review article aims at assessing the ice related problems encountered by offshore structures as well as by ships during their navigation. It also discusses the impacts of local and global ice loads on floating structures and reviews their existing probabilistic models. Moreover, this article covers the dynamic interaction of ice with flexible and rigid structures, and ships. In view of ice loads on marine systems, new design regulations have been introduced by international organizations that are involved in the design and building of ships as well as offshore structures. The ship stochastic stability and the first-passage roll stabilization problem associated with random ocean waves will also be described in an attempt to stimulate future research work dealing with ice impact loads. Moreover, due to the lack of research activities addressing the control problem of ships operating in icy waters, the current article will briefly discuss passive and active control schemes developed for controlling the ship roll motion. There are 529 references cited in this review article. [DOI: 10.1115/1.2777172]

1 Introduction

One of the major goals of the Navy, the Coast Guard, and ship builders is to enhance the capability of their ships in handling extreme environmental conditions. Ships operating in icy waters have to endure additional ice-induced loads on their propulsion systems and appendages. In addition, cold temperatures may reduce the effectiveness of numerous components of the ship, ranging from deck machinery and emergency equipment to sea suctions. Similarly, ice forces may damage structures and shore lines [1].

It is important to measure actual ice loads on wide structures [2] and impact loads induced by wave slamming. Most of the studies reported in the literature have dealt with ice loads on offshore structures [3–14]. The surface areas where ice can grip have to be reduced in order to protect docks from ice forces. This can be done by using piles that are narrow at the water surface, by increasing the span of the deck joists in order to reduce the number of required piles, or by using piles that are very strong and narrow.

Ships operating at low temperatures are prone to icing, which results in shifting their center of gravity, thus causing a decreased initial static stability. These represent dangerous conditions under which a vessel may operate. In particular, extreme latitudes are often associated with steep waves, extreme winds, and possible floating pieces of ice.

One way to alleviate the influence of ice in ship navigation is by holding ice in place or directing its growth and movement. Perham [15] and Kinosita [16] presented some studies to prevent the disaster related to frost heaving, avalanche, snow drifting, snow removal, snow on the roof, snow accretion on electric lines and roads, sea ice, and ice accretion on ships. Ice control such as chemical, electrical, and mechanical methods in navigable waters were addressed by Frankenstein and Hanamoto [17]. Ice carried downstream by ship traffic causes operational problems in and around the lock areas, as well as in restricted channels. Mechanical ice control techniques include the ice boom, air curtain or screen, and icebreaking either by vessels or air cushion vehicle. An ice boom is a barrier made from floating pontoons or timbers held in place by chain or wire rope. An air screen releases large quantities of air at some depth, which induces a diverging current at the surface.

The most efficient means of ensuring navigation in ice is provided by an icebreaker. The latter is a ship designed for breaking the ice and used to escort ships. The basic design features, distinguishing the icebreaker from other types of ships, are mainly the special hull lines along with high local and overall hull strength. It is also driven by a powerful and highly maneuverable propulsion plant (about 900,000 hp), strong screws, and rudder(s). Kashtelyan et al. [18] presented a comprehensive account of the development and design of icebreakers.

Ice jam flooding causes severe damage and may be responsible for loss of life. An ice jam is a stationary accumulation of ice that restricts flow and can cause considerable increase in upstream water levels. At the same time, downstream water levels may drop. Types of ice jams include freeze-up jams, made primarily of frazil ice[1]; breakup jams, made primarily of fragmented ice pieces; and combinations of both [19].

Ice and cold weather conditions affect road vehicle performance due to the low friction and deformable surface material that affects vehicle traction, motion resistance, handling, and maneuvers. A fundamental understanding of both thermal and mechani-

Transmitted by Assoc. Editor W. Shyy.

[1]Fine specules, plates, or discoids of ice suspended in water. In rivers and lakes, frazil ice is formed in supercooled turbulent water.

cal behaviors of snow and freezing/thawing ground in terms of friction and its impact on traction is difficult to quantify [20–24].

In a low temperature environment, the properties of structural materials experience significant variations, which affect the dynamic characteristics of ocean structures. Guidelines for ships operating in Arctic ice-covered waters "take into account that Arctic conditions may include sea and glacial ice[2] that can represent a serious structural hazard to all ships. This is the single most significant factor in Arctic operations." [25]. Structures in arctic regions, such as drilling platforms, foundation piles, bridge piers, and lighthouses, are subjected to violent sea waves and ice loading. Their safe engineering design requires knowledge of ice forces generated under dynamic loading conditions [26–28]. A cable-moored platform subjected to a moving ice flow or field ice rubble experiences undesirable ice loads, which result in undesirable motions. The spectral analysis of recorded ice vibrations revealed a relationship between the period of vibrations and the scale of dynamic processes in a given glacier [29]. The presented spectra of the ice-vibration seismic events display characteristic frequency maxima related to the scale of dynamic processes taking place within a given glacier.

This article presents an assessment of problems related to ice loads, ice impacts, and severe ocean environmental conditions experienced by offshore structures and encountered during navigation of ships. The effects of local and global ice loads and their impacts on ocean ships and structures along with their probabilistic models are discussed in the next section. The dynamic interactions of ice with flexible and rigid structures are covered in Sec. 3. The ice resistance to ship motions is essential to ship design and navigation. It is considered in Sec. 4. Subsequently, the vessel-icing problem is described in Sec. 5. Section 6 will address the stochastic stability and the first-passage problem of ships due to their interaction with random ocean waves. Due to the lack of research work that deals with the control of ships interacting with ice, passive and active control schemes used in controlling the roll ship motion are reviewed in Sec. 7. The article concludes by highlighting the main issues that were resolved in the literature and by addressing the important unresolved ones that need to be considered in future research work.

2 Ice Loads on Ships and Offshore Structures

2.1 Background. The design of vessels and offshore structures requires the knowledge of maximum ice loads and pressures acting on these systems. Equally important is the knowledge of the frequency content of the load, which plays an important role in the dynamic response of ocean systems. In order to understand the dynamic effects of ice on ships and structures, one should have a good background of ice mechanics and ice loads. Ice mechanics involves the mechanical, constitutive, and fracture properties of different forms of ice [30–34]. Sea ice is composed of solid ice, brine, air, and solid salts. Details of the ice microstructure influence significantly its mechanical and physical properties. The brine, air, and solid salts are usually trapped at subgrain boundaries between mostly pure ice lattices. Typically, first-year sea ice has salinity in the range of 4–6% salt. This is much lower than the salinity of seawater (35%). The phase relationship of the ice with temperature is multifarious due to the various salts present in the ice. Several field studies [35–39] have been carried out to measure the properties of sea ice during the melt season. Timco and O'Brien [40] developed the relationship between the flexural strength of first-year sea ice and the brine volume of ice. The need for numerical methods (finite element, discrete element, finite difference) was discussed by Jordaan [41] in the light of the review of mechanics of ice, as well as the boundary conditions for the ice feature.

Sodhi and Morris [42] attributed the observed slight dependence of the frequency on pile diameter to the concept of multiple zones of failure described by Kry [43–45]. It was assumed that the number of failure zones may be proportional to the pile diameter. Accordingly, as the number of failure zones increases, the likelihood of having a certain percentage of the zones failing simultaneously decreases. As the number of zones increases with the increasing pile diameter, the time between simultaneous failures exceeding the threshold percentage increases, thus causing reduction in the characteristic frequency. Similar observations of nonsimultaneous failure of ice made by Kry [43] were also reported by Glen and Blount [46]. Croasdale [47] and Croasdale et al. [48] indicated that the fractures causing spalls tend to propagate to the free edges.

In view of the difficulty of duplicating the characteristics of ice in the field, the formulas for predicting ice loads based on laboratory experiments may not fit well with the actual ice forces measured at the site. Furthermore, the results of available formulas based on laboratory results, in situ experiments, or a combination of both, may produce significant differences due to the basis for the formulas [49].

Zufelt and Ettema [50] presented an extensive account of modeling procedures for ice properties. These properties include two-phase (liquid-solid) dynamics of ice motion and thermodynamic processes associated with ice growth and ice strength. It is not a simple task to fully simulate all processes together in one formulation. Instead, Zufelt and Ettema [50] classified the modeling in two categories: ice-transport (hydraulic) modeling and ice-load modeling. Hydraulic modeling includes similarity of water flow, ice movement, and ice accumulation. Ice-load modeling encompasses similitude of ice forces exerted during ice-structure or ice-ship interaction, ice strength, ice-piece movement around structures and hulls, friction between ice pieces, and ice-piece size.

The interaction force induced by the relative motion between an ice feature and an ocean structure or a vessel is limited by the force required to break the ice sheet. An ice sheet may fail against a ship in bending, buckling, crushing, or a combination of these failure modes. By crushing failure is meant ductile deformation or brittle failure of an ice feature while moving against a ship. Creep deformation of ice leads to simultaneous contact between an advancing ice sheet and a ship, whereas brittle crushing results from fracture and brittle flaking of ice and leads to nonsimultaneous or nonuniform contact across the width of a ship. Masterson et al. [51] observed that the ice behavior is characterized by plastic flow ductile failure during indentation at speeds lower than 3.16 mm/s and by brittle failure above this speed. They found a velocity dependence of pressure in the medium scale in the range of indenter speeds from 0.1 mm/s to 100 mm/s, with the highest pressure at 3.2 mm/s. Jordaan and Xiao [52] analyzed the difference in tensile stresses adjacent to a high-pressure zone for two different rates of loading, taking into account the damage process.

2.2 Local and Global Ice Loads. Ice loads are measured either locally or globally. The line load (local) is estimated by dividing the measured global load by the width of the structure. On the other hand, the global pressure is determined by dividing the measured global load by the product of the width of the structure times the ice thickness. An accurate knowledge of ice forces that are generated during a continuous crushing action of an ice sheet, along with their frequency spectrum, is important in the design and dynamic analysis of ocean systems. Ice forces vary with time according to the resistance offered by the ice sheet. A typical cycle of ice force consists of a gradual increase in the ice force until the ice sheet breaks, at which time the ice force undergoes a sudden decrease due to the clearing of the crushed ice. A new cycle begins when a new contact with another undamaged ice sheet occurs. This cycle may cause the ocean structure to vibrate at its natural frequency, resulting in a complicated ice-structure interaction. Maximum ice forces on structures usually correspond to the

[2]Sea ice is formed by the cooling and freezing of sea water, whereas glacial ice originates on land from snow falling on perennial snow fields.

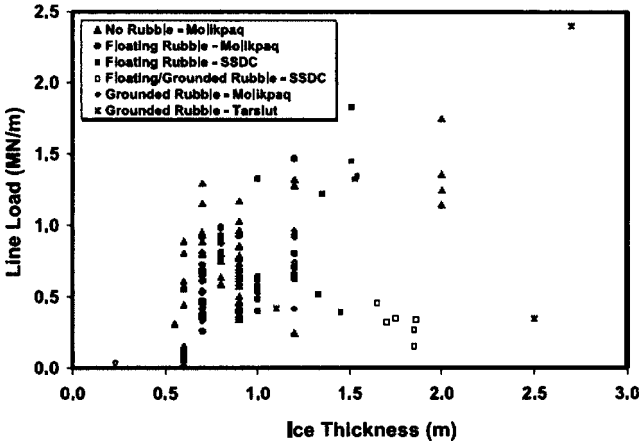

Fig. 1 Dependence of line load on ice thickness for first-year ice loading on the Beaufort Sea structures for different structures and rubble fields [7]

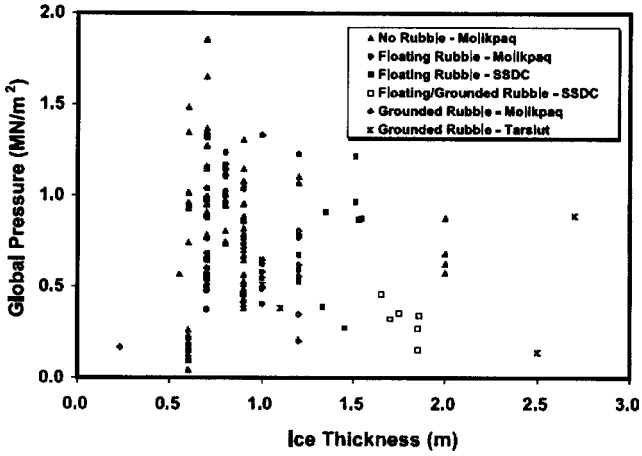

Fig. 2 Dependence of global pressure on ice thickness for first-year ice loading taken from the Molikpaq, single-steel drilling caisson (SSDC), and Tarsiu caisson structures [7]

ultimate strength of ice, occurring when the ice fails. However, the nonhomogeneity and difference in ice microstructure, as well as the influence of salt and temperature, result in a great uncertainty of ice strength.

The prediction of ice loads has been the subject of several studies. These studies proposed a power law to describe the rate-dependent behavior of ice [53–56]. Based on the ice movement pattern with a continuous-velocity field, the total ice load was estimated with the bound theorem for creeping materials. The variation in the strain rate from point to point was taken into account. The fracture behavior of ice was considered by setting fracture limits on the strain rate in compression and tension and by modifying the energy dissipation terms in the zones in which the strain rates exceed those limits.

Johnston [57] reported some results pertaining to the variation of local ice pressure and its interaction with structures. Johnston and Timco [5] and Timco and Wright [8] found that the grounded ice rubble acted as a protective barrier, and the average global load was attenuated by more than 60% due to the presence of the rubble. Timco and Johnston [7] conducted site tests on ocean structures equipped with instruments to measure local and global loads. The structures were subjected to a wide variety of ice conditions that included sheets of first-year ice, pack ice floes (floating ice), second year ice, and multiyear ice in both large sheets and isolated floes. In many cases, especially for the structures placed in shallow waters, the ice is piled up in front of the structure, forming a large rubble field. In some cases, the rubble field was grounded on the seabed over a large area (designated as a grounded rubble field), whereas in other cases, only parts of the rubble field were grounded (grounded/floating rubble field). Figure 1 shows the line load for the first-year sea ice as a function of the ice thickness. The figure reveals that the lower line loads are associated with conditions of a grounded rubble field or a grounded/floating rubble field. It is seen that there is a general increase in the line load with increasing ice thickness for events that do not include grounded rubble.

Figure 2 shows the dependence of the global pressure on the ice thickness for all occasions in which global load information is available. Data from events with grounded rubble resulted in lower global pressure. Although there appears to be a trend of decreasing global pressure with increasing ice thickness, this trend is largely a result of the two highest pressures with 0.7-m-thick ice.

Offshore drilling platforms are usually supported by a multileg structure, which is usually subjected to extreme ice regime conditions. Kato and Sodhi [58] measured the ice forces that are generated during an ice action on two structures located side by side, resembling the legs of offshore structures. There is a trend of increasing load with increasing ice thickness. Other measurements of ice loading were reported by Blanchet and Keinonen [59]. Ice loads on a large offshore structure for the Bohai Bay were evaluated by Lindolm et al. [60]. The structure consists of five similar conical caissons located in a line. The global ice loads and the rubble formation were evaluated in model tests, and the local ice pressures and the dynamic ice-structure interaction were analytically treated. Danilenko et al. [61] conducted a sensitivity analysis of ice load acting on an ice-resistant structure to the contact failure mechanism using three-dimensional boundary element modeling. Full-scale tests of ice-structure interaction were conducted on three multileg jacket platforms in Bohai Sea [62]. Dynamic responses of these structures were recorded continuously, the variations in ice force were measured by load panels, and the failure processes of ice acting on cones and cylindrical pile were observed by video cameras. For the structure with icebreaking cones, the ice sheet fails in bending, but the breaking frequency could coincide with the natural frequency of the structure at a fast ice speed and significant dynamic amplifying could be induced. For the cylindrical structure, two types of vibration are classed. Field observations revealed that sea ice can induce the offshore jacket structure to vibrate in resonance regardless of the fact that ice-breaking cones have been installed.

Riska et al. [63] introduced what is known as a "line load" in which the high-pressure zones are found more often near the center of the ice sheet. Johnston et al. [64,65] presented the results of measured ice loads on slender structures of a diameter ranging from 2 m to 6 m. A number of light piers and navigation channels made in Canada, Finland, and Sweden were instrumented to provide a record of ice loads experienced throughout the winter season. Figure 3 shows the dependence of the measured ice load on the loaded waterline width during interaction. This width is not necessarily identical to the width of the structure at the waterline since only a portion of the waterline width is loaded during the interaction. Note that Fig. 3 does not reveal any trend with the contact width. The measurements included (1) a JZ-20 circular cylinder leg of diameter of 2.03 m, with 6 deg inclination, (2) a cook inlet pile circular cylinder of diameter of 0.91 m, (3) a Hondo structure semicircular of diameter of 2.32 m, with 23 deg inclination, (4) a Pembridge structure circular cylinder of diameter of 0.86 m, (5) a V-shaped St. Regis of width of 1.22 m and 5.7 deg inclination, (6) a V-shaped Rideau River structure of width of 2.0 m, (7) a Yamachiche structure circular cone (15 deg) of base diameter of 4.0 m, curve 1 structure of circular cone (45 deg) of base diameter of 4.0 m, and (8) an LL104 structure

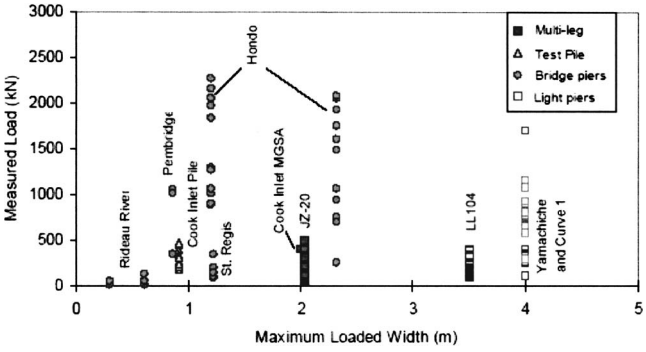

Fig. 3 Dependence of the measured ice load on the waterline width [65]

circular cone (45 deg) of diameter of 3.5 m. Figure 4 shows the dependence of measured ice load on ice thickness for four different slender structures.

Bercha and Danys [66] included the effects of ice sheet in-plane forces and edge moments, as well as transverse loading, on conical structures. A range of results is then corroborated using a finite element simulator having certain refinements over the analytical approach, including a more precise specification of the end actions. Chao [67] presented an assessment to compare several representative prediction models with experimental measurements for global sheet ice forces on conical structures. Differences among the models were identified. Statistical measures of these models were provided so that the uncertainty or accuracy for each of the models can be quantified.

A series of fatigue experiments was carried out in the McMurdo Sound, Antarctica during the summer of 1992. The results presented by Haskell et al. [68] were in the form of a standard fatigue curve (with zero mean stress), which is "stress amplitude" versus "number of cycles to failure," commonly known as an *S-N* curve. The "endurance limit," which is the stress below which the sea ice can withstand an unlimited number of cycles for sea ice in situ, was found approximately half the failure stress. Cole and Dempsey [69] presented selected results of in situ experimental investigations to study the fracture behavior of edge-notched square plate specimens of first-year ice and involved a detailed characterization of the physical properties and thermal state of the ice. Acoustic emissions, which were generated by microcracking, were monitored in the crack tip vicinity and provided insight regarding the size of the process zone. It was found that the viscous deformation rate estimated from the experiments exhibited an increasing power-law exponent with values between 1 and 3. Acoustic emission monitoring indicated that microcracking occurred in a process zone near the crack tip, and the size of the process zone increased with decreasing cyclic loading frequency.

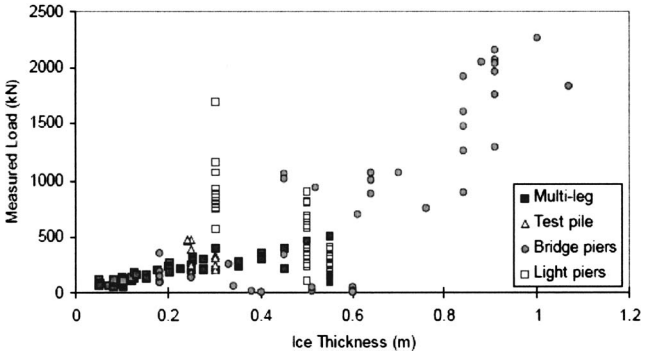

Fig. 4 Dependence of the measured ice load on ice thickness for different slender structures [65]

Katsugari et al. [70] conducted a numerical simulation of a three-dimensional ice-structure interaction using distinct element methods and particle flow code (PFC-3D). The applicability of modified PFC to the simulation of failure mode of ice sheet was tested, and the results were compared with ice tank test data. Barker et al. [71] developed a hybrid Lagrangian–Eulerian model to evaluate ice loads on a 10-m-wide cylindrical pier. There was good agreement between field observations from similar structures and the hybrid model's calculated values. In contrast, forces estimated from analytical formulas were much higher than those from the field measurements.

Ray [72] presented design and measured loads for various ice boom geometries. For the standard Douglas fir rectangular wooden booms, the measured peak line loads vary from 6.7 kN/m to 10.7 kN/m; typical design values reach 16 kN/m. The recorded maximum line load for the huge rectangular steel boom at Beauharnois, Quebec was found to be 46.7 kN/m. For the 1996/1997 season, Cowper et al. [73] reported a peak line load of 14.1 kN/m on the 76 cm steel pontoon Lake Erie boom and a maximum tension of 330 kN in the chain connecting the monitored pontoon to the section cable. Cornett et al. [74,75] and Morse [76] measured the maximum loads at different sites of St. Lawrence River booms constructed of a cylindrical steel pontoon. Morse [77] presented the results of measured ice forces on three booms along the St. Lawrence River and analyzed the structure rupture events of various members. The time-history records revealed (during the consolidation period as the ice grows in area, thickness, and strength) that the load on the booms rises to a peak. Fourier analyses indicated that the flexibility of the ice boom structure filters out high frequency loads.

2.3 Indentation Tests. Indentation tests are usually conducted to measure the dependence of the applied force on the displacement. Some tests were conducted [78–81] to measure the total force and the displacement of the indenter. The reported measurements included local pressures on the faces of spherical and flat indenters. Time-history plots of the total force show the typical sawtooth pattern of gradually increasing force that suddenly decreases to a near zero value, and time-history plots of displacement show a step pattern of slow and fast movements of the indenter. Spencer and Masterson [82] found that the characteristic sawtooth load-time plots are caused by the ice-structure interaction and not by the hydraulic system. Plots of pressure at different points on the indenter revealed a nonuniform distribution of very high and low pressures, indicating nonsimultaneous ice crushing.

Meany et al. [83] studied the characteristics of the failure zone using medium-scale ice indentation tests conducted on Hobson's Choice Ice Island during the spring of 1990. The study included measurements of crushed layer thickness, comparisons of density of ice within the crushed layer to that of the relatively undamaged regions, sieve analysis of ejected particles, and microstructural studies of damage and pressure melting. Swamidas et al. [84] conducted indentation experiments on freshwater ice and developed numerical models for ice damage together with a mechanical model of ice-induced vibration. Modeling of the damage process was used to estimate the thickness and equivalent viscosity of the crushed layer under various circumstances and also to demonstrate the change in pressure distributions at different stages in the loading cycle. Crushing was complicated by the presence of spalling as well as distributed damage. A simple mechanical model, including the structural and far field ice responses, was successfully used in simulating peak forces and the frequency of dynamic loading cycles in a variety of ice and loading conditions. Zou et al. [85] studied the role of fracture and spalling in ice-structure interaction. The most likely regions in which fractures would be initiated from flaws are shear zones with low confining pressure and tensile zones. Since flaws in ice are random in nature, a probabilistic modeling is necessary for the future study of ice fracture and spalling.

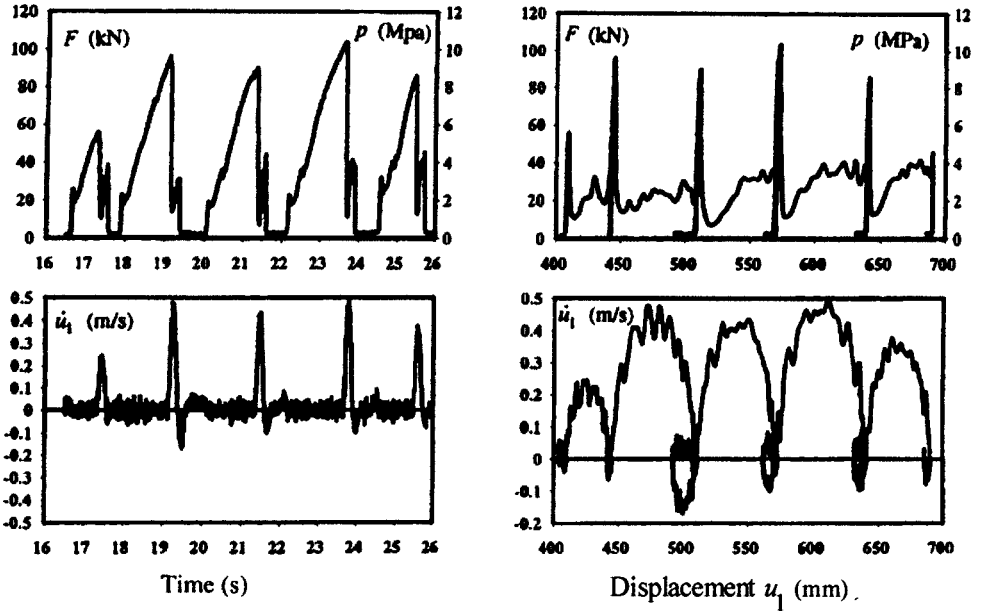

Fig. 5 Quasistatic response with transient vibration for the structure mass=15,000 kg, rate of indentation v=30 mm/s, natural frequency f=2.0 Hz, ice thickness h=100 mm, indenter width D=100 mm [95]

Small-scale indentation tests (see, e.g., Refs. [86–88] and medium-scale tests [89–91] revealed that a ductile to brittle transition zone occurs with changing indentation speed from low to high. Furthermore, the contact interface can be observed in detail for different speeds [88]. The transition between failure modes due to temperature variations were discussed by Sodhi and Haehnel [92]. Medium-scale field indentation tests (MSFITs) included physical properties of ice sheet and measurements of ice sheet deformation (Sakai et al. [93]). Li et al. [94] observed a layer of damaged ice near the contact zone of ice-structure interactions in small-scale, medium-scale, and full-scale tests. These tests revealed a pressure dependent process of damage. Microcracking and recrystallization were observed to be the main types of damage at low confining pressure levels with possible melting at asperities in cracks. Recrystallization and melting were the main types of damage under high confinements.

Kärnä et al. [95] conducted a series of indentation tests in which a compliant structure was pushed into an ice sheet with a nominally constant speed. The time evolution of the resultant ice force and the velocity response are shown in Fig. 5. The dependence of these parameters on the displacement u_1 is also shown on the right-hand plots of Fig. 5. It is seen that the acceleration and the associated mass forces are very small when the global ice force approaches its peak value during a major loading phase. The response was characterized as quasistatic because a nearly static equilibrium exists between the internal and external forces acting on the structure at the events of maximum ice force.

At the events of major peak ice force shown in Fig. 5, the ice fails almost simultaneously in front of the structure, which will start to move forward against the ice edge. This transient vibration process is also termed "spring-back." If the structure is stiff, the spring-back phase is often practically the same as the unloading phase. However, a compliant structure may continue its transient motion after a minimum load has been reached. In this case, the global ice force fluctuates at a low level. This force fluctuation is associated with nonsimultaneous ice failure. Figure 5 reveals an intermittent hysteretic loop appearing in the force-displacement diagram. This hysteresis takes place at the initial stage of a loading phase when the structure moves a little away from the ice edge.

2.4 Ice Impact Loads

2.4.1 Impact Loads on Offshore Structures and Ships. Ice impact loading can cause significant damage to offshore structures and ships. The impact arises when drifting ice sheets, ice floe, and icebergs are moving with considerable speed under the action of environmental conditions. When a fast-moving ice feature crushes against a narrow structure, the force of impact is irregular, random, and contains repetitive fluctuations. The possible interaction effects between the iceberg and waves as well as its interaction with offshore structures was discussed along with the hydrodynamic aspects involved in the analysis of wave-induced motions of icebergs [96]. The results indicated that the surge and heave velocity of model icebergs, with a draft to water depth ratio of less than 0.1, can be greater than 0.8 times the water particle velocity when the iceberg horizontal dimension is less than 0.3 times the wavelength. The random fluctuation can be explained by random variations of ice properties as well as ice failure at random locations along the contact area [97]. Vinogradov [98] described a methodology for simulating the nonstationary random process of the interaction of ice floes with a vessel. El-Tahan et al. [99] developed two different types of elastic impact models for the case of a moored semisubmersible subjected to bergy-bit (a large piece of floating glacier ice) impact. A considerable amount of research has been conducted to understand the process of impact damage initiation and growth along with the identification of impact governing parameters.

Cammaert and Muggeridge [97] classified the impact loads based on the ice feature.

(i) *Ice floe impact loads* [100–104]. For a head-on collision, Kreider [101] estimated the peak force F_p of ice impact by equating the floe kinetic energy and work done by the ice force. This force was described by the following formula:

$$F_p = 2.66h(\rho_i R_s)^{1/3}(p_e R_i V_i)^{2/3} \quad (1)$$

where h is the ice thickness, ρ_i is the ice mass density, R_s is the structure radius, p_e is the average ice-crushing pressure, R_i is the ice floe radius, and V_i is the floe speed. Guttman et al. [105] developed a finite element model, in

which nonlinear elastic elements characterize the ice-structure interaction zone, and nonlinear elastoplastic elements comprise the foundation response.

(ii) *Iceberg impact loads* were considered by Maes and Jordaan [106], who developed phenomenological models that describe the gradual dissipation of the initial transitional energy of the berg during ice crushing at the structure interface.

Powell et al. [107] studied the dynamic ice-structure impact for a large ice floe striking a tubular steel platform. The ice was modeled, taking into account strain rate effects. It was concluded that the static and dynamic results can generally not be correlated and, hence, that dynamic analysis was recommended. Mathematical models of ice feature impacts with an offshore platform or vessel include (i) head-on impacts when an iceberg has a single degree of freedom and an absolutely rigid noncompliant structure [100], (ii) more complex models taking into account the structure compliance and its local and global deformations [102,108–110], and (iii) eccentric impacts [111–113]. Holthe [114] developed sophisticated computer-based models using a three-dimensional time-domain analysis of the coupled iceberg-platform system. These models took into account the iceberg's six degrees of freedom, the structure compliance, and the interaction with soil [115]. Isaacson [116,117] showed that due to the hydrodynamic interaction between an approaching ice feature and a fixed structure, the ice feature tends to deflect to the side and the head-on collision is rather infrequent. The microstructure of ice before and after impact was examined by Kurdyumov and Kheisin [118].

Bhat [119] studied the impact ice loading and the phenomenon of floe splitting as a consequence of initiation and propagation of radial cracks in the impacting floe. It was shown that the splitting load or the fracture limit load reaches its value relatively early in the radial crack propagation process. Subsequently, the crack can propagate dynamically, splitting the floe into pieces and, consequently, the load on the structure falls.

Simple models of impact ice feature on structures include the evaluation of the risk of exceedance of the initial translational energy of iceberg if probability distributions of iceberg mass, velocity, and size were given [106,120]. The successful and safe operation of an Arctic offshore exploration structure depends on the implementation of alert procedures. A computer model was developed by Blanchet [121,122] to perform real-time calculations of engineering risks for each hazardous ice floe interacting with an offshore structure. Specifically, the risk associated with the exceedance of the foundation resistance, assuming that the ice floe will hit the structure, was used to evaluate the levels of alerts.

2.4.2 Eccentric Impact of an Ice Feature. The influence of impact eccentricity on the maximum ice load was addressed by Nevel [113], who developed an analytical solution for simple models of eccentric impact based on the assumption that rotation and displacements of an ice feature throughout the impact are small. It was assumed that the moment arm of the reaction force (the relative position of the contact point and center of mass) is constant. Johnson and Prodanovic [123] extended the work of Nevel [113] for the case of a circular iceberg experiencing an eccentric impact with a circular structure. They found that the impact load in eccentric collisions is approximately two times lower than the one under central impact. It was also indicated that a sufficient amount of the initial kinetic energy of the impacting body can be transferred to the kinetic energy of its rotational motion.

Another class of ice-structure interaction includes the eccentric impact of ice feature with a gravity-based structure (GBS) [112,124]. GBS resist lateral loads solely by its large mass and the friction or shear developed at its base. It was demonstrated that the eccentricity of impact can yield up to 50% drop in the ice force compared to the central direct collisions. Duthinh and Marsden [125] developed a modified closed-form solution for the kinetic energy transformation in the case of eccentric impacts. They also presented numerical simulations for spherical and rectangular iceberg impacts against a cylindrical structure. Croasdale and Metge [126] considered the influence of a possible rotation of iceberg about the horizontal axis during impact.

Croasdale and Marcellus [127] described two stages during the interaction between a large ice feature and a structure. The first stage is characterized by a slowdown of the ice feature during which the structure absorbs its momentum. The force generated during this stage is known as the "limit-momentum load," which is defined as the maximum load developed during the impact of an ice feature against a structure and occurs only when the ice feature is brought to a stop after the impact. Once the ice feature stopped moving, the surrounding pack ice continues to move against it. During this stage, the force generated reaches a limit value referred to as "limit-force load." The limit-force load is governed mainly by the driving forces associated with the ridge-building pressures exerted on an ice feature in contact with a structure and the drag forces on the feature caused by currents and winds.

Coutermarsh et al. [128] performed a series of tests to measure the impact forces generated by free-floating ice beams striking a 45 deg sloped structure. Four beam lengths and impact velocities were used with a fixed beam width and thickness. A coupled fluid/solid finite element program was developed to model the impulsive loads. The structure was modeled as a massless surface that can displace horizontally and vertically without rotation. The solid mechanics portion of the modeled ice is based on linear elastic beam theory including rotary inertia and a static fluid foundation. The numerical model was found to match the experimental peak impact forces to within 10–33% for the majority of the beam lengths. Improvements in the predictions could be realized by including a mechanism for energy loss from the beam to the supporting fluid. The results revealed that structural stiffness greatly affects the impact force in ice/structure interactions.

Matskevitch [129,130] developed linear and nonlinear models of ice-structure interaction under eccentric impact of an ice feature. Bass et al. [124] considered some basic effects of the impact eccentricity on the design ice load using a linearized analytical model. The ice-crushing force was considered to vary in proportion to the indentation depth. It was found that the proportion of the kinetic energy that was converted into rotational motion due to impact eccentricity does not exceed 25% in the case of frictionless contact. Furthermore, the eccentricity was found to reduce the maximum impact load in agreement with the results of Bass et al. [124] and Salvalggio and Rojansky [112]. Matskevitch [130] extended the linearized analysis by considering the nonlinear dependence of the ice-crushing force on the penetration depth. The effect of impact eccentricity on the maximum ice load was found to decrease due to the nonlinearity of ice failure load.

2.4.3 Ice Impact Loads on Composite Structures. The basic morphology of impact damage, its development, and the parameters affecting its initiation, growth, and final size are well documented by Abrate [131]. Ship hulls made of composite materials that are subjected to repeated ice impacts can experience damage consisting of delamination, matrix cracking, and fiber failure. Delamination is the debonding between adjacent laminas. It significantly reduces the strength of the laminate. Furthermore, it was reported that the delamination area increases linearly with the kinetic energy of ice impacting the ship hull.

One must distinguish between the impact of metal projectiles and the ice impact on structures made of composite materials. This difference arises mainly due to the complex material behavior exhibited by the ice, which is very different from metal projectiles conventionally used in impact studies. For this reason, one should understand the complex behavior of ice, which exhibits a strong strain rate dependency. For example, Schulson [132–134] and Batto and Schulson [135] described a ductile to brittle transition of the ice mechanical behavior when the rate of strain is increased from low to high. Other studies revealed that the axial

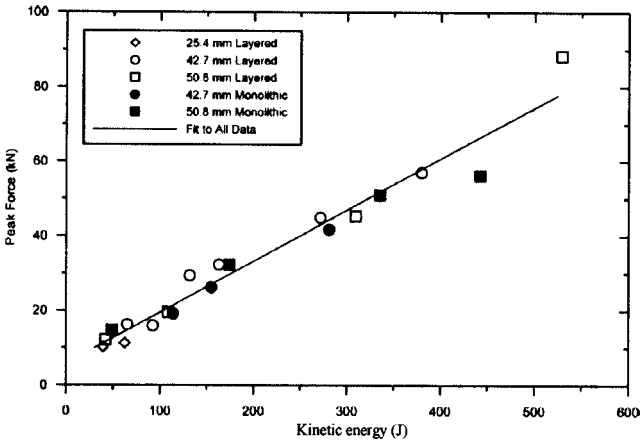

Fig. 6 Dependence of the peak force on the projectile kinetic energy for all normal impact [151]

compression strength of ice increases with strain rate [136–138]. Mellor [136] found that the measured tensile strength is much lower than the compressive strength at strain rates greater than 10^{-5} s^{-1}. It was found that the compressive strength of ice increases dramatically as the temperature decreases from −10°C to −50°C [132]. Under impact conditions, Schroeder and McMaster [139] measured the adiabatic shock (pressure-volume relationship) of ice and found that an extremely large pressure of 23.5 GPa is required to cause a phase change from solid to liquid states. Ice impact also differs from water hydrodynamic impact. Ice impact is associated with solid-body impact phenomena since ice has significant elastic stiffness (9 GPa Young's modulus) and compressive failure strength (10 MPa), as reported in Refs. [30,136,140,141].

The hail-ice impact event that occurred in the Dallas/Fort Worth area in 1995 caused significant damage to composite and metal parts of over 100 aircraft parked outdoors [142]. Impact on composite structures has been reviewed by Abrate [131,143,144]. The impact was classified into the low-velocity and high-velocity regimes. Jackson and Poe [145] analytically studied the transition between high- and low-velocity impacts and highlighted the dramatic differences between the two velocity regimes. It was concluded that the peak force developed during impact is a key parameter in evaluating delamination formation.

Singh et al. [146] measured the force generated by ice impacts using a dynamic measurement device. Pan and Render [147] examined the nonstructural aspects of ice ingestion into turbofan engines. Experimental and numerical studies on high-velocity impact of spherical-shaped ice on thin carbon/epoxy panels were reported in the literature [148–151]. It was found that the measured peak force is linearly proportional to the projectile kinetic energy regardless of the projectile size. For example, Fig. 6 shows the dependence of the peak force on the projectile kinetic energy for tests conducted using different sizes of ice spheres (layered and monolithic compositions). It is seen that all measured points establish a linear relationship between the peak force and kinetic energy. However, for monolithic ice, at higher kinetic energy the maximum force assumed values below the linear relationship. The kinetic energy at which failure initiates (referred to as the failure threshold energy (FTE)) was found to be also linearly proportional to the panel thickness. Impact at kinetic energies exceeding the FTE was found to result in a multiplicity of damage modes. Figure 7 shows time-history records of the impact force of two tests conducted at two different speeds using a layered spherical ball of ice of diameter of 42.7 mm.

The simulation of a ship bow impact with growlers (floating glacial ice masses) was conducted by Gagnon et al. [152] and Gagnon [153]. They measured the loads and pressures from impact experiments of a large impactor against free-floating pieces of growlers. Figure 8 shows the time-history record for a typical test at an impactor speed of 2 m/s with the impact plate at 45 deg. Figure 9 shows the dependence of the growler peak load on the impactor speed for three growler orientations (south direction is perpendicular to the impactor frame, west is along the impactor frame, and southwest is between south and west). It is seen that the average value of the impact load is linearly dependent on the impact speed. This observation is contrary to the one reported by Kim [149] and Kim et al. [151] that the peak force is linearly proportional to the square of the impact speed (kinetic energy). However, the two results are valid because the linear dependence

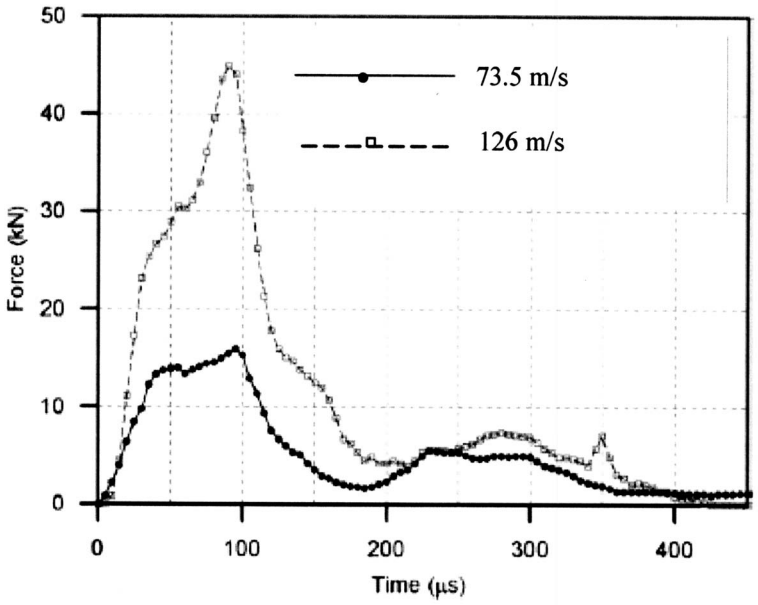

Fig. 7 Time-history records of impact force for two different impact speeds of layered spherical ice of diameter 42.7 mm [151]

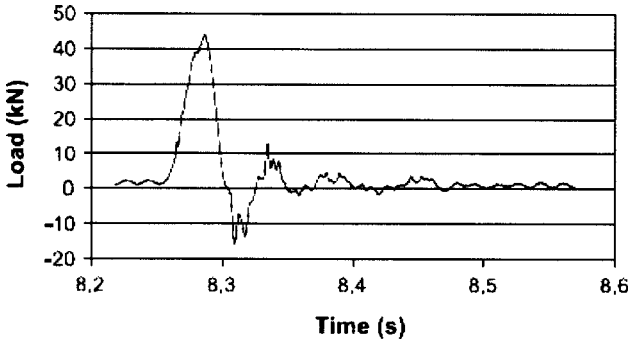

Fig. 8 Impact load-time-history record for a typical test with Growler at an impact speed of 2 m/s with the impact plate at 45 deg [153]

on the speed is taken only for low values of impact speed, while the linear dependence on the square of speed is valid for high values of impact speed.

2.5 Probabilistic Modeling and Uncertainties of Ice Loads

2.5.1 Probabilistic Description. A probabilistic approach for designing ocean structures subjected to ice loading has not yet been developed. However, some progress has been made in estimating the statistical distribution of key parameters. For example, Wright and Timco [13] studied the failure-mode behavior at the Molikpaq caisson during its deployment at the Amauligak I-65 site in the winter of 1985/1986. It was reported that the ice behavior may be categorized according to the failure modes as follows.

- 55% of the time, the structure experienced no load (open water or no ice movement).
- 31% of the time, the ice failed in a mixed mode.
- 9% of the time, the ice failed in creep.
- 4% of the time, the ice failed in flexure (ice/rubble interaction).
- 1% of the time, the ice failed in crushing.

These values were used in a probabilistic analysis of ice loads acting on the Molikpaq by Timco and Frederking [154]. Figure 10 shows the ice thickness as estimated using a random number generator to give three possible values per week—a cold winter (upper curve), an average winter (middle curve), and a mild winter (lower curve). The distribution of the three values was uniform. The values that were selected using the random number generator for the one winter simulated are shown by the dashed curve. The amount of ice interacting with the structure was used to determine

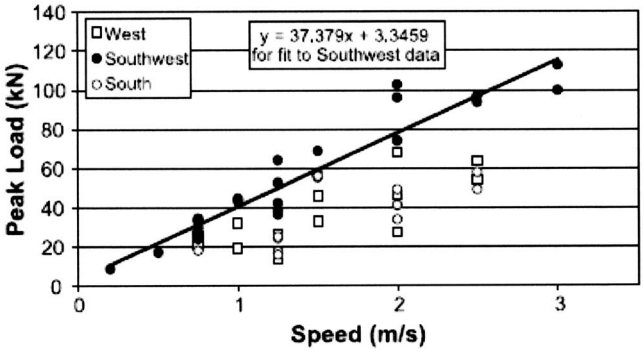

Fig. 9 Dependence of peak load on impactor speed for plate setting 45 deg [153]

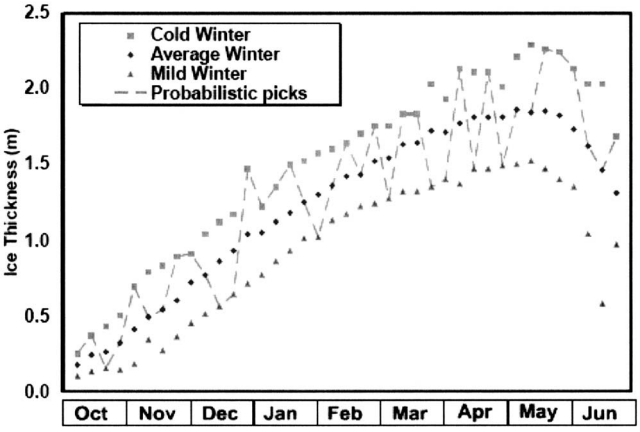

Fig. 10 Ice thickness throughout a winter in the Beaufort Sea showing a cold, average, and mild winter [154]

the number of ice loading events that took place. Wright et al. [155] provided information on the global ice loads on the Molikpaq at the Tarsiut P-45 site during the winter of 1984/1985, and their results are shown in Fig. 11. Figure 12 shows the cumulative distribution as a function of the global pressure for bending, crushing, and mixed-mode failure. These distributions represent loading with level ice with no grounded rubble at the site. Figure

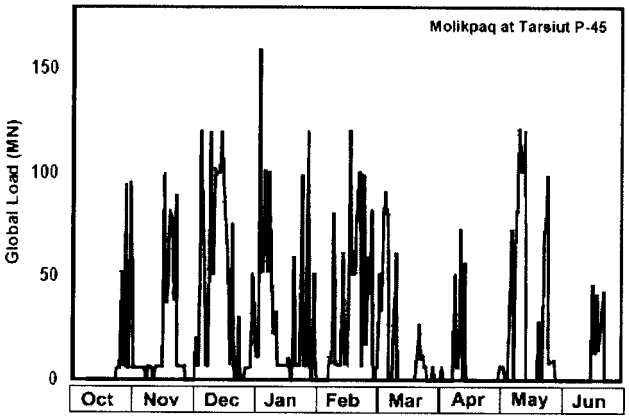

Fig. 11 Global first-year ice loads on the Molikpaq at the Tarsiut P-45 site during the winter of 1984/85 [155]

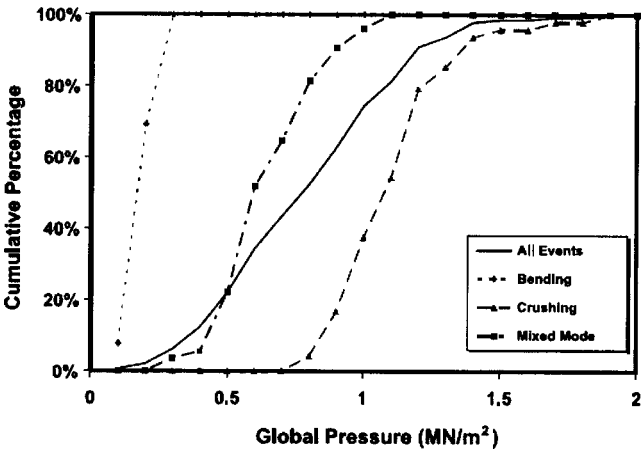

Fig. 12 Cumulative distributions of the global pressure for level ice loading showing the curves for different failure modes of the ice [7]

12 clearly shows the progression of higher global pressures with mixed-mode and crushing ice failure. Local pressures measured by Masterson and Frederking [156] were found considerably higher than the global pressures. Frederking [157] presented an approach for analyzing measured values of local pressure. The probabilistic approach can be used to predict the probability of ice loads acting on ocean vessels to reach a prescribed value based on the ice failure mode. Timco and Frederking [154] developed a simple probabilistic model to predict weekly ice loads. Since there did not appear to be a strong dependence of the global pressure on the ice thickness and floating rubble, the average value for different failure modes was calculated by Timco and Johnston [154]. Based on their analysis, the following predictive equation was proposed:

$$F_{\mathrm{gl}} = T_{fm} w h \tag{2}$$

where F_{gl} is the global load (in MN) on the structure, w is the width (in m) of the structure, h is the ice thickness (in m), and T_{fm} is a failure-mode parameter with the following average values:

$$\begin{aligned} T_{\mathrm{fm}} &= 1.09\ \mathrm{MN/m^2}\ \text{(for ice crushing)} \\ &= 0.83\ \mathrm{MN/m^2}\ \text{(for long-term creep} \\ &\quad \text{(i.e., thermally induced creep))} \\ &= 0.63\ \mathrm{MN/m^2}\ \text{(for mixed-mode failure)} \\ &= 0.18\ \mathrm{MN/m^2}\ \text{(for bending failure)} \end{aligned}$$

These values represent data for ice loading on a wide caisson structure.

Different probabilistic models of high-pressure zones based on the idealization of the high-pressure zones as point loads were developed [64,158–161]. A spatial Poisson process was adopted to model the random number of point loads on a design area, with the size of each load being a random variable. Winkler and Reece [162] used the probabilistic description of multiyear ice ridge loads for conical structures to compute ridge loads as a function of ridge ride-up force, floe driving force, and exposure to multiyear ice.

Full-scale experiments were conducted to measure local and global ice loads. The results showed randomness in ice forces and pressures acting on the structure [163]. Local pressures are considered an important parameter in the design process. Thus, for the design of an offshore rig or a vessel capable of resisting ice forces with adequate reliability, it is necessary to determine ice forces, both global and local, using probabilistic methods. For example, the Canadian Standard Association (CSA) Standard S471 specifies exceedance probabilities for the annual maximum load. The measurements taken on board ships include experiments on CCGS Louis S. St. Laurent, the Cammer Kigoriak, the MV Arctic, the USCGC Polar Sea, the SS Manhattan, and the Oden, which are very valuable. These measurements were analyzed for probabilistic characterization by Carter et al. [164] and Fuglem and Jordaan [165]. Figure 13 shows a sample of measured results taken from two vessels. Figure 13(*a*) was taken from rams by the Polar Sea [166], while the corresponding probability of exceedance is shown in Figure 13(*b*). This case does not reveal any evidence of flexural failure. Figures 13(*c*) and 13(*d*) show the results for the Oden [167] in which flexure failures were evident.

Let the resulting cumulative distribution function be $\Pi_X(x)$, where X is the force or pressure under consideration. Jordaan [168] assumed a Poisson arrival process of loading events, not necessarily with a constant arrival rate. He used the following expression for the distribution of extreme load, Z, which can be derived by writing the expression for zero arrivals in the process, with rate $N[1-\Pi_X(Z)]$, where N is the number of arrivals in a year:

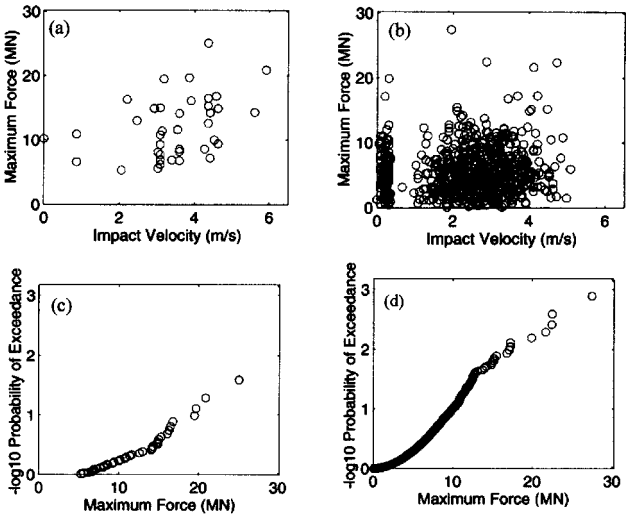

Fig. 13 (*a*) Dependence of maximum force of impact velocity in ramming trials for Polar Sea, (*b*) in Oden, (*c*) probability of exceedance for plot (*a*), (*d*) probability of exceedance for plot (*b*) [171]

$$\Pi_Z(z) = \exp\{-N[1-\Pi_X(z)]\} \tag{3}$$

The choice of period of time could be a year, or the lifetime of the structure, or any other time period that is useful for the case being studied. The probability of exceedance $\Pi_e = 1-\Pi_X(x)$ is

$$\Pi_e = \exp[-(x-x_0)/\alpha] \tag{4}$$

where x_0 and α are constants. Equation (3) takes the form of a double exponential or a Gumbel distribution,

$$\Pi_Z(z) = \exp\{-\exp[-(z-x_0-x_1)/\alpha]\} \tag{5}$$

where $x_1 = \ln N$. Jordaan et al. [159], Morsy and Brown [169], and Brown et al. [170] employed this representation for local ice pressures. Sanderson [32] compiled the main results of ice load measurements and showed how the effective pressure decreases with the nominal contact area. The same trend was confirmed by Masterson and Frederking [156]. The global average pressure P, as a function of nominal contact area A, may be modeled by the power-law relationship

$$P = cA^{-d} \tag{6}$$

where c and d are constants. Sanderson [32] used the value $d = 0.5$, which is consistent with a Weibull distribution describing a material containing random flaws. To deal with material randomness, the coefficient c was represented as a random variable. Jordaan [171] took both c and d as random variables using log-normal and normal distributions, respectively. Consequently, the pressure P is log-normally distributed. Several fits to the data were made for which the mean values of the coefficients c and d were found to be 3 MPa and −0.4, respectively and the corresponding standard deviations were 1.5 MPa and 0.2, respectively [164,172].

The randomness of ice-induced loads was characterized in terms of probability distributions that were fitted to measured ice loads and stress levels. It was assumed that the number of load impacts on the bow of a ship navigating in solid ice, as a function of time, is distributed according to a Poisson law [173]. The measured stress amplitudes on a frame at the bow were found to follow an exponential distribution. Extreme value statistics were applied to the short-term maximum ice-induced pressures measured on board the MS Igrim [174] and to daily maximum ice-induced pressures and stresses on plating and frames measured during the winter of 1978 at the bow of IB Sisu [175]. Similar

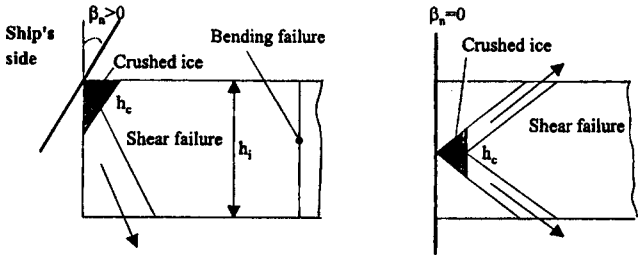

Fig. 14 Ice edge failure process showing the effect of the normal frame angle [190]

approaches were reported in Refs. [176–180]. Varsta [181,182] studied theoretically and experimentally the dynamic bending of level ice. He developed a relation between load level and bow shape, ship's speed, ice thickness, and ice flexural strength. Riska [183] introduced a new approach to calculate ice loads based on the idea of minimal ice pressure.

Carter et al. [164,184] and Fuglem et al. [185] indicated that the design load depends on the number of interactions per unit of time. The greater the number of interactions per unit of time, the further one has to approach the tail of the parent distribution because the design naturally concentrates on extreme values. In formulating the design values recommended by Fuglem et al. [111,186], Jordaan [187], and Brown et al. [188], it is important to distinguish the factors contributing to the number of interactions as opposed to those affecting the failure load itself.

Note that the penetration of a ship into ice by crushing continues until the ice breaks either due to macroscopic shearing or bending failure. With reference to Fig. 14, the ice load increases as long as the crushing area increases before the occurrence of macroscopic bending or shear failure. The normal frame angle β_n is an important parameter in the process and is a function of the waterline angle and frame angle of the hull area under consideration [181]. Kujala [189] developed a statistical model (SM) to describe the ice failure process in ship-ice interaction. The parameters used in the model are level ice thickness, ship's speed, ship's hull shape, ice-crushing strength, and ice flexural strength. Figure 15 illustrates the calculated load on a frame as a function of the normal frame angle with ice thickness as a parameter. Later, Kujala [190] determined the lifetime of maximum ice loads for ice-strengthened ships and obtained the dependence of load level on the main ship parameters and prevailing ice conditions.

2.5.2 Ice Load Uncertainties. It is well known that ice load predictions are subject to uncertainties. Bea [191] summarized the results taken from a CSA sponsored study of the uncertainties associated with extreme environmental loadings acting on offshore structures. The evaluations addressed loading effects that resulted from dynamic and nonlinear interactions of the structures.

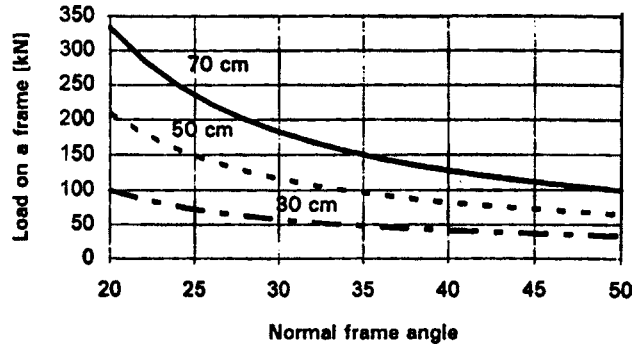

Fig. 15 Dependence of the load on one frame on the normal frame angle for different values of ice thickness [190]

Loading uncertainties were organized and characterized into two categories: (1) inherent randomness (aleatory uncertainty) and (2) analytical variability (epistemic uncertainty). The study addressed the global ultimate limit state performance of three structures: (1) a concrete GBS located off the East coast of Canada (Hibernia), (2) a steel pile template located on the Scotian Shelf off Sable Island, and (3) a caisson retained island located in the Mackenzie Delta area of the Beaufort Sea (Amuligak). The results revealed that it was not possible to develop unambiguous characterizations of uncertainties. In many cases, major sources of uncertainty were not included in probabilistic characterizations. Because of the needs for design code information sensitivity and consistency in demonstrating compliance with target reliability goals, there is a need for well-organized and definitive evaluations of uncertainties in extreme environmental loadings and load effects.

In 1996, a study was undertaken to examine how international experts differed in their ice load predictions, to assess why these differences occurred, and to develop a process to help reach consensus on ice loads. The study involved 14 international groups and looked at ice load scenarios involving level and ridged first-year ice, multiyear ice, and driving forces. As expected, the study highlighted significant differences in ice loads as estimated by worldwide experts and organizations [192].

Wu et al. [193] described a reliability-based methodology that was developed for determining rational design ice loads on offshore structures. The methodology provides a systematic framework to account for type-I (aleatory) and type-II (epistemic) uncertainties in assessing global probabilistic ice hazards. Specifically, a logic-tree based approach is developed to model type-II uncertainties in the assessment of ice hazards. Although the method has a general applicability, Wu et al. [193] considered a wide, vertical-sided GBS in a dynamic annual ice environment. Their results from the reliability-based approach indicated that the modeling of type-II uncertainties plays a significant role in quantifying the ice hazards for determining the design ice load. The developed probabilistic methodology was found to have a broad applicability and can provide a rational framework for calculating design ice loads on other types of structures for arctic offshore development.

In closing this section, it is obvious that the ice loading is a nondeterministic process, nonsmooth due to impact interaction. In addition, its measurements involve several sources of uncertainties that make it imperative to utilize probabilistic description. These facts require further developments to establish phenomenological models that can be used in studying the ice load interaction with offshore structures and ships.

2.5.3 Design Considerations and Regulations. The design of ships and offshore structures should take into account the effect of ice loads. Ice load measurements conducted with vessels navigating in the Baltic were found to exceed several times the design loads. At the design load level, the structure may exhibit some plastic behavior, yet maintaining substantial reserve against actual collapse or rupture. Hakala [194] used the automatic dynamic incremental nonlinear analysis (ADINA) finite element method to study the nonlinear behavior of an ice-strengthened ship shell structure. The plastic limit load was determined using a calculated load-deflection curve. The results of the finite element analysis were compared with well-known formulas of plastic design and also with experimental results. Horrigmoe and Andersen [195] presented the results of a numerical investigation of ice-structure interaction based on finite element analysis. Their formulation included the effects of both material nonlinearities and large deformations. Results from numerical simulations were obtained for different aspect ratios and for varying indenter velocities.

Chiu et al. [196] and Wiernicki [197] applied the plastic theory to investigate the behavior of ship structure subject to ice loads. Refined design standards have been developed and reported by Daley [198]. The design ice loads for the unified requirement for polar ships, developed by the International Association of Classi-

fication Societies (IACS) [199], are described by Daley [27,28,200,201]. The IACS explicitly considers the load carrying capacity of structures in the plastic range [199]. The Finnish-Swedish Ice Class Rules (FSICR) applied design standards for ice-strengthened vessels operating in Baltic Waters [202]. The Finnish Maritime Administration [203–205] introduced guidelines for applying direct calculation approaches in the process of designing structures as an alternative to the FSICR. Classification societies have published guidelines describing direct calculation procedures using nonlinear finite element methods [206,207].

The American Bureau of Shipping (ABS), Det Norske Veritas (DNV), and Lloyd's Register (LR) initiated a joint project to develop a set of classification rules for the hull structure of oil tankers with a length greater than 150 m [208]. Detailed procedures for evaluating alternative structural designs using nonlinear finite element method were outlined in ABS [209]. ABS [207] issued a new set of guidelines on ice class, which provide direct calculation procedures for designing ice-strengthened vessels. They addressed three principal elements in ice strengthening design: alternative side structures, minimum propulsion power requirements, and strength of the propeller. The minimum required engine output power P is determined from the following simple formula $P = \eta_c(R_{ch}/1000)^{3/2}/D_p$, where η_c and R_{ch} are the efficiency of the propeller(s) and the resistance of the vessel, respectively. They can be determined from the tables in the Rules once the geometry of the vessel and propeller(s) are specified [210]. D_p is the diameter of the propeller(s).

Wang et al. [211] addressed the uncertainties associated with ice loads in the FSICR and the Finnish Maritime Administration (FMA) guidelines. They defined extreme ice loads and applied these loads on the side shell between supporting members in evaluating alternative designs using nonlinear finite element methods. An overview of a design procedure for the side structures of ice-strengthened tankers was given by Wang et al. [212,213].

Wang and Wiernicki [214] addressed some issues related to the design, repeated ice loads, and design of other structural components of oil tankers. Plastic deformation theory was used in design formulations for ice impact loads. Although ice strengthening design standards have accepted a certain level of permanent deformations to the side shell, the allowable permanent deformations were not explicitly identified. The latest advances in computer technology and computational software have made it possible to explicitly calculate the permanent deformations of structures, which form the basis for more rational designs. Industry needs have prompted the ABS to develop guidance notes on nonlinear finite element analysis of side structures subjected to ice loads. These notes have provided detailed instructions for structural modeling, material nonlinearity, ice loads, boundary conditions, and acceptance criteria. Wang et al. [215] performed a series of linear and nonlinear finite element methods to investigate the behavior of side stringers. Both the ice loads and the stringer thickness were varied in this study. The impact on the buckling and the ultimate strength of the side stringer were found to be more prominent in the vessel's forebody region.

The Russian Maritime Register of Shipping [216] developed and upgraded its rules on the basis of comprehensive research work as well as the requirements of international conventions and codes. Japan Ocean Industries Association (JOIA) and Mitsubishi Heavy Industries have conducted extensive research projects dealing with the study of ice load acting on marine structures based on field studies, model tests, and refined finite element methods [217–219]. Saeki et al. [220] outlined the development of ice load prediction methods and numerical simulation techniques for ice-structure interaction. They developed analytical simulation algorithms for ice-structure interactions concerning vertical and inclined structures. A numerical simulation of three-dimensional ice-structure interactions was carried out by Katsugari et al. [70] using distinct element methods and PFC-3D. The simulations of ice ride-up on upward and downward breaking were performed on a conical structure model.

3 Ice-Structure Interaction

Ice-structure interaction involves energy sharing in the form of structure oscillations and ice crushing. The ice crushing may result in negative damping that induces self-excited vibration. The concept of negative damping due to decreasing ice-crushing strength was realized by several investigators [156,221–225]. Neill [226] suggested that ice tends to break into fragments of a certain size distribution, which, together with velocity, determines a frequency spectrum.

In studying ice interaction With offshore structures, Peyton [227–229] concluded that the frequency of ice force oscillations, although corresponding closely to the natural frequency of the platform, originated basically from the ice failure mechanism, and there was a great possibility for forced resonant oscillation of the structure. On the other hand, Blenkarn [221] gave a different view that the filtered response to random forces most likely contributed to a major part of the observed dynamic response of Cook Inlet structures. Eranti et al. [230] developed an analytical model for computing the ice force and the structural response on the basis of ice and structure properties as well as their combined properties. The computations were carried out in two phases: penetration leading to ice failure and free vibration of the structure until new contact is established between the ice and structure.

Eranti [231,232] developed a theoretical description of dynamic ice-structure interaction involving transverse and torsional vibrations. The analysis covered cases of continuous crushing against vertical structures as well as combined crushing and shearing against inclined structures. Matskevitch [233] presented the mathematical simulation of ice field action against a wide vertical-faced structure. When there is no adfreeze bond between the ice and the structure surface, ice can slip without friction along the structure. The analytical solution for a structure with a circular cross section was developed in Ref. [233]. The cyclic ice loads formed in crushing failure when ice interacts with vertical compliant structures were investigated by Yue et al. [234] using full-scale structural tests. The results included three ice force modes: quasistatic, steady-state, and random vibration. It was demonstrated that with the change of ice speed, the loading rates of near field ice sheet can make ice fail in three forms including plastic failure, ductile-brittle transition failure, and brittle failure.

Horrigmoe and Andersen [195] presented a comprehensive numerical investigation of ice-structure interaction phenomena using the finite element method. The formulation included the effects of both material nonlinearities and large deformations. The numerical solution was based on a viscoplastic constitutive model for ice. In this model the elastic, creep, and plastic components of strain were additively combined. The constitutive model, which has been developed for general orthotropic (i.e., orthogonal anisotropic) materials, included a variety of creep laws and failure criteria.

3.1 Ice Interaction With Flexible Structures

3.1.1 Basic Studies. The dynamic interaction between an ice feature and a stationary structure is governed by a number of factors, such as the constitutive behavior of the ice, the geometry and flexibility of the structure, the contact conditions of the ice-structure interface, the speed of the ice, and its spatial distribution. The early studies of ice interaction with flexible structures were experimentally conducted by Peyton [227–229,235,236]. His results revealed that the measured response of the structure is greatly dependent on the ice floe. At relatively high velocities, the structure exhibits small-amplitude, high frequency vibrations about a constant mean value. At low ice velocities, the amplitude undergoes severe, low frequency variations between zero and a maximum level that is approximately double the high-velocity mean. The term *ratcheting* was given to this type of oscillation.

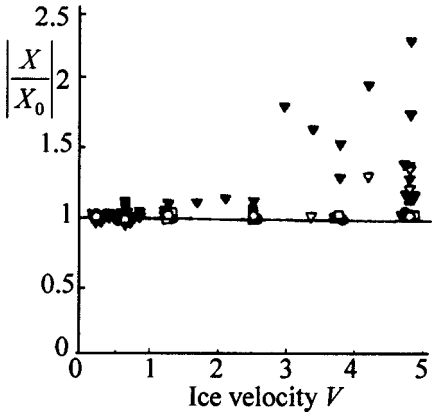

Fig. 16 Dependence of the structure response on ice velocity for different types of structure cross section [238] (● ω_n =16 Hz, ■ ω_n=4.02 Hz, ▼ ω_n=1.27 Hz, single pile of 7.6 cm diameter; ○ ω_n=14.17 Hz, □ ω_n=4.01 Hz, ▽ ω_n=1.27 Hz, two piles of 7.6 cm diameter each)

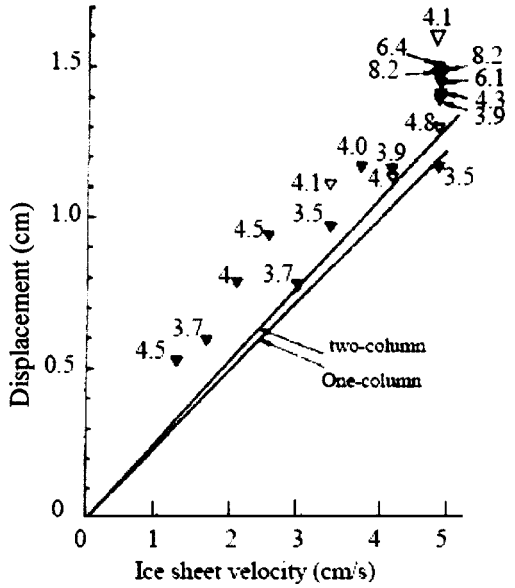

Fig. 17 Dependence of the structure deflection on the ice sheet velocity for different values of ice thickness shown at each point (solid triangles for the one column structure and an empty triangle for the two column structure) [238]

Peyton concluded that the structure receives the most severe loading and acceleration when the ice floe has virtually stopped. Matlock et al. [237] developed a simple model consisting of a mass-spring-dashpot simulating a test pier subjected to a nearly sawtooth ice force. The teeth were uniformly spaced along the time axis, allowing a short time interval for zero ice force. Their numerical solution confirmed the experimental observations of Peyton [227].

Model tests conducted by Toyama et al. [238] observed the occurrence of sawtooth oscillations of relatively rigid structures under ice speed of 0.6 cm/s. For flexible structures, the response was a nearly harmonic oscillation at a high ice speed of 4.8 cm/s. The cycle of oscillation was associated with two ice regimes, namely, elastic ice deformation and ice crushing. They measured the dynamic magnification factor (DMF) defined by the ratio of the maximum structural displacement to static displacement of the structure under the action of the peak ice force. Figure 16 shows the dependence of DMF on the ice sheet speed for different types of structures. Figure 17 shows the dependence of the structure displacement on the ice sheet velocity for different values of ice sheet thickness.

Englebrektson [239] and Nordlund et al. [240] pointed out that all structures have a range of ratios between ice thickness and ice velocities that make them vulnerable to ice-induced vibration and possible simultaneous crushing. For example, the Molikpaq structure in the Canadian Beaufort Sea started to vibrate for a 3 m multilayer ice feature with a drift speed of 0.06 m/s [241].

Tsuchiya et al. [242] conducted experimental investigations to study the effects of the structure's natural frequencies and strain rates on ice-structure interaction. They found that at low ice strain rates, a sawtooth oscillation predominates in both the ice force and the response of the structure, as shown in Fig. 18(*a*). Figure 18(*b*) displays time-history records of the ice force and structure response amplitude under a higher ice velocity of 39.5 mm/s. It is seen that the ice force is random with a constant mean, while the structure response is a narrow band random process. Figure 19 shows the dependence of the predominant structure's natural frequency on the ice velocity. The frequency increases over the lowest range of the ice velocity; then, it asymptotically approaches the structure's first mode natural frequency. Thus, the phenomenon of "locking in" takes place when the structure frequency coincides with the first mode natural frequency. Xu and Wang [243] and Wang and Xu [244] pointed out that a more reasonable description of the ice-induced vibration would be the effect of "frequency locking in" from the nonlinear periodic ice-crushing force and the structural response. The phenomenon displays a similar mechanism to that of the vortex-induced oscillation.

Shih [245] developed a linear oscillator subjected to a dynamic sawtooth ice force in the form

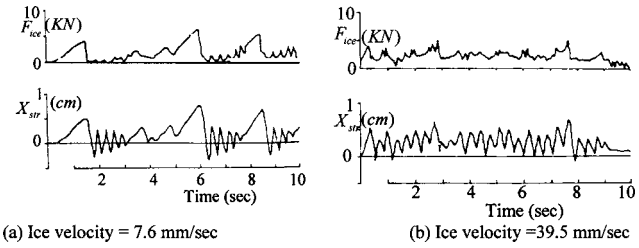

Fig. 18 Time-history records of ice forces and structure displacement at two different ice velocities for a structure natural frequency of 2.89 Hz [248]: (*a*) ice velocity of 7.6 mm/s and (*b*) ice velocity of 39.5 mm/s

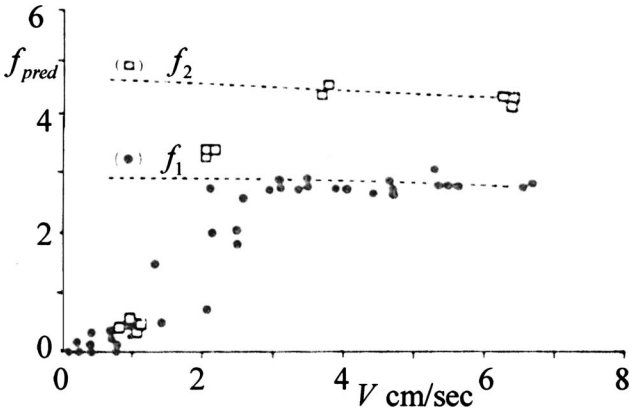

Fig. 19 Dependence of the predominant frequency of structural vibration on ice velocity, showing the structure's first two mode natural frequencies [248]

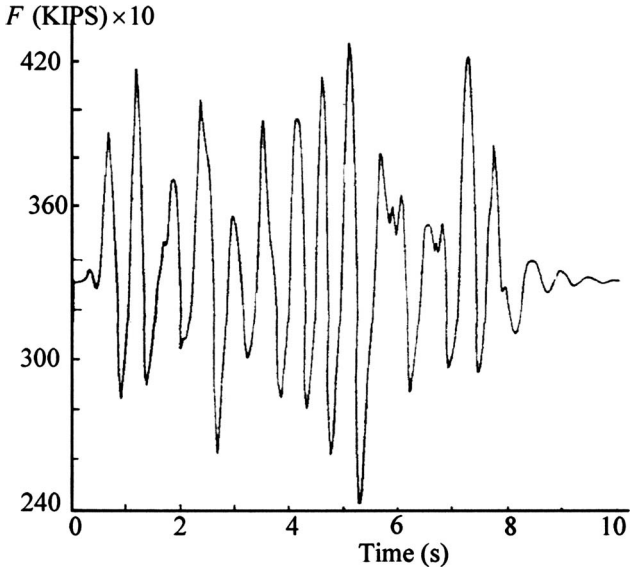

Fig. 20 Typical ice force record acting on a framed tower [255]

$$m\ddot{x} + c\dot{x} + kx = F_n + b_n(t - t_n) \quad t_n \leq t \leq t_{n+1} \tag{7}$$

where m is the mass of the structure, c is the damping coefficient, k is the stiffness of the structure, F_n is the ice force at the beginning of the interval Δt, $\Delta t = t_{n+1} - t_n$ is the time interval of a single ice-crushing force, and b_n is the slope of the force during one time interval. Sodhi [246] presented an extensive review on various models describing ice-induced vibrations of structures.

In a series of papers [247–255], different studies were conducted to estimate the response of framed and monopod offshore towers to ice forces represented by deterministic or stochastic time records. The modeling of ice forces was based on measured records reported by Blenkarn [221] at Cook Inlet. The modeling using a nonstationary random process obtained from filtering a shot noise through a second-order filter. The maximum ice force F developed when an ice cover is cut through by the vertical column of the tower was modeled using Afanasev's [256] formula

$$F = \mu K B h \sigma_0 \tag{8}$$

where μ is the shape coefficient taken as 0.9 for a semicircular cross section, h is the thickness of ice sheet, $K = \sqrt{5(h/B) + 1}$, for $1 \leq B/h \leq 6$, B is the width of the resisting structure, and σ_0 is the uniaxial compressive strength of ice. A typical time-history record of ice force acting on a framed tower is shown in Fig. 20. The mean value of the force was assumed to be produced by the impact of a moving ice floe of constant thickness of 4 ft. The random component was generated artificially and superimposed on the mean value.

Other studies were conducted at low temperatures on fatigue crack propagation in offshore structural steel subjected to random ice loads [257,258]. It was shown that the random ice-induced crack propagation behavior at either ambient or low temperature was different from constant amplitude loading. This is because cracks were propagating faster at low temperature than at ambient temperature.

Sodhi [259,260] observed a dynamic ice-structure interaction due to variable indentation rates during each cycle. Time-history plots of the interaction force took a "sawtooth" pattern. Each cycle of dynamic ice-structure interaction can be divided into the loading, ejection, and separation phases. The tactile sensor data on interfacial pressure exhibited the presence of ductile deformation of ice during the loading phase at low indentation speed and brittle failure of ice during the ejection phase at high indentation

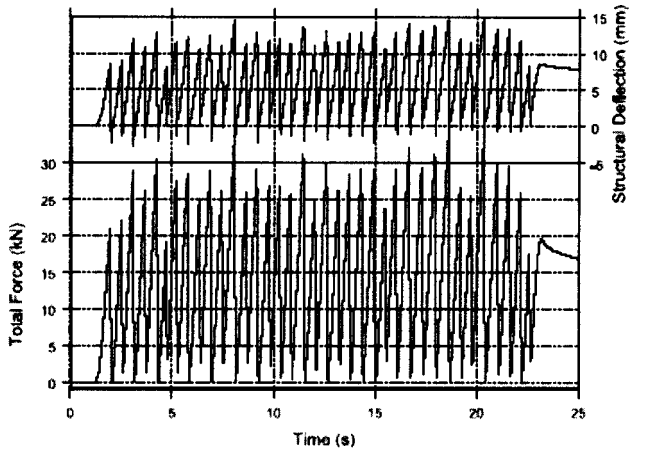

(a) Structure stiffness 2.45 MNm^{-1}.

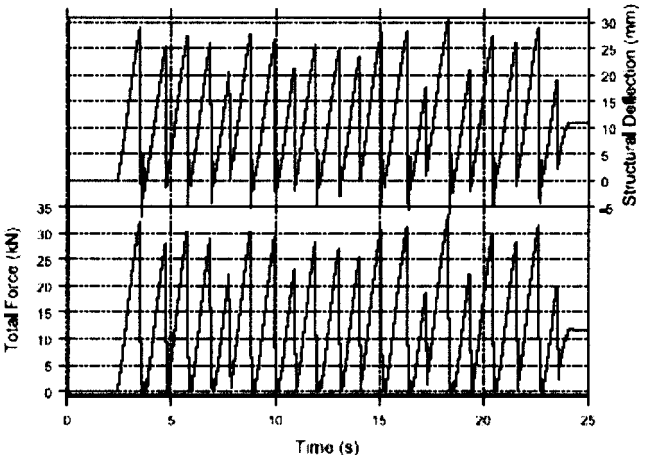

(b) Structure stiffness 1.12 MNm^{-1}

Fig. 21 Time-history records of interaction force and structure deflection on two different structures [260]; structure stiffness of (*a*) 2.45 MN m^{-1} and (*b*) 1.12 MN m^{-1}

speed. Figure 21 shows time-history plots of the interaction force and the structural deflection from two different tests, one with structure stiffness of 2.45 MN m^{-1} and the other with 1.12 MN m^{-1}.

Significant differences between the two interactions as a result of stiffness differences are shown in Fig. 21. For example, the structural deflections were larger in the second test than in the first one. Furthermore, the frequency of intermittent ductile and brittle crushing was higher in the first test than in the second. Though the failure load at the end of the loading phase is variable, the average of the peak values is approximately 25 KN during both tests. The ratio of failure frequency and structural stiffness is 1.85 for the first test and 2.15 for the second. This difference was attributed to the presence and absence of a separation phase during transient vibrations at the end of each loading phase.

Analytical models of dynamic ice-structure interaction were developed in the literatures (see, e.g., Refs. [261–265]). The model considered the crushing with extrusion phenomenon and included two degrees of freedom for the structure and one for the ice sheet. They proposed an indentation failure criterion for full-scale interactions based on a critical crack density. The results predicted lower failure stresses when the size of the structure was relatively large. The combination of microcracks and macrocracks, which occur during the ice-crushing process, was proposed as the pri-

mary cause of size effect for ice crushing. Liu et al. [266] developed a dynamic vibration model for ice-structure interaction. By introducing the broken length of the moving ice sheet, ice-structure interaction was divided into three phases: loading, extrusion, and separation. The dynamic equations of both structure and acting ice sheet and their solutions for each phase were presented, and some results were proposed for both structural designs against ice load and mitigation of ice-induced vibration.

Simple design rules do not provide reliable predictions of ice effects in dynamic interaction conditions. Määttänen [267] reported analytical, experimental, and numerical studies of ice-structure interaction for narrow structures. Kärnä and Trunen [268], Kärnä [269], and Kärnä and Järvinen [270] developed nonlinear models for compliant wide structures. Takeuchi and Saeki [271], Takeuchi et al. [272], and Kärnä et al. [95] considered both narrow and wide structures that have a vertical wall against the ice edge. The ice failure mode at any cross section of the ice edge was assumed to be flaking with ice crushing. Experiments have shown that ice failure occurs sometimes nonsimultaneously and sometimes simultaneously at different points of the ice edge. The change in the failure mode seems to depend on the velocity of the ice floe and on the compliance of the structure.

Discrete element modeling techniques were developed to study ice-structure interaction [273–278]. The discrete element approaches developed in these studies had the capability of accommodating the transition from a continuum to a fragmented state through the application of relatively simple criteria. Selvadurai and Sepehr [279] developed a two-dimensional modeling and applied a discrete element procedure. The modeling took into account the influence of ice viscoplasticity and size dependency in the strength of the ice after fragmentation. It was found that the time-dependent evolution of average contact stress exhibits the characteristic "load accumulation–load shedding" feature observed during many ice-structure interaction phenomena.

3.1.2 Interaction With Offshore Structures. The interaction process of drifting ice fields with offshore structures can cause the structural oscillations. Bekker and Rudetsk [280,281] identified two modes: initial or transition and stable. The initial process is characterized with crushing of the ice sheet bond at the interface zone, penetration, and ice failure. The structural deflection can be monotonic or suddenly changed. The stable process is stochastic and depends on sea ice properties, ice velocity, geometry of structure, and transition process. The failure ice model accompanied with ice-structure interaction was numerically examined by Bekker [282]. Later, Bekker et al. [283,284] developed a hybrid interaction model of system "ice plate–structure support." At the interaction of a structure with an ice sheet, an indentation process takes place with the destruction of ice before a structure by cutting. The approach is based on the numerical modulation of the parameter distribution function of the ice regime and simulation of all possible ice cases characterized by random combination of input parameters. The results of numerical modulation and simulation of all design situations for the whole period of operation of the ice-resistant platform (IRP) establish the probable characteristics of ice loads and number of loading cycles. The numerical experiments for different structure sizes, as well as various directions of ice field impact, were carried out to study the efficiency of the designed model simulating the drifting ice fields/structure interaction. Results include the ice load distribution, number of loading cycles, and penetration time.

High dynamics of ice cover and its considerable thickness require a reliable design of offshore IRPs. Bekker et al. [285,286] proposed a model of mechanical interaction between ice and IRP. The model was based on a numerical simulation of the process when ice cover affects the structure. The proposed model determined those parameters of mechanical interaction between ice cover and a structure such as quantity of load cycles, time of penetration, depth of penetration, and regime of ice load to structure. Similar studies were considered by Makrygiannis et al. [287].

In regions such as the Alaskan and Canadian Beaufort Sea, the ice load is a governing design condition. However, in subarctic areas, such as Cook Inlet of Alaska, Bering Sea, Offshore Sakhalin, and Pohai Bay of China, the governing load is likely to be seismic for slender platforms, which have longer natural periods of vibration. Some of the studies have been done on ice-induced vibration problems of offshore lighthouses in the Gulf of Bothnia, off the coast of Finland. The earthquake response characteristic of offshore platforms in the presence of ice floes is somewhat different from this ice-induced vibration. The problem of nonlinear seismic dynamic responses of a large-scale offshore structure surrounded by thick ice was addressed by Miura and Wang [288]. In modeling the system, a modified joint element was employed to simulate sliding phenomena at the interface between the soil and the structural base. Adashi et al. [289] studied dynamic ice-structure interaction by doing cyclic indentation tests in an ice model basin. They developed a formula suitable for investigating the seismic response of offshore platform, including floating. They also proposed a mathematical model of seismic response analysis. Yamauchi and Kamesaki [290,291] and Yamauchi et al. [292] studied the effects of surrounding ice sheets on the foundation design of GBS under the influence of earthquake ground motion represented by a sine wave. Extensive ice tank tests were performed to simulate an offshore structure placed in moving or nonmoving ice sheets. The test results showed that moving ice sheets affect foundation loads, and an interaction between structure and surrounding ice sheet may mitigate the foundation loads.

The interaction of ice masses with offshore structures is characterized by some physical processes described by Jordaan [171]. Multilayer ice or icebergs can represent a hazard to offshore structures. The pressures within the areas, where compressive forces are transmitted from the structure to the ice, fluctuate considerably both in space and time, with most of the force concentrated intensely in regions known as "high-pressure zones." The center of the high-pressure zone exhibits pressure softening [293,294]. Within the high-pressure zones, the state of stress in the ice is triaxial, varying from low confinement near the edges to high values of contact pressure—up to 70 MPa in measurements—near the center. At lower pressures, found near the edges of the high-pressure zones, microfracturing accompanied by recrystallization occurs, whereas the central areas of high pressure contain highly recrystallized materials. At a certain load, the entire layer is softened and ejection of crushed ice occurs rapidly. The effects of time, temperature, and scale on the formation of high-pressure zones were studied by Dempsey et al. [295]. For both simultaneous and nonsimultaneous contacts, the critical lengths of stable cracking that may occur prior to flaking and flexural failure were found to be strongly linked to the current level of specific pressure parameters.

The influence of ice forces on an offshore structure such as wind turbines was examined by many researchers [296–303]. The stability of these structures due to ice loads is of particular interest. For example, Riska et al. [300] found that the structure response of a slender structure with ice was mildly chaotic. The response dynamics are usually affected by the chaotic ice failure, but dominated by the regular and linear dynamic properties of the structure [304]. Another important aspect is the influence of the broken ice zone around these structures on the emergency evacuation. Timco et al. [305] documented the details of the rubble fields and rubble generation at a number of structure locations in the Beaufort Sea. Timco et al. [306] discussed the size of the broken ice zone around the Molikpaq structure over a range of ice conditions and the implications on emergency evacuation. They also summarized four different evacuation concepts that could be utilized from an offshore structure in ice-covered waters.

Compliant structures having vertical ice walls may suffer from very severe vibrations. Several theories have been proposed to predict these vibrations. However, physical details of this phe-

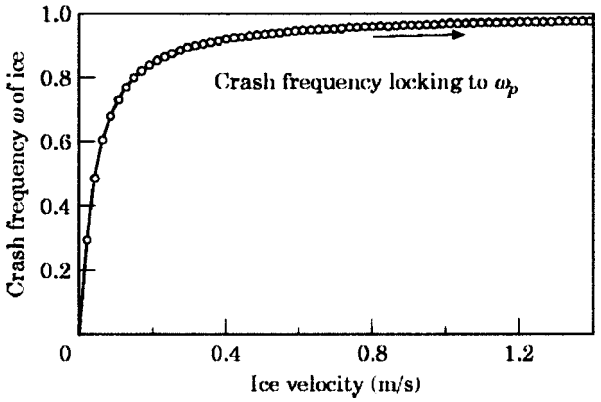

Fig. 22 Dependence of crash frequency on ice velocity [309]

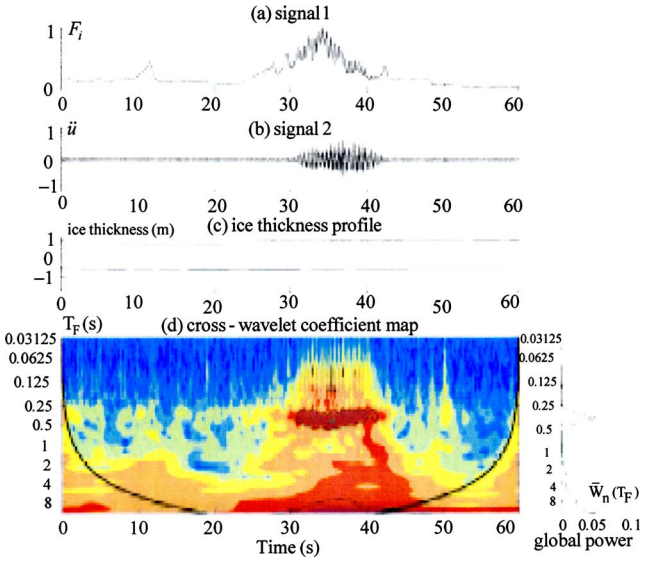

Fig. 23 (*a*) Normalized ice force, $F_i(t)$; (*b*) structure acceleration, $\ddot{u}(t)$; (*c*) ice thickness; (*d*) cross-correlation coefficient map and global wavelet cross spectrum [315]

nomenon are not fully understood. Kärnä et al. [307] addressed the problem of ice-induced vibration of offshore structures. Full-scale measurements made in the Bohai Bay indicated that conical structures may experience excessive vibrations caused by ice. Indentation tests were done at the ARCTEC laboratory at the Hamburg Ship Model Basin, Hamburg to clarify details of ice-induced vibration. Sheets of columnar grained saline ice were used in the tests. The parameters that were varied included the structure's compliance and damping, indentation velocity, and the structural geometry at the waterline.

A two-dimensional finite difference numerical approach was developed by Choi and Rim [308] to study the design ice load and dynamic responses of a slender Arctic structure upon continuous ice movement. A simplified ice-structure interaction model for the system of a slender Arctic offshore structure and a drifting ice floe is proposed. The nonlinear interaction model incorporates the floating ice features, such as crushing strength, thickness, and incoming velocity of ice floes. Interaction forces were calculated using a modified Korzhavin's equation, and a computer program based on a two-dimensional finite difference numerical scheme is developed.

Jin and Hu [309] studied analytically the ice-induced nonlinear vibration of an offshore platform in the North China Sea, where ice exerts a predominant load. They modeled the force of the moving ice by the formula

$$F_{\text{ice}} = B(a_1\dot{\varepsilon} + a_2\dot{\varepsilon}^2 + a_3\dot{\varepsilon}^3)\sin\,\omega t \tag{9}$$

where $\dot{\varepsilon} = \bar{V}_0/4D$, D is the diameter of the pile section where the ice force acts, $\bar{V}_0$ is the relative velocity of the ice with respect to the platform, a_i, $i=1,2,3$ are the optimal fitting coefficients, B is the test constant of the ice force, and ω is the crash frequency of the ice and is a nonlinear function of the ice velocity, as shown in Fig. 22. Usually, the crash frequency is locked to the natural frequency of the pile transverse vibration.

3.1.3 Interaction With Lighthouse Structures. Ice interaction with lighthouse structures is governed by the structure fundamental frequency. In studying such interaction, dynamic ice action events often had to be filtered out at the measurement site [310]. For example, ice load measurements conducted at the Norströmsgrund Lighthouse in the Gulf of Bothnia (Sweden) [311–313] and at the Canadian Confederated Bridge [314] consist of a large amount of unfiltered time records. The characteristic frequency time evolution, together with the applied global ice forces, was estimated by using a wavelet cross-correlation analysis [315]. It was found that the excitations of the Norströmsgrund lighthouse by actions from ice floes are influenced by structural response with dominant frequencies in the same range of frequencies of the response.

Bjerkås [315] estimated the wavelet cross correlation between the measured local ice force $F_i(t)$ and the corresponding acceleration $\ddot{u}(t)$ of the lighthouse structure measured at 16.5 m above seabed. For a 60 s interval with continuously crushing ice with a drift speed of 0.03 m/s and a mean thickness of about 0.9 m, the local ice force $F_i(t)$ and structure acceleration $\ddot{u}(t)$ time record histories are shown in Figs. 23(*a*) and 23(*b*), respectively, where the vertical axis in both plots is normalized. Figure 23(*c*) shows very slight variation of the ice thickness with time. Intervals with ice-induced vibrations were frequently observed when the ice drift speed went from a significant speed down to rest. Figure 23(*d*) shows a map of cross-wavelet coefficients. The horizontal axis displays time in seconds, while the vertical axis represents an equivalent Fourier period. The global cross-wavelet power is plotted on the right of the wavelet map. It is seen that an increase in the load level is triggered around 30 s with a distinct drop followed by an interval with almost steady-state vibrations. The cross-wavelet coefficient reflects a strong correlation for Fourier period T_F slightly faster than 0.5 s. According to the calculations of Engelbrektson [316] and Björk [317], the fundamental frequency of the lighthouse was found to be close to 2.3 Hz and 2.8 Hz, respectively. This implies that the ice load most likely is locked in to a frequency in this range by the response of the structure. The global wavelet spectrum indicates that the most common energy is localized at T_F slightly faster than 0.5 s.

3.2 Ice Interaction With Rigid Bodies. Ice interaction with rigid bodies, such as concrete blocks and rigid structures, is not associated with any significant elastic deformation. Luk [318] analytically studied the influence of an ice sheet on the dynamic characteristics of a cylindrical structure of a circular cross section under dynamic loading using two-dimensional wave theory. Williams and Vipulanandan [319] extended the work of Luk to the case of ice interaction with an isolated, vertical, and cylindrical structure of an elliptic cross section surrounded by an infinite ice sheet. It was found that the damping effects are dominant and ice-structure interaction may be approximated by a first-order dynamical system. Their results provided a measure of the resistance of ice sheet to the structure dynamic motion. Arockiasamy et al. [320] estimated the response of semisubmersible bodies to ice forces.

Chehayeb et al. [321] estimated the global and local pressures generated on a rigid, vertical surface during sea ice deformations in the creeping mode using finite element analysis. Numerical

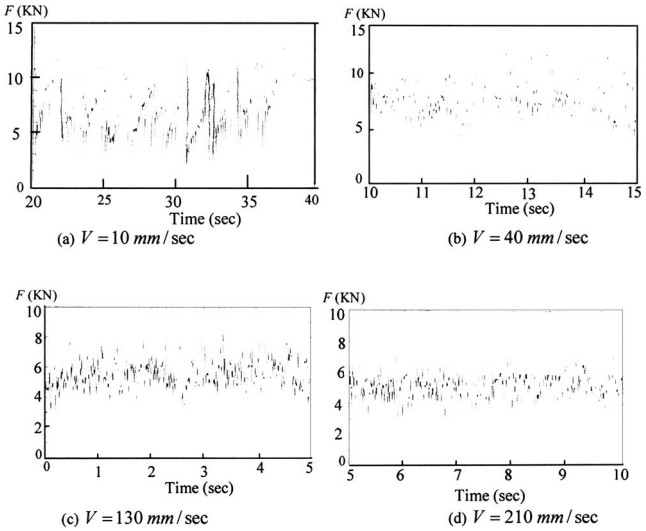

Fig. 24 Time-history records of ice force acting on a rigid cylinder of diameter 200 mm at different values of cylinder velocity [42]

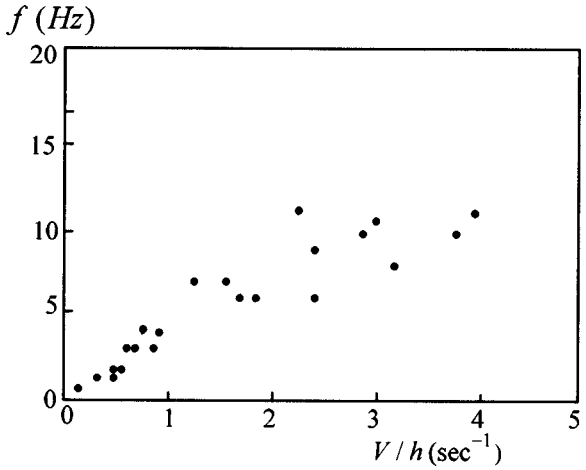

Fig. 25 Dependence of ice force characteristic frequency on the ratio of cylinder velocity-to-ice thickness for a cylinder diameter of 200 mm [42]

simulations were performed under plane stress conditions to assess the influence of interface adfreeze and friction on predicted pressures. A better understanding of the mechanics of ice has led to increased demands for improved computational methods. Current trends in ice mechanics relate principally to creep, global (tensile) fracture, as well as compression fracture (crushing). Suman [322] presented a method for estimating design loads imparted by a floating ice feature to the structure and predicted the behavior of the adfrozen ice plate and the invading ice feature.

Iyer and Kivisild [323] developed a general purpose dynamic finite difference model originally developed for the nuclear industry applications, damage considerations as applied to the fractured ice, and validation of the field tests for the ice cutting semisubmersible drilling vessel (ICSDV) concept. The results for forces and energy were found to be in good agreement with test results.

Friction-induced wear of concrete due to ice-concrete interaction has been the subject of experimental investigations [324–326]. These studies revealed that wear was created due to the combination of two different mechanisms. The first is the general wear due to the progressive erosion of the cement paste and small aggregates by the flow of ice and wear particles along the surface. The second is the catastrophe wear due to a sudden ejection of aggregates from concrete surface after weakening of the cement paste-aggregate bond by general wear.

Sodhi and Morris [42] measured the generated ice forces by pushing rigid cylindrical structures of different diameters at different velocities through an ice sheet. Typical time-history records of ice force acting on a rigid cylinder of diameter of 200 mm measured for four different values of velocity are shown in Fig. 24. The dominant frequency of ice force variations, defined as the characteristic frequency, was determined from the frequency spectra of the force records. The characteristic frequency was found to increase with increasing velocity, as shown in Fig. 25. The frequency plot with respect to the velocity-to-ice thickness ratio reveals a linear relationship, which implies that the average length of the damaged zone is proportional to the ice thickness. The average length of the damaged zone was found to be about one-third of the ice thickness. Furthermore, the effect of pile diameter on the characteristic frequency was difficult to ascertain for a velocity-to-ice thickness ratio greater than 1.5. The characteristic frequency during an interaction of the 500-mm-diameter pile was lower than that of the 50-mm-diameter pile for the same relative velocity. Thus, an increase in the velocity results in an increase in the characteristic frequency, while an increase in the pile diameter causes a decrease in the characteristic frequency.

The influence of interference effects on the dynamic forces experienced by the members of an array of rigid circular cylindrical structures, subjected to steady-state vibration while surrounded by a homogeneous, isotropic, and elastic ice medium of infinite extent was studied by Abul-Azm and Williams [327]. Interference effects were estimated through the modified plane wave approach. Numerical results for two- and four-cylinder arrays indicated that interference effects may significantly alter the amplitude and phase of the reaction force experienced by the array members from that which they would each experience in isolation.

The main categories of structural response are a quasistatic response followed by the transient vibration, the steady-state vibration, and the random response to a wide-band stochastic excitation. Under these conditions, the ice crushes intermittently and causes transient vibrations, which decay before the next event of ice crushing.

The drifting ice field may occasionally induce steady-state vibration in the structure. This kind of response was measured frequently in the Baltic Sea [240,268]. It was shown that if a steady-state vibration arises, the velocity of the structure at the waterline is approximately the same as the ice velocity [238,328–330]. Kärnä et al. [331] considered a very stiff concrete cylinder pushed against sea ice at high speed. The measured time evolution of global force had a random character. The amplitudes of the force fluctuation were very small compared to the mean level of the force. Similar results were reported by Sodhi [332]. Tests with segmented indenters show that random global forces occur in conditions where the local forces fluctuate nonsimultaneously in front of the structure [91,332–334].

On the basis of small-scale indentation tests on ice plates, Korzhavin [335] proposed the following empirical expression to estimate the ice force F on a structure:

$$F = IKmwh\sigma \tag{10}$$

where I is the indentation factor whose value ranges from 1 to 3, k is the constant factor and may assume a value ranging from 0.3 (for nonsimultaneous failure) to 1 (for simultaneous failure), m is the structure shape factor ranging from 0.9 for cylindrical structures to 1 for flat indenters, w is the contact width of the structure with ice, h is the ice thickness, and σ is the uniaxial compressive "strength" of ice. There is much confusion and disagreement on the use of this equation because of different modes of ice failure [32,336,337].

4 Ice-Ship Interaction and Resistance to Ship Motion

4.1 Ice-Ship Interaction. The ship-ice interaction is a complex phenomenon in which interdependence exists between the ship response and the ice forces. The ship response is influenced by transient hydrodynamics, the elastic action of the ship, large motions of the ship, the ice interaction, and the presence of an ice cover. The ice failure process is, in turn, influenced by the ship response. While vessel motions and stability are of some interest, the main concerns are the total force on the bow and the stress distribution along the hull girder.

It has been recognized in the literature that there is a considerable variation in pressure across the compressive interface in ice-structure interaction [43,338]. Improvements in the mechanism of icebreaking having an application to ship icebreakers, offshore drilling platforms, and other structures interacting with ice were reported by Vinogradov et al. [339]. This resulted in a special lever mechanism for ship icebreakers or barrier structures for protecting drilling platforms. Consequently, the horizontal force, which the icebreaker creates or which acts on the structure, was found to be substantially reduced.

Mueller and Ettema [340] conducted an experimental investigation for studying the dynamic behavior of an icebreaker hull moving continuously through an ice sheet. The interaction of ice forces exerted against the hull and the hull's pitching motion was studied on a 1:48-scale model hull of the USCGC "Polar Star" (WAGB10). The dynamic response of the model hull to ice breaking was used to establish the vertical component of the ice forces exerted against the hull and to evaluate the temporal variation of the hull's buoyancy and pitching moment. Uto et al. [341] described the propulsive performance of PM Teshio in a continuous icebreaking mode. Analytical methods to predict the icebreaking performance of a vessel are not reliable, and it is imperative to conduct model tests to optimize different characteristics of ice going vessels [342].

The dynamic interaction between moored tankers and ice features depends on the maximum ice loads acting on tankers. Sandvik [343] and Jolles et al. [344] used simplified model approaches, while Løset et al. [345] and Murray and Spencer [346] conducted ice tank tests to address the feasibility of some conceptual designs. Numerical simulation models based on discrete element modeling techniques were developed to simulate the behavior of vessels moored under the marginal ice zone [347–350]. Each ice floe was represented by a circular disk while boundaries, land formations, and structures were assumed piecewise linear shapes. Disk-disk or disk-structure collisions were modeled as linear viscous-elastic or as a Coulomb friction contact in case of relative tangential sliding. Hansen and Løset [349] found that the results predicted by their model were in qualitative agreement with experimental results; however, the amplitudes tended to be overpredicted. The predicted frequency of oscillation in surge was found to be slightly lower than the measured one.

Jebaraj et al. [351,352] developed a finite element analysis to simulate the interaction between ice and ships. Ice interaction with structures has been treated for two different classes, namely, flexible and rigid ocean systems. In their dynamic analysis for ship/ice impact, the mechanism of load transfer during the interaction was treated as a contact process, taking into consideration the area of contact. Parametric studies were carried out to determine the influence of frame angle of the ship, velocity of impact of the ship, and thickness of the ice sheet on the failure loads.

Noble et al. [353] developed mathematical simulations and physical models. They provided a comparison with full-scale data of the accelerations encountered during various icebreaking and ice transiting operations. The ice interaction modes included continuous level icebreaking, ramming in thick level ice, navigation in floe fields, occasional jamming between floes, and the low probability occurrence of an accidental impact with a large ice feature (ice island or berg) at open water speed. A time-domain solution was obtained to the general problem of the dynamics of a ship under the impact of a moving finite ice floe. A comparison of the model test results with the mathematical model prediction showed good agreement. Daley et al. [354] reported some results on the work conducted at Arctec Canada Limited for the Canadian Coast Guard on the development of a general force and stress equation for head-on ship/ice impact. A methodology for developing local load criteria for ships operating at an ice edge was presented by St. John and Meyer [355]. The details of the ice-structure interaction were discussed, including statistical distributions, of ice impact pressures and force based on measured data and theoretical predictions.

A time-domain simulation of collisions between icebreaking ships and multiyear ice was reported by Phillips and Tanaka [356]. The model, Ithaca Ship, considered the transient ship-ice interaction and fluid-structure phenomena as strongly coupled through ship dynamics. At the Southampton Institute, the polar ship concept design (PSCD) software was developed and enabled a ship designer or operator to assess the effect of a set of parameters on an intended design [357]. The PSCD was developed based on multiyear ice-going ships.

Similarity criteria for ice breaking resistances for conventional ice breaker and air cushion ice breaker were adopted in Refs. [358–360]. A similarity criterion introduced by Goldstein and Osipenko [360] has the form of a characteristic length that incorporates the fracture toughness. It was possible to formulate relations for critical loads or dimensions of fracture pieces that were formed in the process of icebreaker–ice-cover interaction. The characteristic form of the relation was shown for the case of fracture near an icebreaker hull due to cylindrical bending, taking into account the velocity effect of icebreaker motion.

In arctic waters, the presence of floating ice provides several challenges mainly related to loads generated by level ice and pressure ridges. Forces resulting from the interaction of ice and hull were described in terms of the slope of hull at waterline and the coefficient of friction [361]. Enkvist et al. [362] presented an analytical study of ridge resistance, its influence on bow angles. The behavior of ships exposed to ice drifting toward the stern depends on the lateral stiffness of the mooring system and the directional dependency of ice forces (in surge, sway, and yaw). In shallow water, the mooring system will have a high stiffness. Previous analytical studies of the weather varying behavior in level ice revealed that ships tend to strongly maintain a heading parallel to the ice drift direction [363,364]. Løset et al. [365] introduced the "submerged turret loading (STL)" concept for loading oil offshore structures in the North Sea. The feasibility of the STL concept was studied by conducting a number of tests on a model at a scale of 1:36. In level ice, 1.5 m full-scale ice thickness, 720 kPa flexural ice strength, and 0.75 m/s speed, the average total force was 5868 kN with an average line tension in the front line of 2600 kN. The corresponding maximum loads were 8929 kN and 3507 kN. The mean value of the force peaks was 7285 kN with a standard deviation of 932 kN. The measured forces (scaled) in level ice were found to be within the capacity of the STL mooring system. Depending on the ridge consolidation, pressure ridges were found to have the capability of exerting forces that exceed the capacity of the STL system. In broken ice, the average total force did not exceed 2500 kN, and the single mooring line loads were not above 1200 kN.

4.2 Ice Resistance to Ship Motion. Generally, the presence of ice will create a significant resistance to ship navigation. This resistance increases with increasing ice thickness. Existing methods for determining ship resistance in ice included numerical methods, which depend on solutions of equations of motion that describe the dynamic interaction between the ice and the ship, and empirical methods, which depend on model and full-scale icebreaker data to generate empirical correlations for ship resistance. Luk [366] presented a three-dimensional analysis for calculating the level ice resistance for ships that have conventional hull forms. His approach combined a plastic limit analysis used to

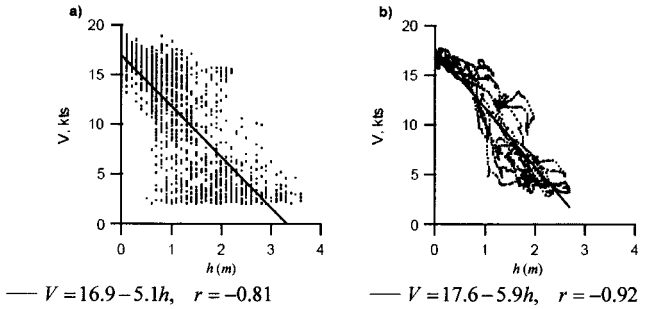

Fig. 26 Dependence of mean speed on mean ice thickness; the lines are linear regression: (*a*) 1 min intervals and (*b*) 30 min running averages [368]

describe the ice failure mechanism, together with the associated ice velocity field and linear and angular momentum balances to determine the average ice resistance for the ship. A review of ship resistance in ice was presented by Peirce [367].

Haas et al. [368] conducted extensive measurements of ice thickness using electromagnetic inductive transducers along the route on board the icebreaker Kapitan Dranitsyn. The dependence of the convoy speed on the ice thickness was obtained, as shown in Figs. 26(*a*) and 26(*b*) for 1 min intervals and 30 min running averages, respectively. The dependence of convoy velocity V in knots (nautical mile per hour, 1 kn=1.689 ft/s) on ice thickness h (in meter) is given by the following linear relationships and the corresponding correlation coefficient r: for Fig. 26(*a*),

$$V = 16.9 - 5.1h \quad r = -0.81$$

for Fig. 26(*b*),

$$V = 17.6 - 5.9h \quad r = -0.92$$

Another well recognized ice force formula based on in situ measured data of ice force on piers is the Schawz formula [369]

$$F = 3.57w^{0.5}h^{1.1}\sigma \tag{11}$$

whose units are in centimeter (for w and h), N/cm^2 (for σ), and N (for F).

Fragments of ice in the form of ice blocks or mush ice add resistance to ship-hull motion. The ice-water medium constitutes two phases. A two-phase flow may be modeled based on a non-Newtonian flow, such as a *Bingham plastic* fluid that was originally proposed to model slurry flows. A Bingham fluid is represented by a threshold shear stress below which there is no motion. Above the threshold value, the shear stress varies linearly with the strain rate as follows:

$$\tau = \tau_0 + \eta\frac{du}{dy} \tag{12}$$

where τ is the shear stress, τ_0 is the threshold yield stress, η is the slope of the shear stress versus the strain rate in the linear region, and du/dy is the velocity gradient. The most significant nondimensional parameter is the *Hedstrom number* (He) defined as [370]

$$\mathrm{He} = \tau_0\rho_m D^2/\eta^2 \tag{13}$$

where ρ_m is the density of the mixture and D is a characteristic dimension.

Resistance tests are performed by towing a ship model at different speeds through ice-covered water. The speeds are usually selected to be the creeping speed, the predicted speed in the given ice condition, and a speed with a value above the one yielding estimated icebreaking performance. The towing force and speed are measured during these tests. The measured total force consists of two parts: the resistance in ice-free water (open water resistance) and the ice resistance. In order to separate these two components, some additional tests in ice-free water should be conducted. The ice resistance consists of two parts: the breaking component and the submersion-velocity component. In order to separate these components a test with creeping speed should be performed in presawn ice. When the ice is presawn, the ice breaking component is eliminated, and the measured ice resistance includes only the submersion-velocity component.

Blanchet and DeFranco [371] reported field data measurements and indicated that the ice force per unit width decreases with the structure width and depends only slightly ice thickness. Løset et al. [372–374] reviewed different studies pertaining to the effective ice pressure. They proposed the following expression for the global load

$$F_{\mathrm{gl}} = pwh \quad p = a_k w^m h^n \tag{14}$$

where m and n are constant factors, a_k is an experimental parameter that depends on ice quality, strength, temperature, and drift speed [375], w is the structure width, and h is the ice thickness. The factor m addresses the uneven contact along the structural width and scale effects in ice crushing. The factor n addresses the uneven distribution of pressure through the entire ice thickness.

Bjerkås [376] indicated that for events with high speed of a rigid body and thin ice, brittle and nonsimultaneous failures usually occur. Furthermore, it was found that the global nominal pressure is stationary and relatively low due to nonsimultaneous peak loads. The effective contact width w_{eff} was found to be always less than the nominal width w. This is a common scenario for wide structures and frequently reported in the literature (see, e.g., Refs. [32,377]).

The influence of hydrodynamic forces acting on iceberg from floating structures was studied in Refs. [378–380]. Other cases include hydrodynamic effects on iceberg collisions [381] and flow about spherical and cylindrical bodies near a plane wall [382–384]. These studies motivated others to consider the hydrodynamic interaction of a transiting tanker and free-floating glacial ice mass (see, e.g., Refs. [356,380,385,386]). In particular, Gagnon [385,386] considered such effects as the ice mass shape, size and orientation, ship model speed, and track proximity. Ice mass shapes included different sizes: spherical, cylindrical, and pyramidal. The observed motion parameters were sway (lateral movement of the ice mass from its initial position perpendicular to the long axis of the tow tank) and surge (movement of the ice mass from its initial position along the long axis of the tow tank). Figure 27 shows the dependence of sway and surge motions on the tanker fore perpendicular position for the small inverted pyramid mass (of base of 0.3×0.3 m^2 and height of 0.26 m) with a separation between the ice mass and the tanker model of 1.375 m and a model speed of 1.24 m/s. It is seen that the ice mass would start to sway and surge away from the tanker (point a in the figure) to a maximum surge value (point b in Figs. 27(*b*) and 27(*c*) and maximum sway value (point c in Figs. 27(*a*) and 27(*c*)). As the long side of the tanker passed, the sway value would stay roughly constant at the maximum value, c in Figs. 27(*a*) and 27(*c*), while the ice mass would surge backward at c in Fig. 27(*b*) until the stern of the tanker came by at which point the ice mass surged forward again and swayed back in toward its original lateral position point d in Figs. 27(*a*)–27(*c*).

Other results of cylindrical and spherical ice masses were reported in Gagnon [385]. With reference to spherical ice masses, it was found that as the tanker speed increased, the maximum sway tended to level off to certain values for each of the spheres. For the medium sphere, the maximum sway increased with increasing speed, while for the large sphere, it decreased with speed. The small sphere exhibited mixed trends. The presence of waves was found to lead to maximum sway values roughly five times the calm water values at the lower speeds for the large sphere ice mass. However, for large and small ice spheres, the effect of

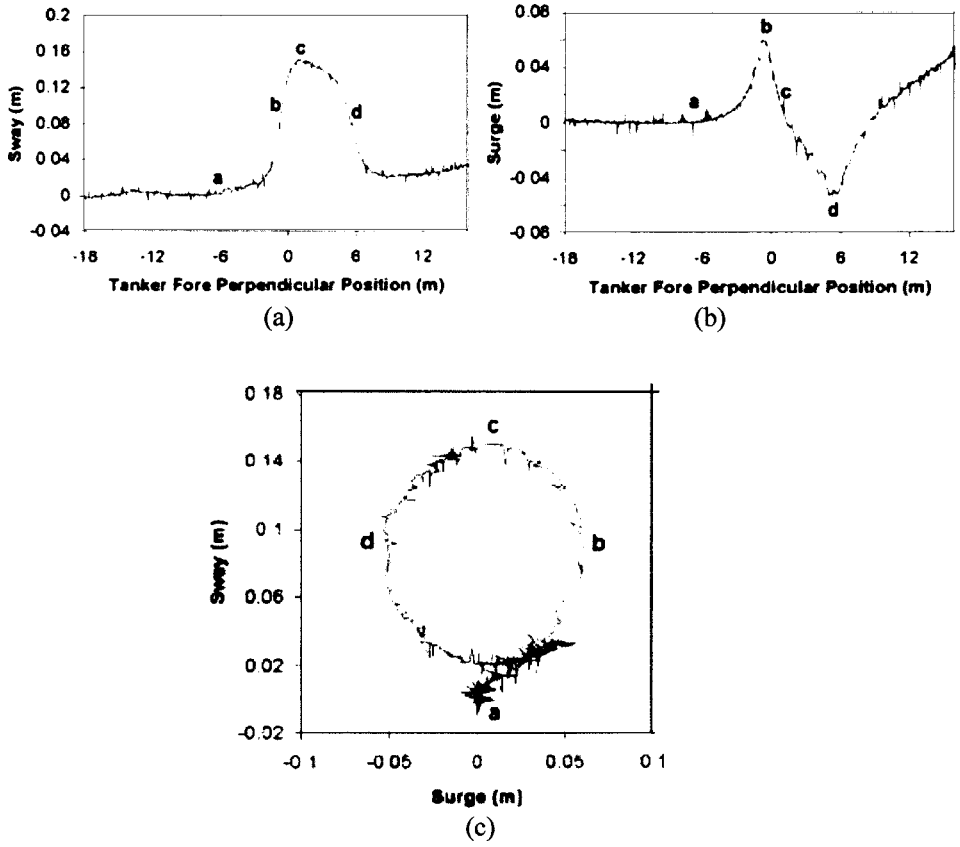

Fig. 27 Dependence of (*a*) sway and (*b*) surge on the model tanker fore perpendicular position; (*c*) sway-surge configuration diagram [386]

waves diminished at higher speeds.

Early studies of ship resistance in ice floes [387–389] revealed that the resistance force has a limiting nonzero value for zero ship speed. Later, Ashton et al. [390] showed a decrease in brash-ice resistance with increasing speed of a Mississippi River two-barge system. They suggested that the decrease may be due to a "trade-off" between decreasing resistance associated with brash-ice accumulation ahead of the two-barge system and increasing boundary-layer friction resistance. This result appears to be in contradiction to the findings of Buzuev and Ryvlin [387] and Kashtelyan et al. [388], who showed that the resistance increases with the ship speed. Based on scale model tests with a 3-m-long hull of a great lake bulk-carrier vessel, Levine et al. [391] obtained the following empirical relationship for hull resistance in brash ice:

$$R = \rho Bh(1.29gh + 1.365V^2) \tag{15}$$

where ρ is the ice density in lb s^2/ft^4, B is the hull beam in ft, h is the ice thickness in ft, g is the gravitational acceleration, and V is the ship speed. Another analytical relationship was developed by Mellor [392] by assuming that a Mohr–Coulomb failure criterion [393] could be used to describe the resistance of a brash-ice layer for a hull on the verge of motion. His model is given by the following relationship:

$$R = BR_p[1 + 2\mu_e(K_1 + K_2N)] \tag{16}$$

where μ_e is the effective friction coefficient, $K_1=L_1/B$, L_1 is the bow length, $K_2=L_2/B$, L_2 is the after-body length in continuous contact with the ice, N is a factor of uncertain value but less than 1, and R_p is the force per unit width of a brash ice in the passive loading state and is given by

$$R_p = 0.5\frac{(1+\sin\phi)}{(1-\sin\phi)}(1-n)\left(1-\frac{\rho_i}{\rho_w}\right) \tag{17}$$

where ϕ is the internal friction angle of brash ice, n is the porosity of the brash-ice layer, and ρ_i and ρ_w are densities of ice and water, respectively.

Greisman [394] proposed the following empirical formula:

$$\left(\frac{R}{R_0}\right)\left(\frac{h_0}{h}\right)\left[\frac{L_0}{L}\right]^{1.5} = 1 + 23.4\left[\frac{V}{\sqrt{gL}} - 0.12\right]^{1.5} \tag{18}$$

where $R_0=25$ lb, $h_0=0.3$ ft, and $L_0=14$ ft are arbitrary values selected for the model tested to normalize the resistance force R, brash-ice layer thickness h, and hull length L, respectively.

Kitazawa and Ettema [395] examined the resistance to ship-hull motion through layers of brash ice (ice fragments of linear size ranging from 0.02 m to 2 m). They found that the resistance to hull motion through brash ice may consist of the following components:

(1) bow resistance associated with shearing or compression of the rubble layer
(2) bow resistance due to submergence of brash ice beneath the hull
(3) bow resistance due to the momentum exchange between the hull and the brash ice
(4) parallel-part resistance due to friction between the hull and the brash ice
(5) stern thrust due to ascension of brash ice at the hull's stern (this is a negative drag force attributable to the contact of rising buoyant ice rubble beneath the stern of a hull)
(6) open water resistance

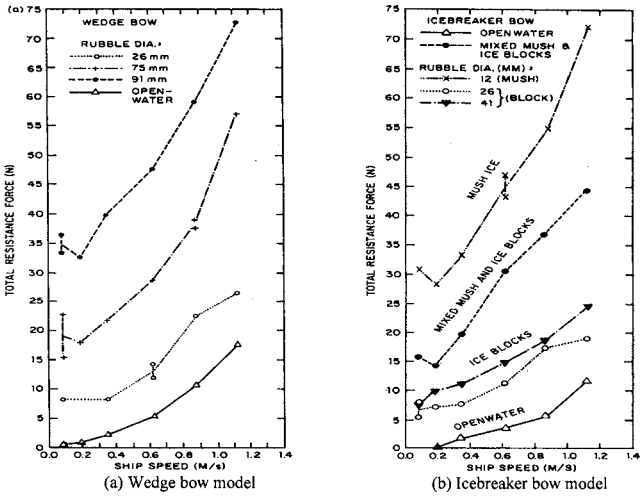

(a) Wedge bow model (b) Icebreaker bow model

Fig. 28 Comparison of total resistance encountered by the (*a*) wedge bow and (*b*) icebreaker bow in rubble comprised of ice blocks, ice mush, and a mixture of ice mush and blocks [396]

The ratio of each component to the total resistance depends on the bow shape, the hull speed, brash-ice characteristics, and channel dimensions. Ettema and Matsuishi [396,397] extended the work of Kitazawa and Ettema [395] and measured the dependence of the total resistance force on ship speed for different sizes of ice rubbles. Figures 28(*a*) and 28(*b*) show this dependence for wedge-bow and icebreaker-bow modes, respectively. It is seen that the total resistance generally increases with the increasing size of ice rubble. Furthermore, the layer comprised of mush ice exerted a greater resistance against the test hull than the layers comprised of discrete ice blocks. Time-history records of ice resistance revealed irregular fluctuations for most cases measured by Ettema et al. [398]. The irregularities were attributed to cyclic adjustments in the hull trim as the ice rubble was submerged and passed beneath the hull. The cyclic adjustments of the trim ice were associated with the unsteady accumulation and the collapse of the ice rubble beneath the bow.

A characteristic feature, reported by Ettema et al. [398], of the ice-rubble displacement by the wedge-bow hull was the collision between individual pieces of ice rubble and the bow, especially for large ice-rubble pieces. The overlap of the processes of shear-zone formation and ice-piece collision led to a fairly irregular time history of resistance for the wedge-bow hull. The overlap of the processes of shear-zone formation and ice-piece collision yields a random time history of resistance for the wedged-bow hull, as shown in Fig. 29. Note that Fig. 29(*a*) shows the force components for ice-rubble diameter $D=91$ mm and hull speed $V=0.62$ m/s, while Fig. 29(*b*) corresponds to $D=26$ mm and $V=0.08$ m/s. It is seen that the mean value of the total resistance is dropped for a small ice rubble and a small hull velocity. Figures 30(*a*) and 30(*b*) show the ice resistance for the icebreaker for two different values of ice-rubble size and hull velocity of $V=0.08$ m/s. It is seen that the ice resistance experienced by the icebreaker exhibits some relatively long-period cycles, which can be attributed to cycle adjustments in hull trim as ice rubble was submerged and passed beneath the hull. The cyclic adjustments of trim were associated with the unsteady accumulation and collapse of ice rubble beneath the bow. This was described earlier by Keinonen [399] as the steady-state "developed condition" of ice ice-rubble accumulation beneath an inclined bow.

It is known that the operation of ice-going vessels depends on the condition of the hull surface. Corrosion increases the roughness of the ship hull, which increases drag and fuel consumption. The hull surface smoothness has been maintained by using coatings and cathodic protection. This problem was addressed by Rennie and Turnbull [400,401] and by Aromaa et al. [402], who utilized controlled and uncontrolled cathodic protection systems for ships' hulls. The cold brackish water is different from ocean water as it has lower salt content, lower conductivity, and higher concentration of dissolved oxygen.

4.3 Interaction With Ship Propulsion System. Navigation in polar waters presents a formidable challenge to ships' propulsion systems as large ice pieces impinging on their propeller blades sometimes result in stresses exceeding the yield strength of the blade material. This can cause damage to propellers and can also spell disaster if a ship becomes disabled in a remote area. To prevent such situations, design practice must be improved and theoretical models of propeller/ice interaction must be validated against experimental data. Several studies have been carried out to estimate load and torques acting on the propeller blades due to ice interaction with the propulsion system. For example, Edwards [403] developed an analytical model for estimating the shaft torque, blade bending moment, and blade turning moment experienced by a propulsion system in ice. The primary variables influencing the level of ice forces, torques, and moments on the propellers were found to be the angle of attack, the maximum depth of cut, the compressive strength of ice, and the pitch angle. Kostilainen [404] discussed the physical modeling of ice transiting ships. The transient behavior of a ship propeller-engine system

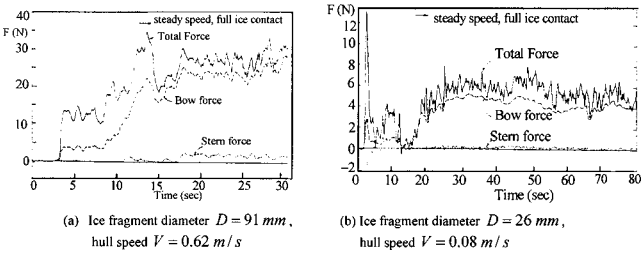

(a) Ice fragment diameter $D=91\,mm$, hull speed $V=0.62\,m/s$ (b) Ice fragment diameter $D=26\,mm$, hull speed $V=0.08\,m/s$

Fig. 29 Time-history records of wedge-bow resistance forces for two different sets of ice fragment size and ship speed [398]

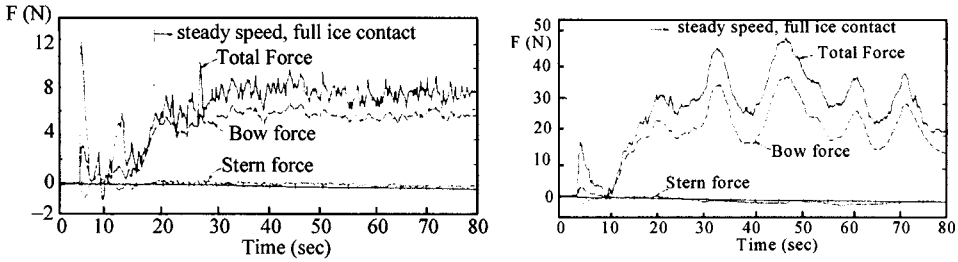

(a) $D=26\,mm$, $V=0.08\,m/s$ (b) $D=12\,mm$, $V=0.08\,m/s$ (mush ice)

Fig. 30 Time-history records of resistance forces of icebreaker bow for two different sets of ice-rubble size and hull velocity [398]

in ice was found to be overlooked in model tests. Kostilainen [404] outlined some methods of modeling the complex ship/ice interaction in maneuvering. Water waves generated by the ships' propeller blades and bow movements interacting with the ice cover were found to produce ice-coupled waves through the ice feature [405].

Browne et al. [406] examined the mechanisms contributing to the loads on both open and ducted propellers in the presence of ice. The model test results were correlated with equivalent full-scale events and were found to be in good agreement. A series of tests on a model of the ice class fixed pitch propeller of the Canadian Coast Guard's R-class icebreakers was conducted in a towing tank [407]. The propeller performance was assessed in both uniform flow and blocked flow behind a nearby simulated ice piece for two blockage configurations and a range of clearances between the block and the propeller blades. Measurements of thrust and torque were made over a range of speeds. The results were used to isolate the separate effects of the extreme wake within which the propeller operates and of proximity of the ice piece.

Morin et al. [408] used fiber optic sensors to measure ice loads at many locations in the propeller blade in order to obtain accurate stress and load distributions. Additional data gathered from the propulsion control system and the ship's navigation equipment was included.

Veitch [409,410] developed a model simulating a marine screw propeller and a submerged ice body. The time simulation predicted the ice contact forces acting on a propeller blade and the motion response of ice. The model included six nonlinear ordinary differential equations for the ice body motion. These equations were solved time stepwise with a numerical integration routine. The propeller was treated as a rigid body with constant rotational and translational velocities. The ice body shape was idealized as spherical. It was found that contact during ice cutting is concentrated near the propeller blade's leading edge. Ice failure on the pressure side (face) of the blade was characterized by an ice chipping process. Veitch [410] indicated several features important to the propeller-ice cutting process, which include the operating conditions of the propeller and the size of the ice body. The propeller-ice contact force was found to depend approximately on the square of the propeller diameter.

Jones et al. [411] discussed results of a joint research project (between the Transport Canada and the Finnish Board of Navigation) dealing with the propeller-ice interaction. The model was used to formulate new machinery regulations for Arctic and Baltic ice class vessels. The model was based on the theoretical analysis and experimental modeling of the physical phenomena involved.

An open water model test was conducted to investigate some issues dealing with the resistance and propulsion, maneuvering, and cavitation performance of a double acting tanker (DAT) [412]. DAT is a ship designed to run astern in heavy ice conditions while remaining hydrodynamically efficient for propulsion in open water conditions. The ship was designed to operate both in ahead and astern conditions for prolonged periods of time. Comprehensive tests of the ship's performance in ice were performed in the ice tank at Masa-Yards Artic Research Centre (MARC). The eight-month model testing and development resulted in a ship with excellent propulsion and maneuvering performance, especially with regard to the high ice class.

5 Vessel Icing and Deterministic Stability

5.1 Vessel Icing. Ice accumulation on ship superstructure[3] components may cause serious problems in reducing ship seakeeping ability and hindering deck operations [413,414]. It results in raising the center of gravity of the vessel and may possibly cause an asymmetry in the ship equilibrium position. As a consequence, the initial static stability of the ship will be reduced. These conditions may result in dangerous operating conditions for a vessel because extreme latitudes are quite often associated with steep waves, severe winds, and possibly floating pieces of ice. Ice accretion presents a serious problem for large ships and floating offshore platforms. This problem becomes even more serious for small vessels. Vessel icing has been known to be the principal cause of the total loss of several vessels. As a result, icing forecasts are an integral part of marine weather forecasts in these low temperature regions [415,416]. The simultaneous loss of two trawlers due to icing [417] motivated researchers to examine and understand vessel icing at a more fundamental level in order to prevent such circumstances from occurring in the future. Subsequent investigations of spray icing models can generally be categorized into SMs, namely, statistical-physical (SPM) and physical-empirical (PEM) models [418]. The SMs are those generally used by forecasters [419], while the physical models are used in more detailed and fundamental studies [420].

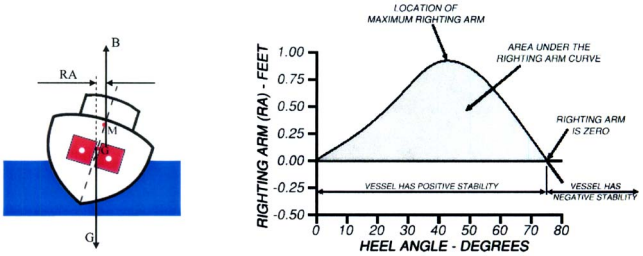

Fig. 31 Dependence of the righting arm on the heel angle [432]

Moreover, U.S. Navy [421] and International Maritime Organization [422] vessel stability codes explicitly consider icing, although they do so in a simplified manner. Icing is not unique to ships, it may also occur on aircrafts [423,424] and electric power lines, where it has been reported to either cause a serious damage or result in a total loss. Much of the theoretical- or physical-based understanding of icing derives from idealized predictions around cylinders applied to electric power lines [425,426]. Vessel icing is known to result from spray, which occurs as the vessel slams into the waves [420]. This spray may then be transported by wind causing an impact on the vessel structure [427–429]. The spray then freezes on the surface of the structure depending on the sea and air temperature, air moisture content, etc. The repetition of this process leads to a significant accumulation of ice on the vessel's superstructure. Moreover, if a vessel heading is not directly into the waves, then an asymmetric icing may occur. This is also associated with a subsequent off-center transverse center of gravity and bias to the vessel [429]. Both of these effects are detrimental to the vessel safe operation.

5.2 Deterministic Stability. Traditional ship stability analysis compares the vessel righting arm curve to a standard or to a steady wind heeling moment [430,431]. With reference to Fig. 31, the righting arm is the horizontal distance between the ship's center of gravity "G" and center of buoyancy "B." Figure 31 also shows the dependence of the righting arm on the heeling angle, and it vanishes at the angle of capsizing [432]. On the other hand, modern analysis methods of ship stability are based on analyzing the vessel's roll motion response either by simulation or by using modern methods of dynamical systems. One method of analyzing nonlinear dynamical systems used by numerous researchers is the analysis of the so-called safe basin [433]. This method consists of numerically integrating a grid of initial conditions in order to determine which initial conditions will lead to bounded motions (safe basin) and which will yield unbounded motions (i.e., capsizing). There are two cases that are generally analyzed, and these are the unbiased and biased cases. The unbiased case involves the

[3]Superstructure refers to any structure built above the main deck of a ship.

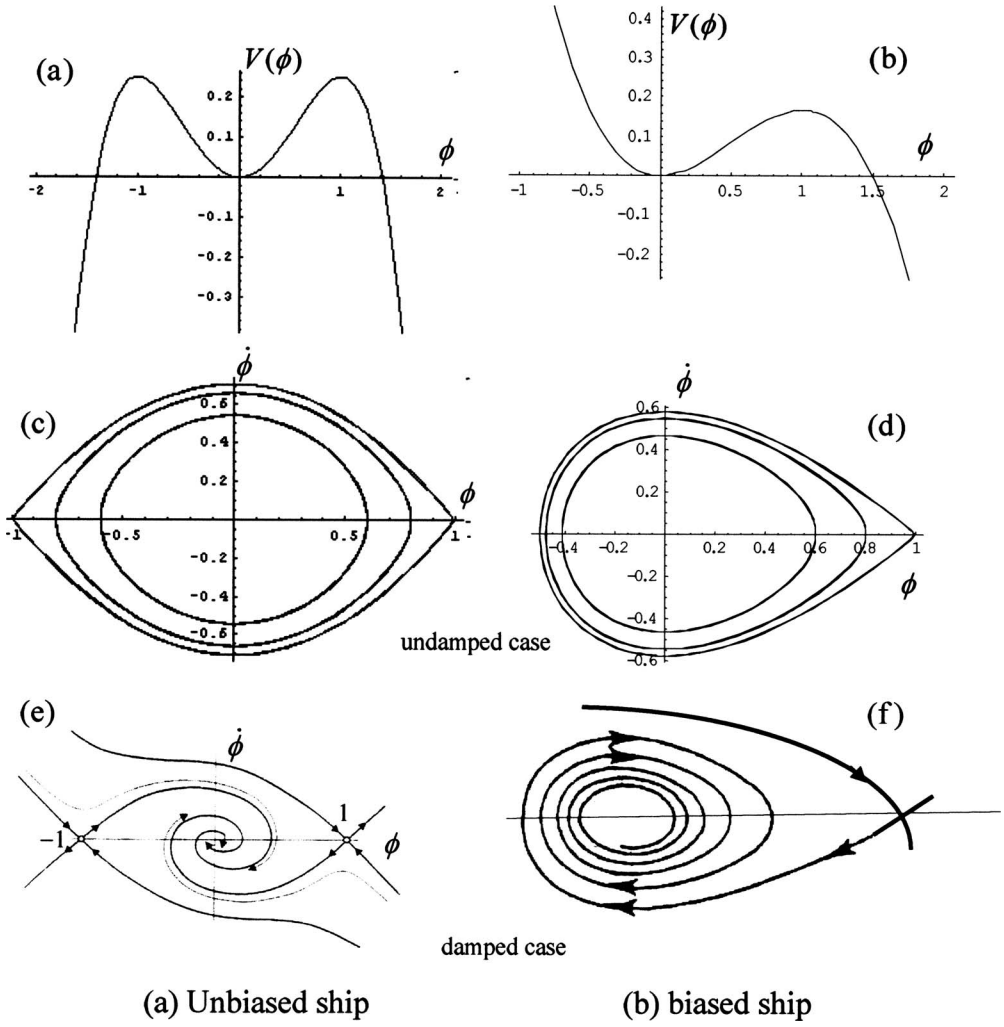

Fig. 32 Potentials and phase portraits of unbiased and biased ships

symmetric ship while the biased case is for an asymmetric ship. The asymmetry may be due to a steady wind moment, cargo shifting, or asymmetric ice accretion. For the case of unbiased ship, the potential energy $V(\phi)$ is two sided, as shown in Fig. 32(a), and may be given by the simple expression $V(\phi)=\frac{1}{2}\phi^2-\frac{1}{4}\phi^4$, where ϕ is the roll angle. For the biased ship, the potential energy may take the form $V(\phi)=\frac{1}{2}\phi^2-\frac{1}{3}\phi^3$ (see Fig. 32(b)). If these potentials are differentiated and used as restoring moments for equations of motion, then the resulting equation of motion becomes a second-order nonlinear differential equation. These cases belong to a class of differential equations referred to as nonhyperbolic (or degenerate). One can also see from Fig. 32 the corresponding undamped phase planes. In both cases, the ship possesses bounded oscillations around the center for a given small initial disturbance. This type of oscillatory motion is depicted by closed curves surrounded by separatrices. The separatrix curves literally separate the bounded oscillatory motions inside from the unbounded rotational motions outside.

The righting arm curve of a ship, known also as the restoring lever, has been represented by an odd-order polynomial up to different degrees [434–437]. Some forms of the restoring moment will be discussed in the next section.

The phase portraits shown in Figs. 32(c) and 32(d) are for the unforced and undamped systems. The inclusion of damping breaks up the homoclinic orbits and the global stable manifolds of the saddle points, which separate the basins of attraction of the point of attraction (the equilibrium position or fixed point). The corresponding orbits are part of a class of differential equations known as hyperbolic, and the corresponding phase portraits are shown in Figs. 32(e) and 32(f).

Once periodic forcing is added to the system, the bounded curves will oscillate periodically in time [435,438]. It should be noted that neglecting the wind bias gives significantly optimistic predictions of the ship safety. However, the simple biased case considered above and by many researchers is only a locally valid approximation. This approximation misses an important region between the safe basin and the capsizing region. This region can only be obtained by considering a more exact approximation to the vessel righting arm curve. This intermediate region has been referred to as the one rotation to the capsize region [439].

The upper bound of the excitation amplitude, beyond which the ship becomes dynamically unstable, is governed by both the damping factor and the excitation frequency. This is reflected by the reduction of the safe basin area with the excitation amplitude. The stability fraction, known in the literature as the normalized safe basin area or safe basin integrity factor (SIF) [440–443], is usually obtained by estimating the ratio of the area of the stable region in the phase plane (area of the safe basin) to the total area encompassed by the homoclinic orbit, which is defined to be the safe basin in the absence of excitation. The stability fraction is strongly dependent on the excitation amplitude. For excitation amplitudes less than a critical value, governed by the excitation frequency, there is no erosion at all for the safe basin. Above this

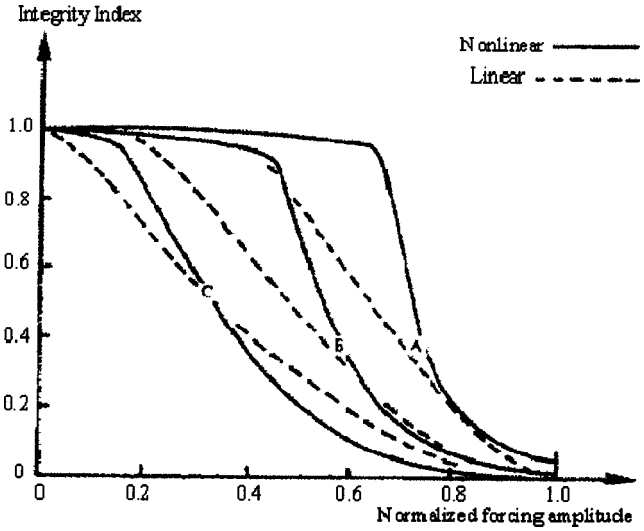

Fig. 33 Integrity curves at different values of damping levels and an equivalent linear system at excitation frequency ω =0.85. Curves A are for β=0.1, B are for β=0.05, and C for β =0.01 [444].

critical value of the excitation amplitude, the area of the safe basin shrinks and the stability fraction drops. As the excitation frequency changes, so does the critical excitation amplitude.

Figure 33 shows the dependence of the integrity index on the excitation amplitude level for the nonlinear oscillator [444]

$$\ddot{x} + \beta\dot{x} + x - x^2 = F \sin \omega t \tag{19}$$

It is seen that the integrity index drops faster for a damping factor, as reflected by curve C. The critical excitation amplitude below which the safe basin remains intact can also be predicted by an analytical method known as the Melnikov method [438,445,446]. There have been two approaches for studying the safe basin. One method involves simulating a grid of initial conditions in order to determine which response remains bounded and which does not. The other approach directly calculates the basin boundary, which is the curve separating the regions of initial conditions with bounded motions from those with unbounded motions [447].

Calculating the basin boundaries is a difficult numerical problem for the damped and forced system. The safe basin boundaries for the damped and forced system are obtained by tracing the solution paths along the manifold's surface as the excitation evolves with time [448]. However, for the unforced system, the manifolds are locally tangent to the eigenvectors of the fixed points, which are obtained by expressing the second-order differential equation of motion as a system of two first-order differential equations. The fixed points are the roots of the nonlinear righting arm curve function. The system of equations is linearized about the fixed point of interest, and the corresponding eigenstructure is obtained.

The motion close to the fixed point is extremely slow. Therefore, an approximation to the unstable manifolds is obtained by moving away from the fixed point a very small distance along the unstable linear eigenvector and then integrating in time from that initial condition. The stable manifold can be approximated in a similar manner, except that one has to integrate backward in time. Once periodic forcing is added to the system, these manifolds, like the steady-state periodic solutions, oscillate periodically with time and an extended phase space with time emerges.

To demonstrate, it is assumed that there is a 25% reduction in the vessel static stability due to icing. The initial stability or metacentric height (i.e., gain margin (GM)) is just the initial slope of the righting arm curve $GZ(\phi)$. Figure 34 is a plot of the vessel static roll restoring moment arm curve as a function of the roll angle; the slope at the origin is the GM. As can be surmised from the figure, this reduction in the initial stability also affects the range of stability by decreasing the angle of vanishing stability or capsizing angle, which is the angle at which the righting arm becomes zero. The change in the righting arm curve can be found using the naval architect's formula, $GZ_m(\phi) = GZ_0(\phi) - G_0G_m \sin(\phi)$, where GZ_0 is the initial righting arm curve, GZ_m is the modified righting arm curve, and G_0G_m is the distance between the initial and modified center of gravity. The reduction in the initial stability significantly affects the vessel roll response magnification curves.

In the previous paragraphs, simplified differential equations were analyzed, which captured the qualitative behavior of the nonlinear system but did not accurately describe an actual vessel.

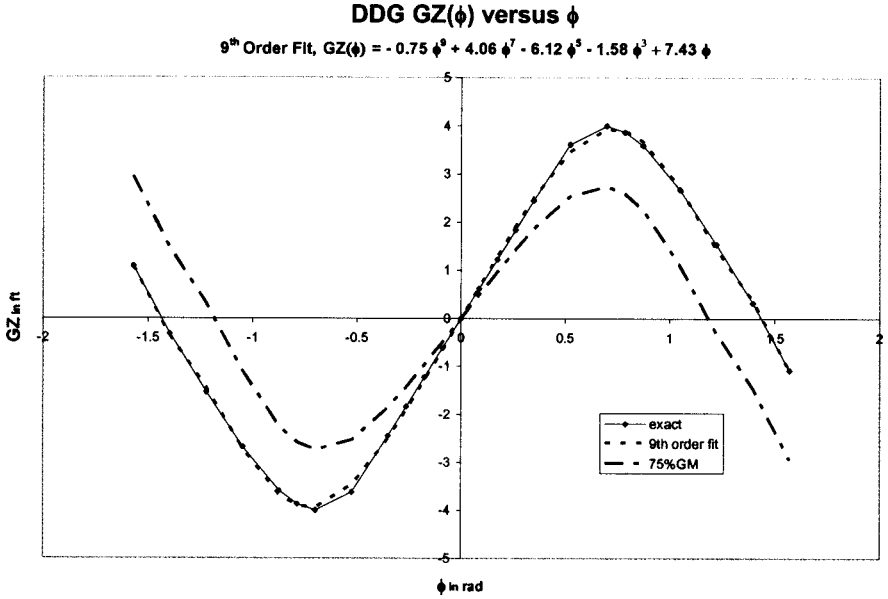

Fig. 34 Righting arm curve: exact versus ninth order fit and reduced righting arm at 100% GM versus 75% GM

The single degree of freedom (uncoupled) roll equation of motion with physical parameters describing an actual vessel may be written in the form [447]

$$[I_{44} + A_{44}(\omega)]\ddot{\phi} + B_{44}(\omega)\dot{\phi} + B_{44q}\dot{\phi}|\dot{\phi}| + \Delta GZ(\phi) = F_4(t) \tag{20}$$

where I_{44} represents the roll moment of inertia, $A_{44}(\omega)$ is the roll added moment of inertia, $B_{44}(\omega)$ is the linear radiated wave damping, ω is the forcing frequency, which is either the wave frequency or the encounter frequency, (both $A_{44}(\omega)$ and $B_{44}(\omega)$ are functions of frequency since they are related to the waves radiated away from the body as the vessel oscillates in response to the incident waves), B_{44q} is the nonlinear viscous roll damping, GZ is the vessel's righting arm curve, Δ is the vessel weight or displacement, and F_4 is the roll wave exciting moment. The linear wave exciting force due to a single frequency harmonic wave can be expressed as $F_4(t)=F_4\cos(\omega t+\gamma_4)$, where F_4 is the amplitude and γ_4 is the phase angle of the wave exciting moment.

Equation (20) is the standard uncoupled single degree of freedom roll equation of motion with nonlinear damping and roll restoring moment. This equation was analyzed using various steady-state and transient methods. The methods used to analyze Eq. (19) consist of path following or continuation methods [448,449] and tracing out the stable (safe-basin boundaries) and unstable manifolds of the periodically forced system in the Poincarè map [448,450]. The path following or continuation method requires an initial starting value, which can be obtained by simply integrating the equation of motion until a steady state solution is obtained. Using this solution as a starting value, the forcing frequency—taken as the bifurcation parameter—is varied, and the curve of stable and unstable harmonic solutions is obtained. Tracing the safe basin boundaries of the periodically forced system is done in a manner similar to what was done with the unforced system, except that now the periodic forcing at a fixed time phase is added to the system of first-order equations. The first step to tracing out the manifolds is to obtain the unstable periodic saddle-type solution at a fixed time phase. Once the unstable periodic solution is obtained, the characteristic multipliers are determined from the Jacobian matrix augmented with the derivative of the periodic forcing with respect to all the state variables. These multipliers are then reinserted back into the augmented Jacobian matrix and eigenvectors are obtained. The stable and unstable manifolds are obtained by moving away from the saddle along these eigenvectors in a manner similar to what was done with the unforced system.

Figures 35(*a*) and 35(*b*) show two different plots of amplitude frequency response curves taken for different values of wave heights and two different values of static stability arms [451]. It is seen that the peaks of the response curves increase with the reduced initial stability. This is particularly dangerous because as the response curve peaks increase, the static angle of vanishing stability will bring the response curve peak closer to the capsizing angle. A more complete picture of the vessel's response is obtained by considering both the steady-state magnification curves and the safe basins as affected by the excitation amplitude and frequency [452].

Falzarano et al. [451] investigated the effects of damping on the safe basin boundaries. This is an alternative approach to the one used by Thompson [433], who investigated the safe basin by integrating a grid of initial conditions. This reduction in initial stability will also affect the vessel's transient response as depicted by the reduction in the size of the safe basin of attraction. Other physical parameters will also affect the safe basin, such as damping. The safe basin calculated herein is at a particular sampling phase relative to the forcing (stroboscopic sampling once per period of the forcing). For example, Figs. 36(*a*) and 36(*b*) show the stable (solid curve) and unstable manifolds associated with the fixed saddle points (unstable saddle-type periodic orbit) located at the angle of vanishing stability or capsizing angle. The stable manifolds are the boundary between the safe basin and the capsizing region. One can see in Figs. 36(*a*) and 36(*b*) how the safe basin area decreases for two different values of damping at the same wave forcing frequency, which is close to the natural frequency. For steeper waves and for a frequency closer to the response peak, the response is even more dramatic.

6 Random Excitation of Ships

6.1 Stochastic Stability Due to Random Waves. As stated earlier, ice loads acting on ocean systems are random in nature and have nonsmooth characteristics when they are of impact type. In full-scale experiments, measurements of ice local and global loads revealed randomness in the ice forces and pressures [7,453]. Thus, one must deal with probabilistic approaches when studying ships' stochastic stability, response, and reliability. The study of ship dynamics in following sea waves was first reported by Froude [454], who observed that ships have undesirable roll characteristics when the frequency of small free oscillations in pitch is twice the frequency of a small free oscillation in roll. It was Pauling and Rosenberg [455] who formulated the analytical modeling of the coupled roll-pitch motion. This coupled motion is described by a set of nonlinear differential equations. The probabilistic theory of ship dynamics was documented by Price and Bishop [456] and Lloyd [457]. If the nonlinear effect of roll is neglected, the pitch equation of motion is reduced to a linear differential equation, which is free from roll motion terms. When the pitch equation is solved, its response appears as a coefficient to the restoring moment of the roll motion, and the roll equation of motion is reduced to the Mathieu equation

$$\ddot{\phi} + 2\bar{\zeta}\omega_n\dot{\phi} + \omega_n^2[1 + \varepsilon\Theta(t)]\phi = \varepsilon M(t) \tag{21}$$

where ϕ is the roll angle, $\Theta(t)$ represents the pitch angle, which is assumed to be a random stationary process, $M(t)$ represents the wave random excitation, $\bar{\zeta}$ is a linear damping factor, ω_n is the natural frequency of the ship roll oscillation, and ε is a small parameter.

The analysis of the ship roll stability in an irregular sea was addressed by some investigators (see, e.g., Refs. [458–460]). The stochastic stability and response of the ship roll motion in random seas have been predicted analytically using the stochastic averaging method [461–464]. Roberts [462] analyzed Eq. (20) for the stochastic stability and statistical response moments using the stochastic averaging method. The sample stability condition of the roll angle amplitude was obtained in the form

$$\bar{\zeta} > \varepsilon^2\omega_n S_\Theta(2\omega_n)/8 \tag{22}$$

where $S_\Theta(2\omega_n)$ is the power spectral density of the random pitch process $\Theta(t)$ at frequency $2\omega_n$. Condition (22) reveals that the onset of instability is not affected by the forcing excitation $M(t)$. If this excitation is removed, the probability density function of the response degenerates into a delta function. The stability conditions of the first moment of the response amplitude is

$$\bar{\zeta} > \frac{3}{16}\varepsilon^2\omega_n S_\Theta(2\omega_n) \tag{23a}$$

The stability condition of the second moment is

$$\bar{\zeta} > \frac{1}{4}\varepsilon^2\omega_n S_\Theta(2\omega_n) \tag{23b}$$

These stability conditions apply only for the case of random sea waves in the absence of ice effects.

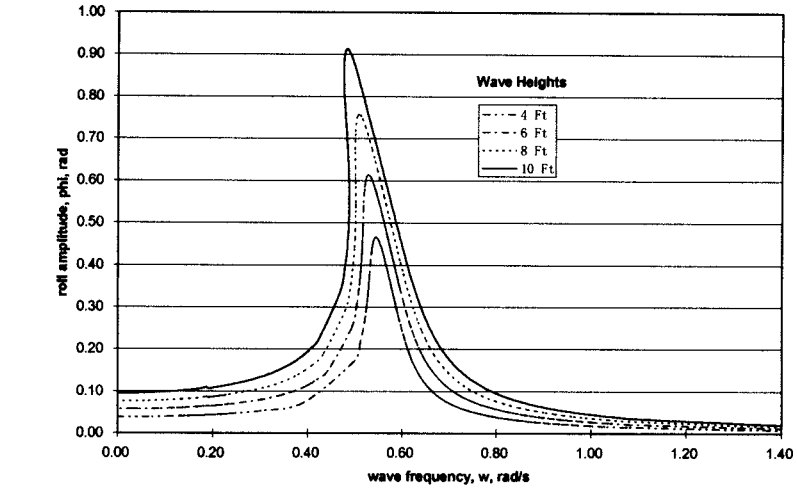

(a) 100% GM

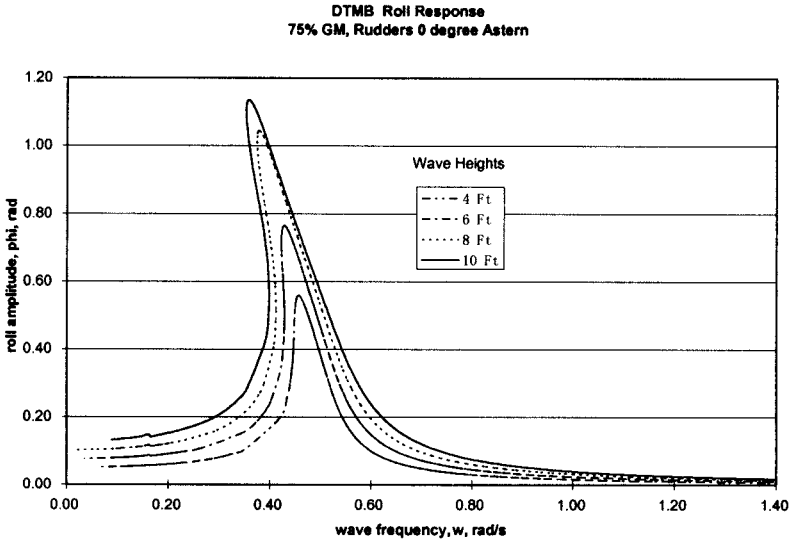

(b) 75% GM

Fig. 35 Roll angle amplitude-frequency response curves for DDG-51 for (*a*) 100%GM and (*b*) 75% GM

6.2 Modeling of Ice Impact. In some cases, ice loads are of impact type and have been assumed as a Poisson arrival process of loading events. A Poisson delta correlated process $M(t)$ is defined as

$$M(t) = \sum_{k=1}^{N(t)} P_k \delta(t - t_k) \tag{24}$$

where $N(t)$ is a homogeneous counting Poisson process, giving the total number of spikes $\delta(t-t_k)$ (Poisson distributed) in the interval $[0,t]$. The P_k terms are identically distributed random variables, which are mutually independent and unaffected by the time instant t_k. The correlations of $M(t)$ are expressed in the form

$$R_M^{(r)}(t_1, t_2, \ldots, t_r) = \lambda E[P^r]\delta(t_2 - t_1)\delta(t_3 - t_1)\cdots\delta(t_r - t_1) \tag{25}$$

where $E[\cdot]$ denotes the expectation and $\lambda > 0$ is the mean arrival rate of impulses in unit time. When λ approaches infinity and, at the same time, $\lambda E[P^2]$ keeps a constant value, the Poisson white noise approaches the normal white noise. The treatment of dynamical systems under Poisson random processes has been considered in Refs. [465–472].

Ship hull–ice loading has been measured either with actual ships or small-scale model basin tests, or controlled field tests [473]. The impact of a ship hull with an ice cusp was experimentally simulated by Gagnon et al. [474]. The prediction of global ice loads on offshore structures was considered by Bjerkås [376], who showed how the effective structure width is affected by changes in the failure mode of the ice sheet to a vertical structure. It was found that a simultaneous failure took place during ductile crushing and static loading with the drift speed/ice thickness ratio from 0 s^{-1} to 0.063 s^{-1}.

The continuous indentation of a ship or offshore structure into an ice sheet was examined by Karr et al. [475,476] and Troesch et al. [477]. The impacting ship or offshore structure was represented by a mass-spring-dashpot system having a constant velocity relative to the ice sheet. The nonlinear dynamic response was due to intermittent ice breakage and intermittent contact of the structure with the ice. Periodic motions were found, and the peri-

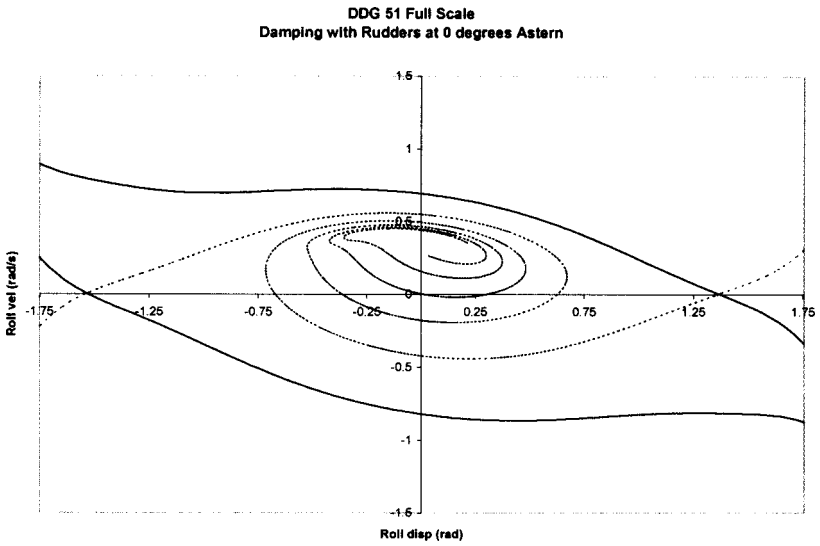

(a) 100% GM

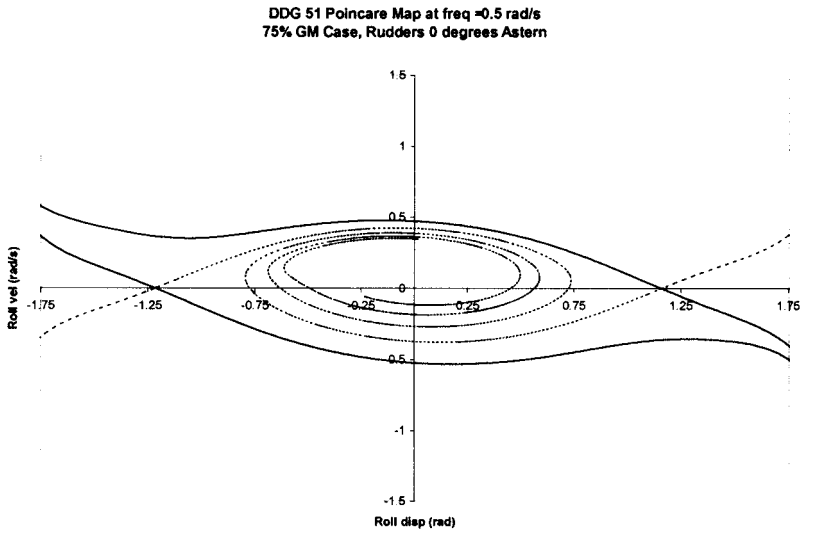

(b) 75% GM

Fig. 36 Safe basin of attraction for DDG-51 with (*a*) 100% GM and (*b*) 75% GM. (—, stable; - - - -, unstable)

odicity for a particular system was found to be dependent on initial conditions. For a representative system, a Poincarè map was presented showing the fixed points. A description of some of the effects of random variations in system parameters was also discussed.

6.3 Ship Roll Dynamics in Random Ocean Waves

6.3.1 Analytical Modeling. The above results did not take into account the nonlinear effects of drag and restoring moments. The nonlinear damping moment is proportional to the product of the roll velocity times its absolute value and acts in a direction opposite to the velocity. This is usually represented by the expression $a\dot{\phi}|\dot{\phi}|$, where a is a constant determined experimentally. Usually, the restoring moment is nonlinearly dependent on the roll angle. The nonlinear equation of the ship motion in random beam sea involves a nonhomogeneous external moment $M(t)$, in addition to parametric noise $\xi(t)$, and may be written in the form

$$\ddot{\phi} + 2\tilde{\zeta}\omega_n\dot{\phi} + a\dot{\phi}|\dot{\phi}| + \bar{\Gamma}(\phi) + \xi(t)\varphi = M(t) \tag{26}$$

where $\bar{\Gamma}(\phi)$ is the restoring moment.

Different representations of the restoring moment have been proposed in the literature. For example, Roberts [461,462] and Falzarano and Zhang [478] represented $\bar{\Gamma}(\phi)$ by the polynomial

$$\bar{\Gamma}(\phi) = \omega_n^2\phi(1 + e_2\phi^2 + e_4\phi^4 + \cdots) \tag{27a}$$

Moshchuk et al. [491] proposed the following representation:

$$\bar{\Gamma}(\phi) = \omega_n^2 \sin(\pi\phi/\phi_s) + \tilde{\gamma}(\pi\phi/\phi_s) \tag{27b}$$

where ϕ_s is the capsizing angle and the function $\tilde{\gamma}(\pi\phi/\phi_s)$ accounts for the difference between the exact function $\bar{\Gamma}(\phi)$ and $\omega_n^2 \sin(\pi\phi/\phi_s)$. Huang et al. [464] assumed a fifth-order polynomial restoring moment, while Senjanović et al. [479] proposed the following seventh-order polynomial of the restoring moment:

$$\bar{\Gamma}(\phi) = k_1\phi + k_3\phi^3 + k_5\phi^5 + k_7\phi^7 \tag{27c}$$

where $k_1 > 0$, $k_3 < 0$, $k_5 > 0$, and $k_7 < 0$ for a damaged vessel, but $k_7 = 0$ for an intact vessel.

The critical roll angle ϕ_c at which the restoring moment vanishes, i.e., $\bar{\Gamma}(\phi)$, defines the condition of the capsizing ship. Most of the research work deals with the first exit time at which this angle is reached.

The nonlinear damping expression has received special treatment in the literature, and approximate equivalent expressions have been proposed. For example, Spanos and Chen [480] have replaced it by an equivalent viscous damping. Dalzell [481] and Bruce [482] replaced it by an equivalent polynomial having the form

$$\dot{\phi}|\dot{\phi}| = \sum_{n=1}^{\infty} a_{2n+1}\dot{\phi}^{2n+1} \quad n = 1,2,\ldots \tag{28}$$

where the coefficients a_i are determined either by a least squares fitting or by comparison with a certain probability distribution. Jiang et al. [483] considered three types of damping moments. These are the usual effects that are treated as linear and quadratic in the roll velocity, plus a frequency-dependent effect that captures the dissipation of energy caused by the generation of waves radiated away from the rolling vessel.

Senjanović et al. [484] used the wave energy spectrum to determine random roll excitation. The probability of ship survival was obtained in terms of the sea state, vessel speed, and heading angle. The probability of survival was determined by estimating the ratio between the areas of the safe basin with and without wave excitation. Arnold et al. [435] presented the results of a case study of ship roll dynamics described by the differential equation

$$\ddot{\phi} + \phi - \phi^3 + \dot{\phi}|\dot{\phi}| + \delta\phi \sin 0.8t + \varepsilon\xi(t) = 0 \tag{29}$$

For a small random noise, $\varepsilon = 0.01$, Arnold et al. [435] found a similar bifurcation as in the case of purely periodic forcing, i.e., $\varepsilon = 0$. However, when the noise level was increased to $\varepsilon = 0.05$, the random attractor appeared as a single point for all values of δ for which it exists; i.e., there was no bifurcations which "announce" capsizing. The capsizing was also declared by the termination of the top Lyapunov exponent. Lin and Yim [445] adopted the generalized Melnikov method to provide an upper bound on the domain of the potential chaotic roll motion in the presence of periodic excitation with random noise. They found that the presence of the random noise enlarges the boundary of the chaotic domains and bridges coexisting attracting basins in the local regimes. Probabilistic methods have been employed in combination with Melnikov function approaches [483,485,486]. Senjanović et al. [484] studied the safe basin of ships rolling in rough sea. The rough sea was represented as a sum of harmonic waves with a given wave energy spectrum.

The probabilistic characteristics of irregular rolling in the regime of parametric resonance were studied in Refs. [487–489]. Leavdou and Palazzi [490] evaluated the operational risk of parametric roll oscillations using numerical simulations with the large amplitude motions program (LAMB). It was shown that in order to obtain reliable results, one realization is not enough and that distribution of the parametric roll response might be different from Gaussian.

In the absence of parametric excitation, the ship roll equation of motion may be written in the form [491]

$$\ddot{\phi} + 2\tilde{\zeta}\omega_n\dot{\phi} + a\dot{\phi}|\dot{\phi}| + \omega_n^2 \sin(\pi\phi/\phi_s) + \tilde{\gamma}(\pi\phi/\phi_s) = M(t) \tag{30}$$

Introducing the nondimensional parameters $\tau = \omega_n t\sqrt{\pi/\phi_s}$, $q = \pi\phi/\phi_s$, $2\tilde{\zeta}\sqrt{\phi_s/\pi} = \varepsilon\zeta$, $a\pi/\phi_s = \varepsilon\eta$, $\tilde{\gamma}(q)/\omega_n^2 = \varepsilon\gamma(q)$, and $M(t)/\omega_n^2 = \sqrt{\varepsilon}W(\tau) + \varepsilon\bar{m}$, $0 < \varepsilon \ll 1$, Eq. (30) can be written in the state vector form,

$$q' = p \quad p' = -\sin q - \varepsilon\zeta p - \varepsilon\eta p|p| + \varepsilon\gamma(q) + \sqrt{\varepsilon}W(\tau) + \varepsilon\bar{m} \tag{31}$$

$W(\tau)$ is a white noise of intensity ν. The unperturbed and perturbed characteristics of Eqs. (31) are discussed in the next sections.

6.3.2 Unperturbed Analysis. If ε is set to zero, Eqs. (31) are reduced to the well-known nonlinear equations of the free oscillation of a simple pendulum,

$$q' = p \quad p' = -\sin q \tag{32}$$

These equations possess the Hamiltonian

$$H = \frac{p^2}{2} + 2\sin^2(q/2) \tag{33a}$$

$$q'^2 = 2[H - + \sin^2(q/2)] \tag{33b}$$

Each level of the energy H corresponds to a periodic closed orbit in the phase space $\{q,p\}$. Level $H=2$ corresponds to the unstable equilibrium position $q = \pm\pi$ and is characterized by two different homoclinic orbits. Periodic motion is only restricted in the domain $D = \{(q,p)|H \leq H_c\}$, where $H_c = 2 - \tilde{h}$ ($\tilde{h} > 0$ is sufficiently small) is the critical energy level above which capsizing takes place and the trajectories will be structurally unstable. The general solution of Eqs. (33) when $H < 2$ can be obtained in the form

$$\tau = \pm \int_{q_0}^{q} \frac{dq}{2\sqrt{k^2 - \sin^2(q/2)}} \tag{34}$$

where $k = \sqrt{H/2}$ and q_0 is the initial value of the angle q. For $k^2 < 1$, the angle q can take any value within a range governed by the condition $k^2 - \sin^2(q/2) = 0$. In this case, q is given by the two roots $q_1 = -2\sin^{-1}k$ and $q_2 = 2\sin^{-1}k$. Accordingly, the angle q fluctuates between q_1 and q_2, and the corresponding period of oscillation is

$$T = \pm \int_{q_1}^{q_2} \frac{dq}{\sqrt{k^2 - \sin^2(q/2)}} \tag{35}$$

The general solution of Eqs. (32) can be expressed in terms of elliptic functions using the following transformation:

$$\sin(q/2) = k\sin\psi \tag{36a}$$

$$p = 2k\cos\psi \tag{36b}$$

where $\sin\psi = \pm\sqrt{2H - p^2}/\sqrt{2H}$. Differentiating Eq. (36*a*) with respect to τ and substituting into Eq. (33*b*) gives

$$\psi'^2 = 1 - k^2\sin^2\psi \tag{37}$$

The solution of this equation takes the form

$$\tau = \pm \int_0^{\psi} \frac{d\bar{\psi}}{\sqrt{1 - k^2 \sin^2 \bar{\psi}}} = F(\psi, k) \tag{38}$$

where $F(\psi,k)$ is known as the incomplete elliptic integral of the first kind. Solution (38) assumes that at $t=0$, $\psi=0$. The upper limit ψ is referred to as the amplitude of the function $F(\psi,k)$ and is written as $\psi=am\tau$. Relations (36) can be written in terms of elliptic functions as

$$p = 2k\cos(am\tau) = 2kcn\tau \quad q = 2\sin^{-1}(ksn\tau) \tag{39}$$

where $sn\tau$ and $cn\tau$ are the Jacobian elliptic functions, and k is the modulus.

6.3.3 First-Passage Problem. Reliability of ship operations under Gaussian or non-Gaussian random sea waves deals with the probability that the ship will not capsize. One may estimate the ship reliability in terms of the probabilistic characteristics of the time at which the roll motion first exits from the safe domain. When ship capsizing is defined by the first exit of response from a safe domain of operation, the reliability is referred to as a first-passage problem. For ships whose response is described by a Markov process, the mean value of the exit time is usually governed by a partial differential equation known as the Pontryagin–Vitt (PV) equation [492].

The first-passage problem of ship's nonlinear roll oscillations in random sea waves has been considered by Roberts [461,462], Cai and Lin [493], Cai et al. [494], and Moshchuk et al. [491,495]. Roberts [461,462] developed an approximate theory based on a combination of averaging techniques and the theory of Markov processes. His analysis resulted in a simple expression for the distribution of the ship roll angle. Cai et al. [493] adopted the same modeling and introduced a parametric excitation term. They used the modified version of quasiconservative averaging. Moshchuk et al. [491] determined the mean exit time of the perturbed ship motion by solving the Pontryagin's partial differential equation using the method of asymptotic expansion. It was found that the mean exit time is extremely large for any excitation intensity less than a critical value above which it experiences exponential decay.

The perturbed equation of motion Eq. (30) of the ship, $\varepsilon \neq 0$, may be written in the standard form of the Itô stochastic differential equation

$$d\mathbf{Z}(\tau) = \mathbf{f}(\mathbf{Z},\tau)d\tau + \mathbf{b}(\mathbf{Z},\tau)d\mathbf{B}(\tau) \quad \mathbf{Z} = \{Z_1 \cdots Z_n\}^T \quad \mathbf{Z}(\tau=0) = \mathbf{Z}_0 \tag{40}$$

where

$$\mathbf{Z}(\tau) = \begin{Bmatrix} q(\tau) \\ p(\tau) \end{Bmatrix} \quad \mathbf{B}(\tau)$$

are vectors of the Brownian motion. The Pontryagin equation that describes the expected value of the exit time from region D is [491]

$$\mathbf{f}(\mathbf{Z},\tau)\frac{\partial U(\mathbf{Z})}{\partial \mathbf{Z}} + \frac{1}{2}\mathrm{Tr}\left\{\frac{\partial}{\partial \mathbf{Z}}\frac{\partial^T U(\mathbf{Z})}{\partial \mathbf{Z}}[\mathbf{b}(\mathbf{Z},\tau)\nu\mathbf{b}^T(\mathbf{Z},\tau)]\right\} \quad U(\mathbf{Z})|_{\Gamma} = 0 \tag{41}$$

where $\Gamma=\partial D$ is the boundary of region D. The boundary condition $U(\mathbf{Z})|_{\Gamma}=0$ implies that the expected values of the exit time starting from Γ is zero. The Pontryagin equation of system (30) takes the form

$$LU(\mathbf{Z}) = p\frac{\partial U}{\partial q} - \sin q\frac{\partial U}{\partial p} + \varepsilon\left\{[-\zeta p - \eta p|p| + \gamma(q) + \bar{m}]\frac{\partial U}{\partial p} + \frac{\nu}{2}\frac{\partial^2 U}{\partial p^2}\right\} = -1 \tag{42}$$

where L is the generator of the Itô process, which governs many response functions such as the expected value of exit time, $U(\mathbf{Z})$, from region D. This equation is subject to the boundary conditions,

$$U|_{H(q,p)=H_c} = 0 \quad |U(0,0)| < \infty \tag{43}$$

Note that if the nonlinear conservative system is subjected to a random excitation with zero mean, i.e., by setting $\zeta=\eta=\bar{m}=0$, then Eq. (42) will have an exact solution given by the expression

$$U(q,p) = \frac{2}{\varepsilon\nu}[H_c - H(q,p)] \tag{44}$$

The corresponding generator L can be decomposed into two operators, i.e.,

$$L = L_1 + \varepsilon L_2 \tag{45}$$

where the first operator, L_1, represents derivative in the direction of motion of the unperturbed system,

$$L_1 = p\frac{\partial}{\partial q} - \sin q\frac{\partial}{\partial p} \tag{46}$$

The second operator, L_2, is due to perturbations and is defined as follows:

$$L_2 = [-\zeta p - \eta p|p| + \gamma(q) + \bar{m}]\frac{\partial}{\partial p} + \frac{\nu}{2}\frac{\partial^2}{\partial p^2} \tag{47}$$

The solution of Eq. (42) for the exit time U is not a simple task. For the one-dimensional case, the Pontryagin equation has an exact solution given by Feller [496]. For two-dimensional problems of slightly perturbed conservative systems, the averaging method of Khasminskii [497,498] reduces the problem to the one-dimensional case. Khasminskii's theorem has been widely used for ship roll dynamics by Roberts [461,462] and for other applications [493,499]. The method of asymptotic expansion developed by Khasminskii [500] has the advantage over the averaging method because the first-order expansion leads to a solution identical to the one obtained by the averaging method. Furthermore, higher-order terms in the asymptotic expansion provide improved accuracy especially for the contribution of all nonlinearities that both the first-order asymptotic expansion and the averaging method failed to include.

The essence of the asymptotic expansion technique is briefly outlined; however, for a detailed account, the reader should refer to Khasminskii [500] and Moshchuk et al. [491,495]. The solution of the partial differential equation (Eq. (42)) can be split into two functions

$$U(q,p) \approx U_n(q,p) + G_n(q,p) \tag{48}$$

This representation implies that the mean exit time U consists of two parts. The first $U_n(q,p)$ accounts for the averaged value of time taken by the trajectory in domain D, while the second $G_n(q,p)$ stands for the influence of the boundary and is thus referred to as the boundary-layer solution. The function $U_n(q,p)$ should satisfy the equation $LU_n(q,p)=-1$ with possibly higher-degree of accuracy, while the function $G_n(q,p)$ should satisfy the homogeneous equation $LG_n(q,p)=0$ and compensate for the residual in the boundary condition $U|_{\Gamma}=0$. Basically, the expected exit time is governed by the Pontryagin equation $LU_n(q,p)=-1$. However, this equation will not satisfy the boundary condition by itself alone unless one introduces a function that will take into

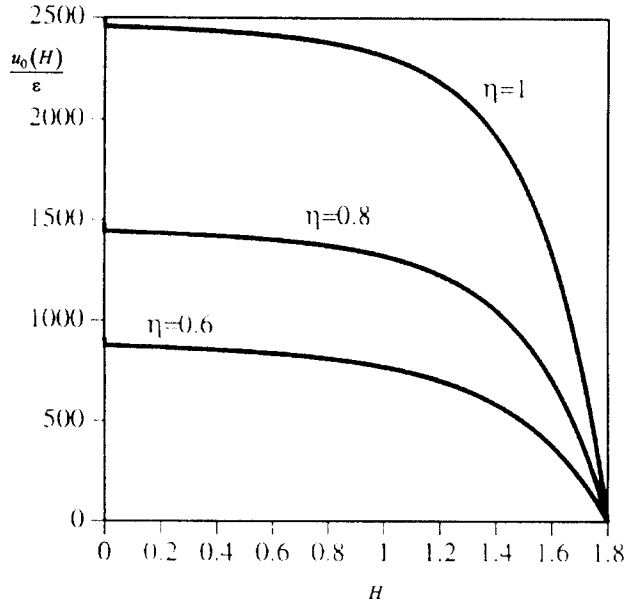

Fig. 37 Dependence of the mean exit time on the initial energy H for different values of the nonlinear damping coefficient η [491]

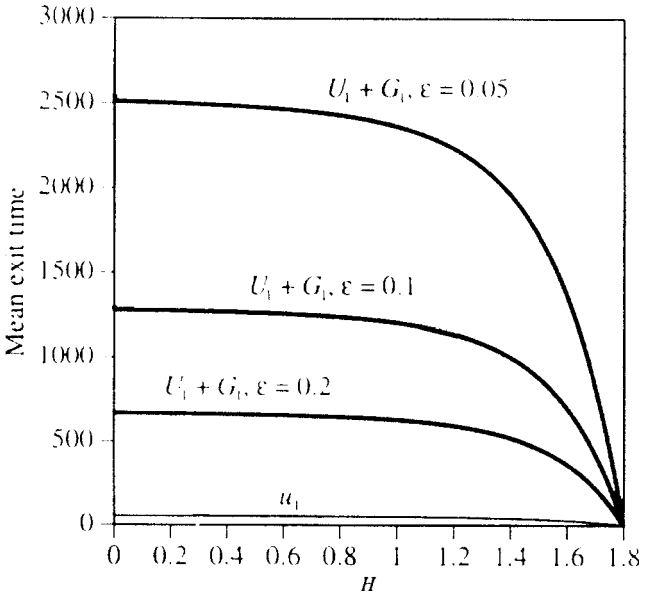

Fig. 38 Dependence of the mean exit time on the initial energy level for different values of ε, $\zeta=\eta=\nu=1$, $\bar{m}=0.5$, $\bar{\gamma}=0.15$ [495]

account the effect of the boundary condition. If the two equations $LG_n(q,p)=0$ and $LU_n(q,p)=-1$ are added, one gets the equation $L(U_n+G_n)=-1$. In this case, one needs to match the boundary condition by choosing an appropriate function G_n.

The first-passage problem of ship capsizing was treated within the framework of the first-order approximation of the Pontryagin equation

$$LU_n(q,p) = L\left(\frac{u_0}{\varepsilon} + u_1 + \varepsilon u_2 + \cdots\right) = -1 \tag{49}$$

The solution of Eq. (49) for system (31) was obtained by Moshchuk et al. [491]. Figure 37 shows the dependence of the mean exit time $u_0(H)/\varepsilon$ on the initial level H for different values of the nonlinear hydrodynamic drag coefficient, $\eta=0.6, 0.8, 1.0$, and under a constant excitation level $\nu=1$. The effect of η is seen to increase the mean exit time for a given energy level. It is also seen that the mean exit time remains almost constant for a wide range of initial energy level up to $H=1.4$ and then experiences a steep drop until it reaches zero at $H=1.8$, which was taken as the critical value. Note that the value $H=2.0$ is the exact critical value. However, it was avoided as it would result in singularity in higher-order approximation [495]. The influence of the excitation level ν on the mean exit time was found to have an inverse effect.

A second-order approximation was considered by Moshchuk et al. [495] including the contribution of the boundary layer, which compensates for the residual in the boundary condition at the barrier. Figure 38 shows the contribution of the second-order approximation, together with the boundary-layer effect. It is seen that the first-order approximation is more conservative and leads to a smaller mean exit time than the second-order solution. As ε increases, the mean exit time decreases. The effects of the mean value of excitation, $\bar{m}$, and the amplitude of the additional nonlinear restoring moment, $\gamma(q)$, are found to have similar effects in reducing the mean exit time. One may notice that the critical value of the ship energy level at which capsizing takes place is taken to be less than $H=2$, which corresponds to the homoclinic orbit of the unperturbed system. For $H=2$, the first-order approximation gives similar results with resolvable singularities. However, for the second-order approximation, the value of the critical energy level must be less than 2 to avoid singularity.

7 Ship Controls in Icy Waters

7.1 Challenges in Controlling Ship Motions. The dynamics of marine vessels are highly nonlinear and strongly influenced by unpredictable environmental disturbances stemming from severe winds, random sea waves, and currents. This problem is further complicated when ships are required to operate under severe cold weather conditions. This is because ice-infested waters will expose ships to considerable and unpredictable ice forces and impact loads. In addition, the ice accretion on the exposed ship surfaces has a tendency to significantly vary the numerical values of the ship parameters, thus inducing unstructured uncertainties in the system in addition to all external disturbances that were mentioned earlier.

Normally, the ship dynamics involve both hard and soft nonlinearities. The latter stems from the aerofoil shape of the hull that generates forces and moments, which are functions of the square of the ship forward speed. On the other hand, the hard nonlinearities are associated with the rudder travel saturation and slew rate limitations. Therefore, the task of controlling the ship dynamics is usually classified as designing a controller for a nonlinear and highly uncertain system [501].

In spite of these difficult issues, the ship is required to accurately perform track-keeping and course-changing tasks while being able to attenuate the undesirable roll motion. To the best of our knowledge, passive and active ship control problems involving navigation in ice-infested waters represent potential research issues that are still in the early stage of their development. Therefore, only control schemes that were developed for ships operating under no ice loading conditions will be briefly reviewed in this section. Specifically, the focus will be restricted to roll motion stabilizers.

7.2 Ship Roll Control Problem. In rough weather conditions, excessive roll-induced oscillations may be discomforting and fatiguing to passengers, may reduce the crew efficiency, degrade the fighting capabilities of warships, and damage the contents of containers in cargo ships. These factors cause an inherent degradation in ship operability. Monk [502] indicated that the ability of crew members would be impaired by 20–30% if the ship undergoes a rms roll motion of 6 deg and by 50% if the ship experiences a rms lateral acceleration of 0.07 g. Therefore, in an attempt to deal with the undesirable effects of excessive roll os-

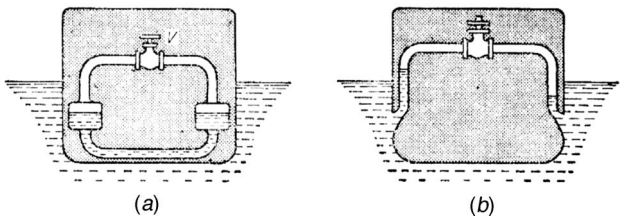

Fig. 39 Frahm's antiroll ship tanks: (*a*) two tanks each half filled with water (old type); (*b*) modern blister construction of Frahm's antirolling tanks [525]

cillations, the ship captain may be forced to slow down the ship, alter its course, or suspend its allotted mission [503,504]. Such measures would ultimately lead to undesirable delays in performing the tasks or reaching the desired destination of the ship.

Among the ship's six degrees of freedom (i.e., surge, sway, heave, roll, pitch, and yaw), the roll oscillation is considered to be the most critical component of the ship motion. Large amplitude roll oscillations can be generated at resonance by relatively small wave forces. These oscillations can be significantly attenuated by applying forces/moments that are out of phase with the excitation forces. Moreover, the forces required to counteract the roll motion are relatively small compared to the ship's weight. Many studies have shown that the roll motion can be significantly reduced by fitting the marine vessel with a roll stabilization system. Most notable roll stabilization techniques are the antiroll tanks [505–512], the active and passive fins [503,511,513–517], the rudder roll stabilization (RRS) system [515,518–523], and the integral fin/rudder roll stabilization system (INFRRS) [503,515]. The next sections describe and assess the main results pertaining to these four techniques.

7.2.1 Roll Stabilization by Antiroll Tanks. Antiroll tanks have been introduced as mechanical absorbers to attenuate the ship roll motion. The advantages of passive U-tube antiroll tanks stem from the fact that they do not have moving parts and require little maintenance. However, they occupy a very significant portion of the ship's hull. They can be classified as passive [505–507,509–511,524], controlled passive [508], and active [512]. The motion of the ship causes appropriate masses of fluid, water or reserve fuel, to flow side by side between tanks that are mounted at specific heights and distances from the ship's centerline. The resistance in the connection between the tanks is tuned so that the fluid motion is out of phase with the ship roll motion, thus generating opposing moments that will minimize the adverse effects of wave-induced excitations [505,511].

Frahm [524] introduced an antiroll tank in the form of a U-tube. This is shown in Fig. 39 (taken from Den Hartog [525]). In this system, a moment opposing the roll motion of the ship is generated by the oscillating fluid. Figure 39(*a*) depicts the old version of Frahm's antiroll system, which consists of two half-full tanks that are connected at the bottom by a water pipe and at the top through an air pipe fitted by a *V* valve. Figure 39(*b*) shows a newer version of Frahm's antiroll system in which the lower pipe connecting the tanks is omitted and replaced by the open ocean. The "blisters" are extended along two-thirds of the length of the ship and are subdivided into three or more compartments by vertical partitions. Stigter [507] derived the equations of motion of the fluid in a passive U-tube antiroll tank and determined the coupling terms between the ship and the tank. Lewison [510] proposed a scheme to optimize the design of free-surface passive tanks. Abdel Gawad et al. [505] aimed at optimizing the performance of passive U-tube tanks over a wide range of excitation frequencies. They focused on determining optimal values for the tank damping, mass, and location with respect to the ship's center of gravity. Moreover, their study demonstrated a 67% reduction in the ship roll motion for a well-tuned and well-designed U-tube tank. Furthermore, Vugts [509] designed and compared the performances of four passive tanks in reducing the roll motion for the same ship.

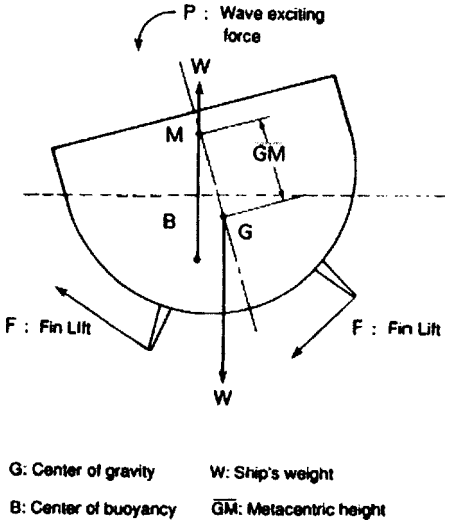

Fig. 40 Principles of roll reduction by fin stabilizer [513]

Bell and Walker [508] examined two differently controlled antiroll tanks. The first is controlled by valves mounted in the water channel. The second is controlled by valves in the air channel. In active antiroll tanks, either air pressure or a pump is used to move the fluid between tanks. Webster [512] examined the control of pump-activated U-tube tanks. He demonstrated the superiority of active antiroll tanks over passive ones in reducing the ship roll motion.

Treakle, III et al. [504] designed a proportional-integral-derivative (PID) controller for an onboard moving weight to mimic the motion of the fluid in an active antiroll-tank system. The simulation results demonstrate that the moving weight system is very effective in reducing the ship roll motion.

It should be emphasized that both antiroll tanks and moving weights are independent of the vessel forward speed. As a consequence, both systems have the advantage of being effective when the ship is not underway or moving at low speeds.

It should be pointed out that the design of existing active antiroll tanks should be modified in order to ensure that these systems operate as intended under extreme low temperatures. Furthermore, the controller of the onboard moving weight system should be robust to structured uncertainties induced by the weight shift that is caused by the ice accretion on the ship.

7.2.2 Roll Stabilization by Fins. The fin stabilization system generates a moment to oppose the wave-induced roll moment on the ship. Its stabilizing moment is produced by the lift forces on the airfoil sections, which may be all or partly moveable with or without flaps [511]. Therefore, to alleviate the roll motion, ships have been equipped with either passive or active fin stabilizers. Figure 40 shows a schematic diagram of fin stabilizer adopted from Kawazoe et al. [513]. The stabilizer is basically used to provide additional damping to the ship roll motion. However, they must have a very large size in order to be effective in attenuating the ship roll oscillations; thus, their usage becomes limited [515].

Under a "beam-sea" state, the ship oscillates heavily at its own natural frequency, particularly when the wave natural frequency matches that of the ship. A common way of dealing with this problem is to increase the damping by equipping the ship with bilge keels [505]. Figure 41 shows the effectiveness of bilge keels. At resonance, the roll angle is reduced by almost 33%.

The active fin stabilizers have been successfully implemented to enhance the operational effectiveness of warships in rough

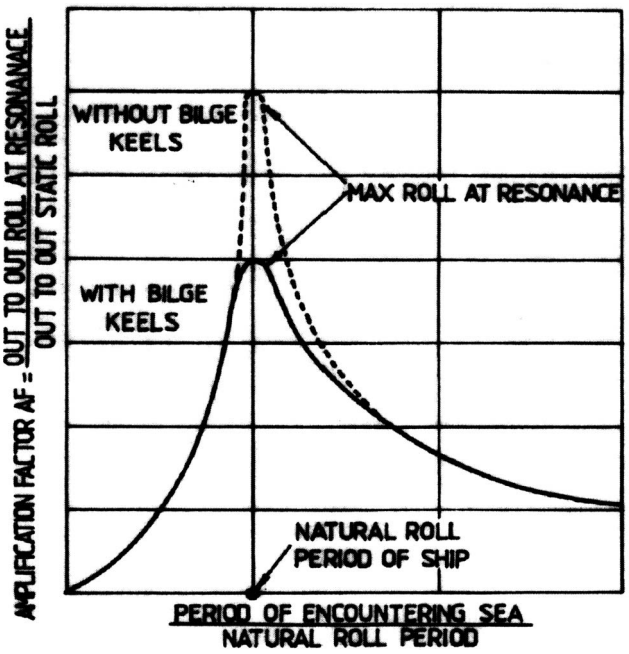

Fig. 41 Amplification factor [511]

weather [503,516]. They use winglike appendages that are usually controlled based on measured roll angular displacement and velocity. The fins are hydraulically rotated in phase with the ship roll motion at long wave periods, in phase with the roll acceleration at short periods and out of phase at a ship resonance period [511,517]. Note that the hydrodynamic forces exerted on the fins are proportional to the square of the ship forward speed. Therefore, at high speeds, large stabilizing moments can be generated by having the fins undergo small rotations. Andrew et al. [516] showned the operational effectiveness for the same frigate with and without fin stabilizers to be 0.851 and 0.649, respectively. This claim was also supported by Crossland [503], who confirmed in his study that the performance of a ship with a fin stabilizer is superior to that of a ship without a stabilizer, as shown in Fig. 42. However, at low ship speeds, the effectiveness of the fins is greatly reduced, and their role becomes similar to additional bilge keels [511]. Crossland [503] demonstrated that there are few differences between the performances of ships with or without fin stabilizers at slow speeds. To address this shortcoming, a coupled system consisting of an antiroll tank and a fin stabilizer have been suggested in order to enhance the ship operational effectiveness at both high and low speeds [505,511].

Initial control strategies for fin stabilizer systems were developed based on the assumption that the roll was mainly induced by beam-sea and "following-sea" states. In the beam-sea state, the objective of the control strategy is to enhance the damping characteristic of the ship. The control action is assigned as follows [511]:

$$\text{control signal} = \text{roll velocity} - 10\,\%\ \text{roll angle} \quad \text{(for the beam-sea state)} \tag{50}$$

Note that the roll angle was included to compensate for the time lag between the initiation and the actual movement of the fins. However, in the following-sea state, the ship is tilted at the contour of the waves in an irregular manner. In this case, the controller objective is twofold. First, it has to induce additional damping into the system in order to attenuate the roll oscillations of the ship. Second, it has to restore the upright position of the ship. The control action is specified as [511]

$$\text{control signal} = \text{roll velocity} + 63\,\%\ \text{roll angle} \quad \text{(for the following-sea state)} \tag{51}$$

However, the sea seldom acts purely in either state. Therefore, a more sophisticated controller, capable of handling the ship nonlinearities and being robust to disturbances that are generated by randomly varying environmental conditions, is required.

Katebi et al. [514] designed three controllers for an active fin stabilizer system. The first consists of a PID controller whose gains are tuned based on the classical control theory. The second is a PID controller whose gains are tuned based on an optimization scheme. The third consists of a robust H_∞ controller, which is suitable for handling systems with significant model variations over their operating range. This controller is an optimization scheme that combines conventional and robust control methodologies within a single design framework. It is basically designed to minimize the effect of the wave disturbance input on the roll angular displacement of the ship. All controllers were designed to satisfy two stability and three performance criteria. The stability criteria pertain to the GM and phase margin (PM). It was demonstrated that the conventional PID controller can only account for one of the specified criteria in its design. The digital simulation results illustrated the superiority of advanced control schemes over conventional ones in attenuating the wave-induced roll motion of the ship.

Crossland [503] adopted the three controllers described by Katebi et al. [514] to quantify the improvement in the ship operational performance that can be attributed to the choice of the control strategy used in the fin stabilizer system. The performance criterion was based on the average percentage time operability (PTO) of the ship. All simulations were based on an antisubmarine warfare (ASW) mission of a warship in the North Atlantic. Moreover, they assumed a short-crested sea state where the waves approach the ship from one direction. However, a cosine-squared spreading of the wave energy around the primary wave direction was considered. The results revealed that none of the control strategies considered in this study yields the best performance throughout the entire range of the ship speed/heading combinations. A control strategy may yield a better performance than others in one range of ship speed/heading combinations and may perform worse than others in a different range. It should be stressed that this conclusion should only be applicable for the type of controllers that were considered in Crossland's study [503].

Yang et al. [526] developed a robust adaptive fuzzy controller (RAFC) to stabilize the ship roll motion through an active fin stabilizer. The ship is considered to be an uncertain system whose dynamics are described by a nonlinear second-order differential equation. The universal approximation capability of fuzzy systems has been exploited in this study to construct a fuzzy system that yields an upper bound for the system uncertainties. The RAFC has been designed based on the Lyapunov direct method in order to ensure that the closed-loop system trajectory converges exponen-

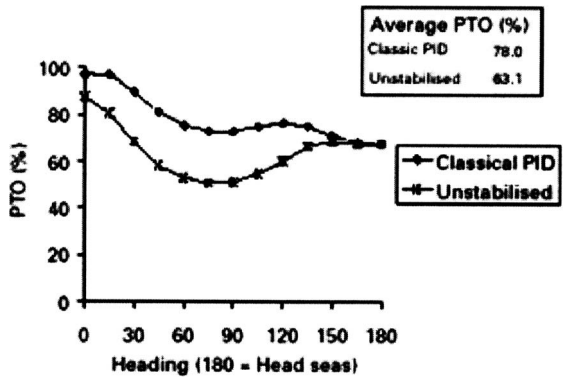

Fig. 42 PTO at 15 knots in the North Atlantic [503]

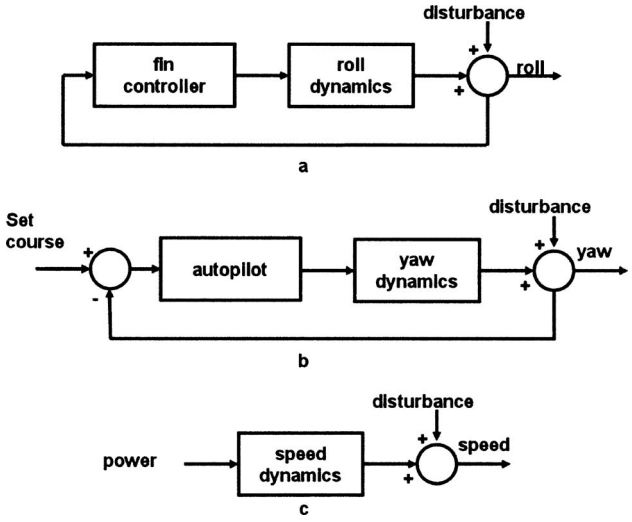

Fig. 43 Independent control strategies for the yaw and roll motions of the ship [527]

tially to a closed-ball surrounding the equilibrium state with a prescribed radius. The wave effect is modeled as an external disturbance consisting of a sinusoidal signal with a peak amplitude of 7 m. The digital simulation results illustrated the effectiveness of the proposed controller in significantly reducing the amplitude of the ship roll motion when the ship is subjected to a sinusoidal wave external disturbance.

Most control strategies tend to ignore the coupling terms between the yaw and the roll motions of the ship. This strategy is reflected in Fig. 43 where the roll and yaw motions are being controlled independently [527]. However, modern warships are required to be highly maneuverable. The design configuration that meets this requirement has resulted in a strong interaction between the roll and yaw motions of the ship. This strong coupling has to be accounted for in the design of the controller. Otherwise, it will have a significant detrimental effect on the ability of the ship to provide a stable platform during maneuvers, thus adversely impacting the operational efficiency of the ship. Roberts and Towill [528] designed a model-based linear multivariable controller that considers both the yaw and the roll motions of the ship. Their technique implemented a decoupling algorithm that decomposed the system into two independent control loops. However, the performance of this controller is hinged on the accuracy of the dynamic model of the ship.

Sutton et al. [527] addressed the problem of reducing the roll motion of the ship that is induced by both the rudder and sea disturbances. Their model accounts for the effect of yaw on the roll motion. This is illustrated in Fig. 44, which also reveals that the ship model considers the dynamics of the fins and rudder servomechanisms along with their saturation limiters. Their study proposed a fixed-rule-based fuzzy logic controller (FLC) for the fin stabilizer system that uses both the roll angle and its time derivative as input variables and the fin demand as the output variable. It should be emphasized that the FLC design was solely based on the ship roll motion. Their simulation results exhibit the effectiveness of their proposed controller in reducing the roll motion. Moreover, the performance of the FLC was found to be considerably more robust than that of traditionally designed multivariable controllers. However, its implementation may become impractical due to the lengthy computational time required to evaluate the large rule base of the controller. Sutton et al. [527] suggested a self-organizing or adaptive FLC, whereby the rules may be automatically generated or modified based on their contribution to the performance of the closed-loop system, as a viable alternative to the fixed-rule-based FLC.

7.2.3 Rudder Roll Stabilization System. There is a great interest in increasing the functionality of the rudder to include both ship steering and roll reduction. The rationale is to eliminate the need for equipping ships with conventional fin stabilizers in order to reduce the roll motion. Many studies have been conducted to evaluate the effectiveness of the RRS system as a potential tool for roll reduction (see, e.g., Refs. [515,518–523]). The RRS system uses a moment generated by the rudder to significantly attenuate the roll motion. This has been achieved with a negligible effect on the yaw motion of the ship. The RRS system remains one of the primary roll control devices in use on U.S. Navy ships. However, the roll stabilization system loses its effectiveness at low ship speeds. In addition, a significant increase in the slew rate of the rudder is required if rudders are to replace fins.

7.2.4 Integrated Fin/Rudder Roll Stabilization System. In contrast to the RRS system, which aims at replacing the fin stabilizer, the INFRRS system utilizes both systems in an attempt to combine their advantages for further enhancement of the ship stabilization. In assessing the advantages of the INFRRS system, Crossland [503] used the PTO as a measure of the operational

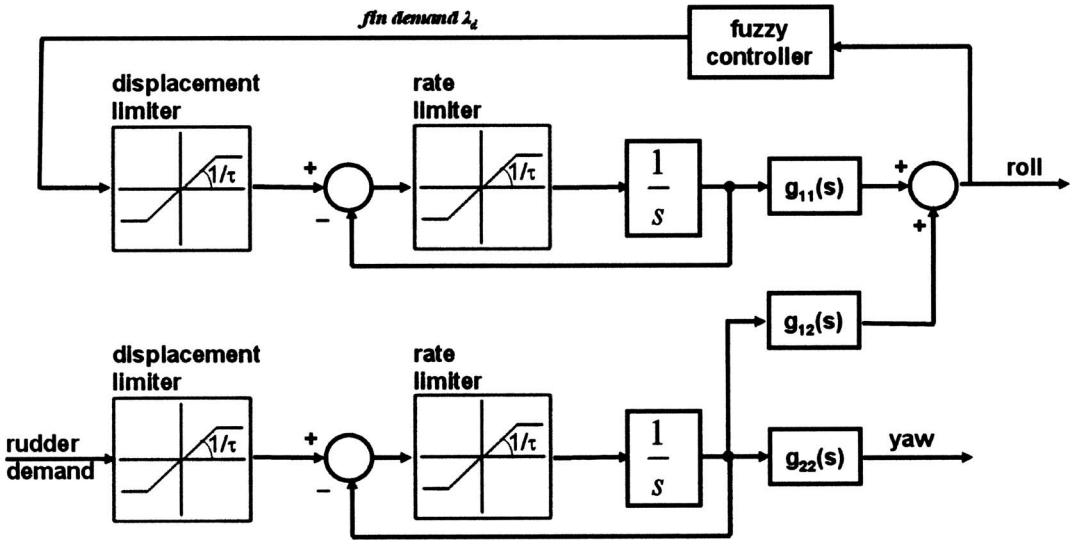

Fig. 44 Proposed control strategy [527]

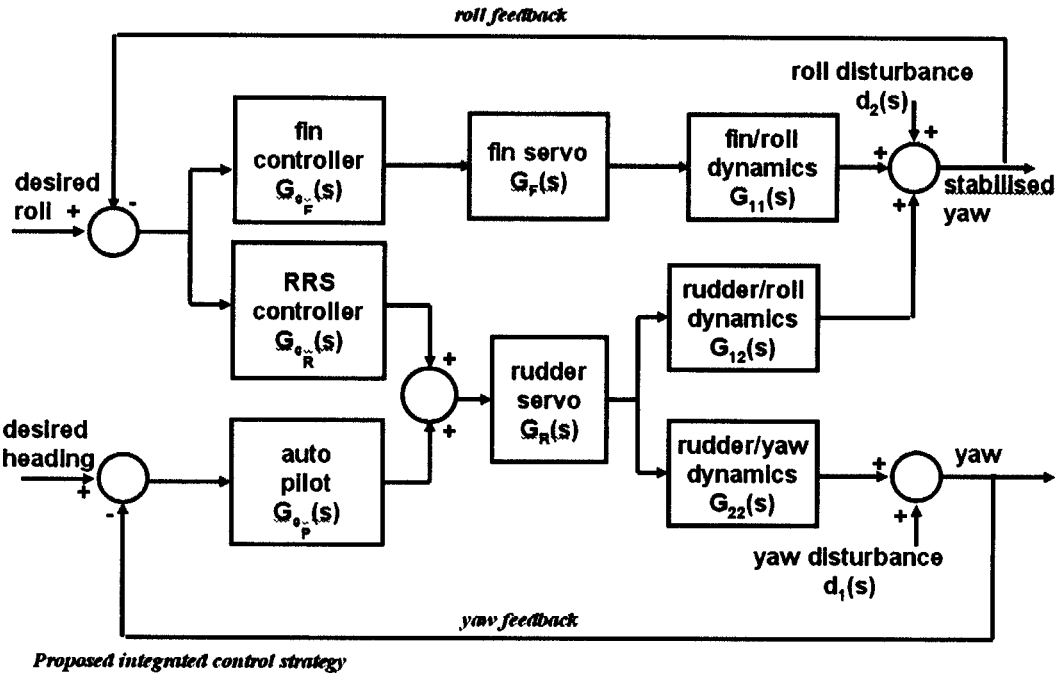

Fig. 45 Proposed INFRRS system [515]

performance of the ship. He has demonstrated that the INFRRS can lead to an improvement of about 3.8% in PTO of ASW frigates over the level achievable by a standard fin roll stabilizer system. Most importantly, this improvement was realized without requiring an increase in the slew rate of the existing rudder.

Roberts et al. [515] have also used an INFRRS system to attenuate the roll motion of frigates in the Royal Navy. Their model considered both the roll and yaw motions of the ship. However, they ignored the effect of the roll on the yaw motion of the ship. This is clearly reflected in Fig. 45. The rudder control signal is composed of two independent components. The first is designed to yield a good course-keeping characteristic of the ship autopilot system, while the second is introduced to aid the fin controller in attenuating the roll angle of the ship (see Fig. 45). Both the rudder roll controller and the autopilot controller have been designed based on the H_∞ methodology. Their study demonstrated that the classical RRS controller, consisting of a typical lead-lag compensator [457], achieves a better roll reduction at the ship's resonance roll frequency. However, the performance of the H_∞ RRS controller was found to be consistently better over the entire encountered frequency range and resulted in a reduced rudder activity than that required by the classical RRS controller. Moreover, the H_∞ controller has been shown to be robust to system's uncertainties and possesses good disturbance rejection characteristics.

Most importantly, Roberts et al. [515] showed that the existing rudder system can be used effectively to assist the active fin stabilization system in attenuating the ship roll motion without generating significant disturbances on the yaw motion.

7.2.5 Control Issues Pertaining to Ice Loading on Ships. It should be emphasized that none of the control strategies discussed herein takes into consideration the effects of ice loading and ice impact in its design. As mentioned earlier, the ice effects tend to increase the structured uncertainties of the system and/or introduce additional external disturbances, which may adversely affect the performance of the ship.

Hill et al. [529] proposed a control strategy for a Canadian Coast Guard icebreaker featuring a diesel-electric propulsion system. The latter consists of three marine diesel engines driving three synchronous generators that supply power to cycloconvertor transformers, which in their turn are needed by the propulsion motors. Note that in this system, the ship propellers are directly coupled to the propulsion motors. Among the advantages of the diesel-electric propulsion system is its ability to use fixed pitch propellers that are more efficient and less expensive than the controlled pitch propellers that are needed by the geared diesel drives. Furthermore, this propulsion system has the capability of transmitting larger rated torque at low ship speeds than the geared diesel drives. Moreover, the diesel engines in a diesel-electric propulsion system do not have to be slowed down in order to reverse the direction of the propeller rotation, a task often required to dislodge blocks of ice that managed to stall some of the ship propellers. Note that such maneuvers are not possible without slowing down the diesel engines in geared diesel systems. In this study, the proposed control strategy of the propulsion system relies on two control loops to limit the power that can be delivered to the synchronous motors. The rationale is to prevent the diesel engines from stalling and the generators from overloading when the propulsion system experiences sudden or sustained overloads usually associated by ice impact and stiff ice resistance.

In light of these difficulties, the ship control problem under severe cold weather conditions represents a very challenging task that needs to be addressed by future research activities. The studies discussed above tend to suggest that a nonlinear robust controller capable of adapting itself to the unpredictable environmental disturbances of the ship is needed. Adaptive fuzzy controllers or fuzzy-tuned robust nonlinear controllers seem to be potential candidates for this challenging problem since they account in their structures for both system nonlinearities and uncertainties.

8 Conclusions

Ships and offshore structures may encounter severe loads from ice impacts and random ocean waves. This problem presents formidable tasks to the navigation, safe operation, controls, and stabilization of ships. Depending on the thickness and conditions of ice, these interactions may result in repeated impacts that would ultimately lead to structure fatigue and may, under severe conditions, cause ship capsizing. The estimation and measurements of ice loads, which have been examined extensively in recent studies, have been summarized in the beginning of this article. Experimental measurements of ice loads have been classified in the lit-

erature as local and global loads. They were found to be random in nature and were expressed in terms of probabilistic measures. One of these measures is considered to be the Poisson distribution when the number of ice-load impacts is random.

Moreover, this review article addresses governing factors of ice loads such as its mechanics and properties. A typical cycle of ice force resisting an ocean structure consists of a gradual increase in the ice force until the ice is broken. Thus, the cycle involves a sudden drop in the force exerted on the structure due to the clearance created by the ice that is being crushed. The repetition of this cycle revealed a sawtooth pattern in the time domain according to indentation test results. It should be mentioned that this loading pattern is known to be caused by ice-structure interaction. Furthermore, the ice-crushing process results in negative damping to the ship motion due to the drop in the resistance. Full-scale structural test measurements have revealed three ice-load modes: quasi-static, steady-state, and random fluctuations. These measurements involve uncertainties due to ice nonhomogeneity and differences in the ice microstructure.

The results reviewed herein provide valuable information pertaining to ice impact loads, which were found to be linearly dependent on the impact speed (for a low speed range) or on the square of the speed (for a high speed range). Ice impact on ship hulls made of composite materials can cause delamination, matrix cracking, and fiber failure. The nonlinear dynamic response of a ship or an offshore structure was found to be due to intermittent ice breaking and ice contact with the structure. Models of ice impact loads on ship roll dynamics have been presented in the literature; however, no attempt has yet been made to analyze the resulting equation of motion for stability and response characteristics.

One of the major issues reported in the literature is the ice resistance to ship motions. The resistance to the hull motion through brash ice was found to be due to different components that were described in Sec. 4. Among these factors are the bow resistance associated with shearing or compression of the rubble layer, the resistance associated with the submergence of brash ice beneath the hull, and the resistance to the momentum exchange between the hull and the brash ice. Another important and serious problem encountered during the navigation of ships in ice infested waters is the ice-interaction with the propulsion system. This problem has the potential of damaging the propellers and leaving ships stranded in remote areas. A great deal of study has been devoted to improve the design of propulsion systems. These studies estimated the loads and stress distributions of the propeller blades due to the ice interaction. In view of the additional ice loads on marine systems, new design regulations have been introduced to enable ships and offshore structures to withstand loads induced by extreme environmental conditions.

It is a common knowledge that the ice accretion on a ship has a tendency to raise its center of gravity and possibly cause an asymmetry in its equilibrium position. This will result in a significant reduction in the initial static stability of the ship. Many studies have addressed the dynamic stability of vessels due to icing and tried to establish safe basins (initial conditions) for the ship roll motion. The stochastic stability of ships and its first-passage problem have been addressed for ship roll dynamics operating in random sea waves. No such effort has yet been made to investigate this stability problem in the presence of ice-ship interaction. Furthermore, stochastic dynamic modeling of ships involving ice impact loadings has not been tackled in the literature, and it is still an open area for potential research activities.

Moreover, this article has briefly summarized the work done in developing antiroll tanks and moving weights whose performances are not affected by the vessel forward speed. Consequently, they have the advantage over other antiroll schemes in being effective when the ship is not underway or is moving at slow speeds. On the other hand, active fins can produce large stabilizing moments at high ship speeds. The performances of ships with fin stabilizers have been shown to be superior to those without stabilizers. Other approaches, such as the RRS system, have relied on increasing the functionality of the rudder to perform both ship steering and roll reduction tasks. Several studies have demonstrated the viability of such an approach. However, the slew rate of the rudder must be significantly increased if the RRS system is to replace the fins. To relax this requirement, the INFRRS stabilization system is introduced whereby the existing rudder assists the fin stabilization system in attenuating the ship roll motion. It should be emphasized that the effectiveness of RRS, INFRRS, and fin stabilization systems is greatly reduced at low ship speeds. It should be stressed that none of the control schemes discussed herein have dealt with ships navigating in ice-infested waters. Passive and active control schemes are very valuable in preventing ships from capsizing due to ice accretion on their superstructures. The enhancement of their performances under extreme weather conditions necessitates the development of robust nonlinear controllers that are capable of adapting to the constantly varying and highly uncertain environmental conditions.

Acknowledgment

This work is supported by a grant from ONR under Award No. N00014-05-1-0040. Dr. Kelly B. Cooper is the Program Director. The authors would like to thank one of the reviewers who provided additional references and suggested a number of improvements to the article.

References

[1] Jones, K. F., and Mulherin, N. D., 1998, "An Evaluation of the Severity of the January 1998 Ice Storm in Northern New England," U.S. Army Cold Regions Research and Engineering Laboratory, Snow and Ice Division, Report for FEMA Region 1.

[2] Kry, P. R., 1980, "Ice Forces on Wide Structures," Can. Geotech. J., **17**, pp. 97–113.

[3] Hardy, M. D., Jefferies, M. G., Rogers, B. T., and Wright, B. D., 1998, "DynaMAC: Molikpaq Ice Loading Experience," Klohn-Crippen, Calgary, AB, Canada, PERD/CHC Report No. 14-62.

[4] Frederking, R. M. W., Timco, G. W., and Wright, B. D., 1999, "Ice Pressure Distribution From First-year Sea Ice Features Interacting With Molikpaq in the Beaufort Sea," *Proceedings of the Ninth International Offshore and Polar Engineering Conference ISOPE'99*, Brest, France, Vol. II, pp. 541–548.

[5] Johnston, M. E., and Timco, G. W., 2003, "Ice Loads on the SSDC During its Beaufort Sea Deployments," *Proceedings of the 17th International Conference on Port and Ocean Engineering Under Arctic Conditions, POAC'03*, Norwegian University of Science and Technology, Vol. 1, pp. 213–222.

[6] Timco, G. W., and Johnston, M., 2003, "Ice Loads on the Molikpaq in the Canadian Beaufort Sea," Cold Regions Sci. Technol., **37**, pp. 51–68.

[7] Timco, G. W., and Johnston, M., 2004, "Ice Loads on the Caisson Structures in the Canadian Beaufort Sea," Cold Regions Sci. Technol., **38**, pp. 185–209.

[8] Timco, G. W., and Wright, D. B., 1999, "Load Attenuation Through Grounded Ice Rubble at Tarsiut Island," *Proceedings of the 15th International Conference on Port and Ocean Engineering Under Arctic Conditions, POAC'99*, Helsinki University of Technology, Espoo, Finland, Vol. 1, pp. 454–463.

[9] Timco, G. W., Johnston, M., and Frederking, R., 1999, "The NRC Ice Load Catalogue (2 Volumes)," NRC National Research Council of Canada, Report No. HYD-CTR-058.

[10] Timco, G. W., Johnston, M., and Frederking, R., 1999, "The NRC Ice Load Catalogue," *Proceedings of the 15th International Conference on Port and Ocean Engineering Under Arctic Conditions, POAC'99*, Helsinki University of Technology, Espoo, Finland, Vol. 1, pp. 444–453.

[11] Timco, G. W., Johnston, M., and Frederking, R., 1999, "First-Year Ice Ridge Loads on the Molikpaq," *Proceedings of the Fourth International Conference on Development of the Russian Arctic Offshore, RAO99*, Krylov Shipbuilding Research Institute, St. Petersburg, Russia, Pt. II, pp. 172–179.

[12] Timco, G. W., Johnston, M., and Frederking, R., 2001, "The NRC Ice Load Catalogue: Phase 2," NRC National Research Council of Canada, Report No. HYD-CTR-094.

[13] Wright, B., and Timco, G. W., 1994, "A Review of Ice Forces and Failure Modes on the Molikpaq," *Proceedings of the 12th International Association of Hydraulic Engineering and Research Symposium on Ice*, Trondheim, Norway, Vol. 2, pp. 816–825.

[14] Wright, B., and Timco, G. W., 2000, "First-Year Ridge Interaction With the Molikpaq in the Beaufort Sea," Cold Regions Sci. Technol., **32**, pp. 27–44.

[15] Perham, R. E., 1981, "Ice Control Arrangement for Winter Navigation," Tetsu-To-Hagane/Journal of the Iron and Steel Institute of Japan, **2**, pp. 1096–1103.

[16] Kinosita, S., 1982, "Control of Snow and Ice in Hokkaido, Japan," *ASCE Journal of the Technical Councils of ASCE: Proceedings of the ASCE*, 108(TC1), pp. 34–43.

[17] Frankenstein, G., and Hanamoto, B., 1983, "Methods of Ice Control," ASCE

Design for Ice Forces: A State of the Practice Report. Paper presented at the ASCE Annual Convention., New Orleans, LA, pp. 204–215.
[18] Kashtelyan, V. I., Ryvlin, A. Y., Faddeyev, O. V., and Yagodkin, V. Ya., 1973, *Icebreakers*, Draft Translation 418, National Technical Information Service Document No. AD-767 457, Springfield, VA.
[19] USACE, 1994, *Ice Jam Flooding: Causes and Possible Solutions*, Department of the Army, U.S. Army Corps of Engineers, Washington, DC, 20314-1000EP1110-2–11.
[20] Shoop, S. A., 1995, "Vehicle Bearing Capacity of Frozen Ground Under Soft Substrate," Can. Geotech. J., **32**, pp. 552–556.
[21] Azarnejad, A., and Hrudey, T. M., 1998, "Numerical Study of Thermal Ice Loads on Structures," Can. J. Civ. Eng., **25**(3), pp. 557–568.
[22] Shoop, S. A., Haehnel, R., Kestler, K., Stebbings, K., and Alger, R., 1999, "Finite Element Analysis of a Wheel Rolling in Snow," *Proceedings of the Tenth International Conference on Cold Regions Engineering*, Lincoln, NH, pp. 519–530.
[23] Shoop, S. A., Lacombe, J., and Haehnel, R., 2001, "Modeling Tire Performance for Winter Conditions," Tire Technology International, Annual Review of Tire MaterTire Manufacture Technology, pp. 10–14.
[24] Shoop, S. A., Richmond, P. W., and Lacombe, J., 2006, "Overview of Cold Regions Mobility Modeling at CRREL," J. Terramech., **43**, pp. 1–26.
[25] IMO, 2001, "Guidelines for Ships Operating in Arctic Ice-Covered Waters," International Maritime Organization, EP46/6; 2002, ibid., and DE 45/27 (http://www.uscg.mil/hq/g-m/MSE4/stdimofp46-06.pdf and http://www.tc.gc.ca/marinesafety/CES/Arctic/IMO-guidelines.pdf).
[26] Daley, C. G., and Riska, K., 2000, "Conceptual Framework for an Ice Load Model," www.engr.mun.ca.
[27] Daley, C. G., 2002, "Application of Plastic Framing Requirements for Polar Ships," Mar. Struct., **15**, pp. 533–542.
[28] Daley, C. G., 2002, "Derivation of Plastic Framing Requirements for Polar Ships," Mar. Struct., **15**, pp. 543–559.
[29] Gorski, M., 2004, "Predominant Frequencies in the Spectrum of Ice-Vibration Events," Acta Geophys. Pol., **52**(4), pp. 457–464.
[30] Michel, B., 1978, *Ice Mechanics*, Presses de l'Universite Laval, QB, Canada.
[31] Hamza, H., 1986, "Application of Fracture Mechanics Techniques to Ice-Structure Interaction Problems," *Proceedings of the International Association of Hydraulic Research, IAHR Symposium on Ice*, University of Iowa, IA, Vol. 1, pp. 329–347.
[32] Sanderson, T. J. O., 1988, *Ice Mechanics: Risks to Offshore Structures*, Graham and Trotman, London.
[33] Jordaan, I. J., Xiao, J., and Zou, B., 1993, "Fracture and Damage of Ice: Towards Practical Implementation," *Proceedings of the First International Mechanics Meeting of ASME, ASCE, SES*, Charlottesville, VA, Paper No. AMD 163, Ice Mechanics, pp. 251–260.
[34] Dempsey, J. P., 2000, "Research Trends in Ice Mechanics," Int. J. Solids Struct., **37**, pp. 131–153.
[35] Johnston, M. E., and Frederking, R., 2001, "Decay of the First Year Sea Ice: A Second Season of Field Measurements," NRC Report No. HYD-TR-69.
[36] Johnston, M. E., and Frederking, R., 2001, "Decay Induced Changes in the Physical and Mechanical Properties of First-Year Sea Ice," *Proceedings of the Port and Ocean Engineering Under Arctic Conditions (POAC'01)*, Ottawa, ON, Vol. 3, pp. 1395–1404.
[37] Johnston, M. E., Frederking, R., and Timco, G., 2001, "Seasonal Decay of First-Year Sea Ice," NRC Report No. HYD-TR-058.
[38] Johnston, M. E., Frederking, R., and Timco, G., 2002, "Properties of Decaying First-Year Sea Ice: Two Seasons of Field Measurements," *Proceedings of the 17th International Conference on Okhotsk Sea and Sea Ice*, Mombetsu, Hokkaido, Japan, pp. 303–311.
[39] Timco, G. W., and Johnston, M. E., 2002, "Sea Ice Strength During the Melt Season," *Proceedings of the 16th International Association of Hydraulic Engineering and Research (IAHR) Symposium on Ice*, Denedin, New Zealand, Dec. 2–6, pp. 187–193.
[40] Timco, G. W., and O'Brien, S., 1994, "Flexural Strength Equation for Sea Ice," Cold Regions Sci. Technol., **22**, pp. 285–298.
[41] Jordaan, I. J., 1986, "Numerical and Finite Element Techniques in Calculation of Ice-Structure Interaction," *Proceedings of International Association for Hydraulic Research (IAHR) Symposium on Ice*, University of Iowa, Iowa City, IA, Vol. 2, pp. 405–441.
[42] Sodhi, D. S., and Morris, C. E., 1986, "Characteristic Frequency of Force Variations in Continuous Crushing of Sheet Ice Against Rigid Cylindrical Structures," Cold Regions Sci. Technol., **12**, pp. 1–12.
[43] Kry, P. R., 1978, "A Statistical Prediction of Effective Ice Crushing Stresses on Wide Structures," *Proceedings of the Fourth International Association of Hydraulic Research Symposium on Ice Problems*, University of Lulea, Lulea, Sweden, Aug. 7–9, pp. 33–47.
[44] Kry, P. R., 1979, "Implications of Structure Width for Design Ice Forces," in *Proceedings of the International Union of Theoretical and Applied Mechanics (ITAM) Symposium*, P. Tryde, ed., Copenhagen, pp. 179–193.
[45] Kry, P. R., 1981, "Scale Effects in Continuous Crushing of Ice," *Proceedings of the Fifth International Association Hydraulic Research Symposium on Ice Problems*, Laval University, QB, Canada, Jul. 27–31, pp. 565–580.
[46] Glen, I. F., and Blount, H., 1984, "Measurements of Ice Impact Pressures and Loads Onboard CCGS Louis S. St. Laurent," *ASME Proceedings of the Third Offshore Mechanics and Arctic Engineering Symposium*, New Orleans, LA, Vol. III, pp. 246–252.
[47] Croasdale, K. R., 1975, "Ice Forces on Marine Structures," *Proceedings of the Third International Association of Hydraulic Engineering and Research (IAHR) Symposium on Ice Problems*, Hanover, NH, pp. 315–337.
[48] Croasdale, K. R., Morgenstern, N. R., and Nuttal, J. B., 1977, "Indentation Tests to Investigate Ice Pressures on Vertical Piers," J. Glaciol., **19**(81), pp. 301–312.
[49] Yue, Q. J., 1996, "Ice Force Measurement and Ice Load Prediction for the JZ20-2 Platform Structure," Dalian University of Technology, Research Report.
[50] Zufelt, J. E., and Ettema, R., 1996, *Model Ice Properties*, U.S. Army Corps of Engineers, Cold Regions Research and Engineering Laboratory, CRREL Report No. 96-1.
[51] Masterson, D. M., Spencer, P. A., Nevel, D. E., and Nordgren, R. P., 1999, "Velocity Effects From Multi-Year Ice Tests," *Proceedings of the 18th International Conference on Offshore Mechanics and Arctic Engineering (OMAE)*, St. John's, Newfoundland, Canada, Paper No. OMAE99/P&A, p. 1127.
[52] Jordaan, I. J., and Xiao, J., 1992, "Interplay Between Damage and Fracture in Ice-Structure Interaction," *Proceedings of the 11th International Symposium on Ice*, AB, Canada, Vol. 3, pp. 1448–1467.
[53] Bruen, F. J., and Vivatrat, V., 1984, "Ice Force Prediction Based on Strain-Rate Field," ASME J. Energy Resour. Technol., **106**(4), pp. 509–514.
[54] Vivatrat, V., and Kreider, J. R., 1981, "Ice Force Prediction Using a Limited Driving Force Approach," *Proceedings of the Annual Offshore Technology Conference*, Houston, TX, Vol. 3, pp. 471–485.
[55] Vivatrat, V., Chen, V., and Bruen, F. J., 1984, "Ice Load Prediction for Arctic Near-Shore Zone," Cold Regions Sci. Technol., **10**(1), pp. 75–87.
[56] Vivatrat, V., and Chen, V. L., 1985, "Ice Load Prediction With the Use of a Rate-Dependent Anisotropic Constitutive Law," *ASCE Proceedings of the Conference Arctic'85*, Civil Engineering in the Arctic Offshore, San Francisco, CA, pp. 942–952.
[57] Johnston, M. E., 1994, "Variation of Local Ice Pressures During Ice-Structure Interaction," Ph.D. thesis, Memorial University of Newfoundland.
[58] Kato, K., and Sodhi, D. S., 1984, "Ice Action on Two Cylindrical Structures," *Proceedings: Annual Offshore Technology Conference*, Houston, TX, Vol. 1, pp. 159–166.
[59] Blanchet, D., and Keinonen, A., 1988, "Ice Load Measurements at the Phoenix: Harrison Bay Winter 1986–1987," CANMARY/Valmet, Calgary, AB, Canada, pp. 1–208.
[60] Lindolm, J. E., Makela, K., Bo, Z. C., 1993, "Structure-Ice Interaction for a Bohai Bay Oil Production Project," *Proceedings of the Third International Offshore and Polar Engineering Conference (ISOPE)*, Offshore Mechanics & Polar Engineering Council (OMPEC), pp. 538–547.
[61] Danilenko, V. I., Goldstein, R. V., and Osipenko, N. M., 1995, "Study of Multi-Scale Deformation and Failure of Ice Cover at Interaction With Ice-Resistant Structure," *Proceedings of the 14th International Conference on Offshore Mechanics and Arctic Engineering—OMAE*, Copenhagen, Vol. 4, pp. 17–20.
[62] Yue, Q. J., and Bi, X., 2000, "Ice-Induced Jacket Structure in Bohai Sea," J. Cold Reg. Eng., **14**(2), pp. 81–92.
[63] Riska, K., Rantala, H., and Joensuu, A., 1990, "Full Scale Observations of Ship-Ice Impact," Helsinki University of Technology, Report No. M-97.
[64] Johnston, M. E., Croasdale, K. R., and Jordaan, I. J., 1998, "Localized Pressures During Ice-Structure Interaction: Relevance to Design Criteria," Cold Regions Sci. Technol., **27**, pp. 105–117.
[65] Johnston, M. E., Timco, G. W., and Frederking, R., 1999, "An Overview of Ice Loads on Slender Structures," *Proceedings of the 18th International Conference on Offshore Mechanics and Arctic Engineering—OMAE99*, St. John's, Newfoundland, Canada, Jul. 11–16, Paper No. OMAE-99-1152.
[66] Bercha, F. G., and Danys, J. V., 1975, "Prediction of Ice Forces on Conical Offshore Structures," *Proceedings of the Third International Symposium on Ice Problems*, Hannover, Germany, pp. 447–458.
[67] Chao, J. C., 1992, "Comparison of Sheet Ice Load Prediction Methods and Experimental Data for Conical Structures," *Proceedings of the International Offshore Mechanics and Arctic Engineering Symposium*, Arctic/Polar Technology, Calgary, Alberta, Vol. 4, pp. 183–193.
[68] Haskell, T. G., Robinson, W. H., and Langhorne, P. J., 1996, "Preliminary Results From Fatigue Tests on In Situ Sea Ice Beams," Cold Regions Sci. Technol., **24**(2), pp. 167–176.
[69] Cole, D. M., and Dempsey, J. P., 2004, "In Situ Sea Ice Experiments in McMurdo Sound: Cyclic Loading, Fracture, and Acoustic Emissions," J. Cold Reg. Eng., **18**(4), pp. 155–174.
[70] Katsugari, K., Kawasaki, T., Seto, H., and Hayashi, Y., 1998, "Distinct Element Simulation of Ice-Structure Interactions," *Proceedings of the Eighth International Offshore and Polar Engineering Conference*, Montreal, Canada, Vol. 2, pp. 395–401.
[71] Barker, A., Sayed, M., and Timco, G., 2002, "Numerical Simulation of Ice Interaction With a Wide Cylindrical Pier," *Proceedings of the 11th International Conference of Cold Regions Engineering Cold Regions Impacts on Transportation and Infrastructure*, pp. 617–628.
[72] Ray, J., 1982, "Engineering and Design, Ice Engineering," Department of the Army Corps of Engineers, Engineering Manual EM 1110-2-1612, Office of the Chief Engineers, Washington, D.C.
[73] Cowper, B., Abdelnour, R., Yuxiang, G., and Grissman, R., 1997, "Ice Load Measurements on the Lake Erie-Niagra River Ice Boom: 1996/97," *Ninth Workshop on River Ice, Fredericton*, NB, Canada, Canadian Committee on River Ice Processes and Environment, Fredericton, NB, Canada.
[74] Cornett, A. M., Frederking, R., Morse, B., and Dumont, S., 1997, "Ice Boom Loads in the St. Lawrence River: 1994-95 and 1995-96," *Proceedings of the Seventh International Offshore and Polar Engineering Conference, ISOPE'97*,

Honolulu, HL, Vol. II, pp. 442–448.
[75] Cornett, A. M., Frederking, R., Morse, B., and Dumont, S., 1998, "Review of Ice Boom Loads in the St. Lawrence River: 1994-97," *Ice in Surface Waters*, Z. Shen, ed., Balkeman, Rotterdam, pp. 53–59.
[76] Morse, B., 2000, "Ice/Structure Interaction: Factors Affecting Ice Loads on Wide Structures," Panel on Energy Research and Development (PERD)/ Canadian Hydraulic Center (CHC), PERD/CHS Report No. 10-56.
[77] Morse, B., 2001, "Dynamics of Ice Forces on Booms," Cold Regions Sci. Technol., **33**, pp. 29–43.
[78] Sunder, S. S., 1986, "Ice Load Prediction During Indentation," *Proceedings of the First International Conference on Ice Technology*, Cambridge, MA, pp. 297–309.
[79] Frederking, R. M. W., Jordaan, I. J., and McCalum, J. S., 1990, "Field Tests of Ice Indentation of Medium Scale, Hobson's Choice Ice Island, 1989," *Proceedings of the Tenth International Association of Hydraulic Engineering and Research (IAHR) Symposium on Ice*, Espoo, Finland, Vol. 2, pp. 931–944.
[80] Masterson, D. M., Frederking, R., Jordaan, I. J., and Spencer, P. A., 1993, "Description of Multi-Year Ice Indentation Tests at Hobson's Choice Ice Island—1990," *Proceedings of the 112th International Conference on Offshore Mechanics and Arctic Engineering (OMAE)*, Glasgow, Scotland, Vol. IV, pp. 145–155.
[81] Gagnon, R. E., 1998, "Analysis of Visual Data From Medium Scale Indentation Experiment at Hobson's Choice Ice Island," Cold Regions Sci. Technol., **28**, pp. 45–58.
[82] Spencer, P. A., and Masterson, D. M., 1993, "Dynamic Analysis of the Medium Scale Hydraulic Ice Indentation Apparatus," *Proceedings of the 12th International Conference on Offshore Mechanics and Arctic Engineering (OMAE)*, Glasgow, Scotland, Vol. IV, pp. 105–111.
[83] Meaney, R., Kenny, S., and Sinha, N. K., 1991, "Medium-Scale Ice-Structure Interaction: Failure Zone Characterization," *Proceedings of the 11th International Conference on Port and Ocean Engineering Under Arctic Conditions, POAC*, Vol. 1, pp. 126–140.
[84] Swamidas, A. S. J., Jordaan, I. J., Jones, S. J., and McKenna, R. E., 1991, "Modeling of the Ice Failure Processes in Ship/Ice Interaction," *Proceedings of the 11th International Conference on Port and Ocean Engineering Under Arctic Conditions, POAC*, St. John's, Newfoundland, Canada, Vol. 2, pp. 685–703.
[85] Zou, B., Xiao, J., and Jordaan, I. J., 1996, "Ice Fracture and Spalling in Ice-Structure Interaction," Cold Regions Sci. Technol., **24**(2), pp. 213–220.
[86] Muhonen, A., Kärnä, T., Järvinen, E., and Riska, K., 1992, "Laboratory Indentation Tests With Thick Freshwater Ice," Laboratory of Naval Architecture and Marine Engineering Otaniemi, Report No. M-122, pp. 1–397.
[87] Thukuri, J., 1995, "Experimental Observations of the Brittle Failure Process of Ice and Ice-Structure Contact," Cold Regions Sci. Technol., **23**, pp. 265–278.
[88] Sodhi, D. S., 1998, "Non-Simultaneous Crushing During Edge Indentation of Freshwater Ice Sheets," Cold Regions Sci. Technol., **27**, pp. 179–195.
[89] Masterson, D. M., Nevel, D. E., Johnson, R. C., Kenny, J. J., and Spencer, P. A., 1992, "The Medium Scale Iceberg Impact Test Program," *Proceedings of the International Association of Hydraulic Engineering and Research (IAHR) Symposium on Ice*, Banff, AB, Canada.
[90] Fransson, L. Å., and Nyström, M., 1994, "Non-Simultaneous Ice Failure on Wide and Narrow Offshore Structures," *Proceedings of the International Association of Hydraulic Engineering and Research (IAHR) Ice Symposium*, Norway, Vol. 2, pp. 774–783.
[91] Kawamura, M., Takeuchi, T., Akagawa, S., Terashima, T., Nakazawa, N., Matsushita, H., Aosima, M., Katsui, H., and Sakai, M., 1996, "Ice-Structure Interaction in Medium Scale Field Indentation Tests," *Proceedings of the 13th International Association of Hydraulic Engineering and Research (IAHR) Ice Symposium*, Beijing, Vol. 1, pp. 228–236.
[92] Sodhi, D. S., and Haehnel, R. B., 2003, "Crushing Ice Forces on Structures," Cold Regions Sci. Technol., **17**, pp. 153–170.
[93] Sakai, M., Aoshima, M., Katsui, H., and Suzuki, M., 1997, "Medium-Scale Field Indentation Tests: Measurements of Ice Sheet Deformation Under Ice-Structure Interactions by Means of Photogrammetry," *Proceedings of the Seventh International Offshore and Polar Engineering Conference*, Honolulu, HI, Vol. 2, pp. 383–386.
[94] Li, C., Jordaan, I., and Barrette, P., 2003, "Damage and Microstructural Changes in Ice in Compression During Interaction With Structures," Key Eng. Mater., **251–252**, pp. 431–436.
[95] Kärnä, T., Kamesaki, K., and Tsukuda, H., 1999, "A Numerical Model for Dynamic Ice-Structure Interaction," Comput. Struct., **72**, pp. 645–658.
[96] Arunachalam, V. M., Murray, J. J., and Muggeridge, D. B., 1987, "Short Term Motion Analysis of Icebergs in Linear Waves," Cold Regions Sci. Technol., **13**, pp. 247–258.
[97] Cammaert, A. B., and Muggeridge, D. B., 1988, *Ice Interaction With Offshore Structures*, Van Nostrand Reinhold, New York.
[98] Vinogradov, O. C., 1986, "Simulation Methodology of Vessel-Ice Floes Interaction Problems," *Proceedings of the International Symposium on Offshore Mechanics and Arctic Engineering (OMAE)*, Tokyo, Japan, Vol. 4, pp. 601–606.
[99] El-Tahan, H., Swamidas, A. S., and Arockiasamy, M., 1985, "Response of Semi-Submersible Models to Bergy-Bit Impact," *Proceedings of the International Conference on Part and Ocean Engineering Under Arctic Conditions (POAC)*, Narssarssuaq, pp. 544–554.
[100] Cammaert, A. B., and Tsinker, G. P., 1981, "Impact of Large Ice Floes and Icebergs on Marine Structures," *Proceedings of the International Conference on Port and Ocean Engineering Under Arctic Conditions, POAC'81*, QB, Canada, Vol. 2, pp. 653–662.
[101] Kreider, J. R., 1984, "Summer Ice Impact Loads From Multiyear Floes," *Proceedings of International Association of Hydraulic Engineering and Research (IAHR) Symposium on Ice*, Hamburg, Vol. 2, pp. 55–66.
[102] Croteau, P., Rojansky, M., and Gerwick, B. C., 1984, "Summer Ice Floe Impact Against Caisson-Type Exploratory and Production Platforms," *Proceedings of the International Conference on Offshore Mechanics and Arctic Engineering, OMAE'84*, Vol. 3, pp. 228–237.
[103] Cox, J. R., 1985, "Ice Floe Impact Forces on Vertical-Sided Structures," *Proceedings of the ASCE Conference on Arctic'85*, New York, pp. 211–219.
[104] Evans, R. J., and Parmerter, R. R., 1985, "Ice Forces Due to Impact on a Sloping Structure," *Proceedings of the ASCE Conference on Arctic'85*, New York, pp. 220–229.
[105] Guttman, S. I., Puskar, F. J., and Bea, R. G., 1984, "Analysis of Offshore Structures Subject to Arctic Ice Impact," *Proceedings of the International Conference on Offshore Mechanics and Arctic Engineering, OMAE'84*, New Orleans, Vol. 3, pp. 238–245.
[106] Maes, M. A., and Jordaan, I. J., 1984, "Probabilistic Analysis of Iceberg Loads on Offshore Structures," *Proceedings of the International Association of Hydraulic Engineering and Research Symposium (IAHR) on Ice*, Hamburg, Vol. 2, pp. 175–188.
[107] Powell, G., Schricker, V., Row, D., Hollings, J., and Sause, R., 1985, "Ice-Structure Interaction of an Offshore Platform," *Proceedings of the Conference Arctic'85*, San Francisco, CA, pp. 230–238.
[108] Swamidas, A. S. J., and Arockiasamy, M., 1984, "Iceberg Impact Forces on Gravity Platforms," *Proceedings of the Third Cold Regions Engineering specialty Conference, Edmonton*, Vol. 1, pp. 431–458.
[109] Swamidas, A. S. J., and Arockiasamy, M., 1986, "Structural Integrity of Semi-Submersibles and Gravity Platforms to Berg-Bit/Iceberg Impact," *Proceedings of the 18th Annual Offshore Technology Conference*, Houston, TX, Paper No. OTC-5087, pp. 39–49.
[110] Duthinh, D., 1984, "The Head-On Impact of an Iceberg on a Vertical, Gravity-Based Structure," *Proceedings of the Specialty Conference on Computer Methods in Offshore Engineering*, Halifax, NS, Canada, pp. 397–412.
[111] Fuglem, M. K., Duthinh, D., Lever, J. H., and Jordan, I., 1991, "Probabilistic Determination of Iceberg Collision Design Loads for Floating Production Vessels," *Proceedings of IUTAM-IAHR Symposium on Ice-Structure Interaction*, St. John's, Newfoundland, Canada, pp. 459–482.
[112] Salvaggio, M. A., and Rojansky, M., 1986, "The Importance of Wave-Driven Icebergs Impacting an Offshore Structure," *Proceedings of the Offshore Technology Conference OTC'86*, Paper No. OTC 5086, Vol. 1, pp. 29–38.
[113] Nevel, D. E., 1986, "Iceberg Impact Forces," *Proceeding of the International Association of Hydraulic Engineering and Research Symposium (IAHR) on Ice*, Iowa City, IA, Vol. 3, pp. 345–365.
[114] Holthe, K., 1989, "A Numerical Model for Predicting the Response of Concrete Gravity Platforms to Iceberg Impact," *Proceedings of the Tenth International Conference on Port and Ocean Engineering Under Arctic Conditions-POAC'89*, Luleå, pp. 527–536.
[115] Alekseev, Yu. N., Belijashov, V. A., Sazonov, K. E., and Starovoitov, O. M., 1991, "New Aspects of Ice/Structure Interaction Problems," *Proceedings of the First International Offshore and Polar Engineering Conference*, Edinburgh, Scotland, pp. 515–519.
[116] Isaacson, M., 1987, "Ice Mass Motion Near Offshore Structure," ASME J. Offshore Mech. Arct. Eng., **19**, pp. 209–210.
[117] Isaacson, M., 1988, "Influence of Wave Drift Force on Ice Mass Motions," *Proceedings of the Seventh International Conference on Offshore Mechanics and Arctic Engineering, OMAE'88*, Houston, TX, Vol. 2, pp. 125–130.
[118] Kurdyumov, V. A., and Kheisin, D. E., 1976, "Hydrodynamic Model of the Impact of a Solid on Ice," Prikl. Mekh., **12**(10), pp. 103–109.
[119] Bhat, S. U., 1988, "Analysis for Splitting of Ice Floes During Summer Impact," Cold Regions Sci. Technol., **5**(1), pp. 53–63.
[120] Maes, M. A., Jordaan, I. J., Appleby, J. R., and Fidjestøl, P., 1984, "Risk Assessment of Ice Loading for Fixed Structures," *Proceedings of the International Offshore Mechanics and Arctic Engineering Symposium, OMAE'84*, LA, Vol. 3, pp. 220–227.
[121] Blanchet, D., 1990, "Design Criteria for Wide Offshore Structures," Can. Geotech. J., **27**(6), pp. 701–725.
[122] Blanchet, D., 1991, "Application of Ice/Structure Interaction Concepts to a Real Time Ice Risk Assessment Computer Model," *Proceedings of the Sixth International Cold Regions Engineering Conference*, West Lebanon, NH, pp. 650–665.
[123] Johnson, R. J., and Prodanovic, A., 1989 "Calculation of Iceberg Impact Forces," *Proceedings of the International Conference on Port and Ocean Engineering Under Arctic Conditions-POAC'89*, Vol. 2, pp. 546–556.
[124] Bass, D., Gaskill, H., and Riggs, N., 1985, "Analysis of Iceberg Impact With Gravity-Base Structures at Hibernia," *Proceedings of the Fourth International Conference on Offshore Mechanics and Arctic Engineering (OMAE'85)*, Vol. 3, pp. 255–259.
[125] Duthinh, D., and Marsden, S., 1986, "Iceberg Impact Load on a Gravity-Based Structure," *Proceedings of the Fourth International Conference on Cold Regions Engineering*, Anchorage, Alaska, pp. 82–92.
[126] Croasdale, K. R., and Metge, M., 1989, "Structure Geometry and Ice Interaction," *Proceedings of the IUTAM Symposium on Ice-Structure Interaction*, St. John's, Newfoundland, Canada, pp. 641–668.
[127] Croasdale, K. R., and Marcellus, R. W., 1981, "Ice Forces on Large Marine Structures," *Proceeding of International Association of Hydraulic Engineering and Research (IAHR) Symposium on Ice*, QB, Canada, Vol. 2, pp. 755–765.

[128] Coutermarsh, B. A., McGilvary, W. R., and Sodhi, D. S., 1992, "Floating Ice Beam Impact Against a Sloped Structure," *Proceedings of the 11th International Offshore Mechanics and Arctic Engineering Symposium*, Arctic/Polar Technology, Calgary, AB, Canada, Vol. 4, pp. 173–181.
[129] Matskevitch, D. G., 1997, "Eccentric Impact of an Ice Feature: Linearized Model," Cold Regions Sci. Technol., **25**, pp. 159–171.
[130] Matskevitch, D. G., 1997, "Eccentric Impact of an Ice Feature: Nonlinear Model," Cold Regions Sci. Technol., **26**, pp. 55–66.
[131] Abrate, S., 1998, *Impact on Composite Structures*, Cambridge University Press, Cambridge, UK.
[132] Schulson, E. M., 1990, "The Brittle Compressive Fracture of Ice," Acta Metall. Mater., **38**(10), pp. 1963–1976.
[133] Schulson, E. M., 1997, "The Brittle Failure of Ice Under Compression," J. Phys. Chem. B, **101**(32), pp. 6254–6258.
[134] Schulson, E. M., 2004, "Compressive Shear Faults Within Arctic Sea Ice: Fracture on Scales Large and Small," J. Geophys. Res., 109(C7), 23 pp.
[135] Batto, R. A., and Schulson, E. M., 1993, "On the Ductile-to-Brittle Transition in Ice Under Compression," Acta Metall. Mater., **41**(7), pp. 2219–2225.
[136] Mellor, M., 1979, "Mechanical Properties of Polycrystalline Ice," *IUTAM Symposium, Proceedings of Physics and Mechanics of Ice*, P. Tryde, ed., Copenhagen, Springer, New York, pp. 217–245.
[137] Mellor, M., and Cole, D. M., 1982, "Deformation and Failure of Ice Under Constant Stress Or Constant Strain-Rate," Cold Regions Sci. Technol., **5**(3), pp. 201–219.
[138] Jones, S. J., 1997, "High Strain-Rate Compression Tests on Ice," J. Phys. Chem. B, **101**(32), pp. 6099–6101.
[139] Schroeder, R. C., and McMaster, W. H., 1973, "Shock-Compression Freezing and Melting of Water and Ice," J. Appl. Phys., **44**(6), pp. 2591–2594.
[140] Nadreau, J. P., Mawwar, A. M., and Wang, Y. S., 1988, "Triaxial Testing of Freshwater Ice at Low Confining Pressure," *ASME Proceedings of the Seventh International Conference Offshore Mechanics and Arctic Engineering*, pp. 117–124.
[141] Melanson, P. M., Meglis, I. L., and Jordaan, I. J., 1998, "The Failure of Ice Under Impact Conditions: Refinement of the Constitutive Model," Research and Development (PERD)/Canadian Hydraulic Center (CHC), PERD/CHS Report No. 7–82.
[142] Saul, M., and Lunford, J. L., 1995, "Damage From Hail Grounds Nearly 100 D/FW Planes Passengers Scramble as Scores of Flights Cancelled," Dallas Morning News, May 1, p. 1A.
[143] Abrate, S., 1991, "Impact on Laminate Composites," Appl. Mech. Rev., **44**(4), pp. 155–190.
[144] Abrate, S., 1997, "Impact on Laminate Composites: Recent Advances," Appl. Mech. Rev., **50**(11), pp. 517–544.
[145] Jackson, W. C., and Poe, C. C., Jr., 1992, "The Use of Impact Force as a Scale Parameter for the Impact Response of Composite Laminates," NASA Technical Memorandum 104189, U.S. Army Aviation Systems Command (AVSCOM), Techical Report No. 92-B-001.
[146] Singh, S., Masiulaniec, K. C., DeWitt, K. J., and Britton, P. K., 1994, "Measurements of the Impact Forces of Shed Ice Striking a Surface," *Proceedings of the 32nd Aerospace Science Meeting and Exhibit*, AIAA Paper No. 94-0713.
[147] Pan, H., and Render, P. M., 1998, "Studies Into Hail Ingestion of Turbofan Engines Using a Rotating Fan and Spinner Assembly," Aeronaut. J., **102**(1011), pp. 45–51.
[148] Lange, M. A., and Ahrens, T. J., 1987, "Impact Experiments in Low-Temperature Ice," Icarus, **69**(3), pp. 506–518.
[149] Kim, H., 1998, "The Damage Resistance of Composite Structures to High Velocity Ice Impacts and Their Tolerance to Impact Damage," Ph.D. thesis, Department of Mechanical and Environmental Engineering, University of California Santa Barbara.
[150] Kim, H., and Edward, K. T., 2000, "Experimental and Numerical Analysis Correlation of Hail Ice Impacting Composite Structures," AIAA J., **38**(7), pp. 1278–1288.
[151] Kim, H., Welch, D. A., and Edward, K. T., 2003, "Experimental Investigation of High Velocity Ice Impacts on Woven Carbon/Epoxy Composite Panels," Composites, Part A, **34**, pp. 25–41.
[152] Gagnon, R. E., Cumming, D., Ritch, R., Browne, R., Johnston, M., Frederking, R., McKenna, R., and Ralph, M., 2002, "Overview of Bergy Bit Impact Trials," *Proceedings of the International Association of Hydraulic Engineering and Research (IAHR)*, University of Otago, Dunedin, New Zealand, pp. 458–465.
[153] Gagnon, R. E., 2004, "Analysis of Laboratory Growler Impact Tests," Cold Regions Sci. Technol., **39**, pp. 1–17.
[154] Timco, G. W., and Frederking, R., 2004, "Probabilistic Analysis of Seasonal Ice Loads on the Molikpaq," *17th International Symposium on Ice*, Saint Petersburg, Russia, June 21–25, Vol. 2, pp. 68–76.
[155] Wright, B., Pikington, G. R., Woolner, K. S., and Wright, W. H., 1986, "Winter Ice Interactions With an Arctic Offshore Structure," *Proceedings of Eighth International Association of Hydraulic Engineering and Research Symposium on Ice*, Iowa City, IA, Vo. III, pp. 49–73.
[156] Masterson, D. M., and Frederking, R., 1993, "Local Contact Pressures in Ship/Ice and Structure/Ice Interactions," Cold Regions Sci. Technol., **21**, pp. 169–185.
[157] Frederking, R. M. W., 2003, "Determination of Local Ice Pressures From Ship Transits in Ice," *Proceedings of the International Society of Offshore and Polar Engineers (ISOPE'03)*, Honolulu, HA, Paper No. 2003-JSC-393.
[158] Jordaan, I. J., Appleby, J., and Fidjestoel, P., 1983, "Ice-Structure Interaction: Some Recent Veritas Approaches," J. Can. Pet. Technol., **22**(6), pp. 55–57.
[159] Jordaan, I. J., Maes, M. A., Brown, P. W., and Hermans, I. P., 1993, "Probabilistic Analysis of Local Ice Pressures," ASME J. Offshore Mech. Arct. Eng., **115**, pp. 83–89.
[160] Maes, M. A., 1989, "Uncertainties and Difficulties in Codified Design for Ice Loading," *Proceedings of the Eighth International Offshore Mechanics and Arctic Engineering Symposium*, Hague, The Netherlands, Vol. 4, pp. 97–103.
[161] Zou, B., 1996, "Ships in Ice: The Interaction Process and Principles of Design," Ph.D. thesis, Memorial University of Newfoundland.
[162] Winkler, M. M., and Reece, A. M., 1986, "Probabilistic Model for Multiyear Ice Ridge Loads on Conical Structures," *IAHR Symposium on Ice*, University of Iowa, Vol. 1, pp. 159–170.
[163] Jordaan, I. J., and Xiao, J., 1999, "Compressive Ice Failure," *Proceedings of the International Association of Hydraulic Engineering and Research (IAHR) Symposium on Ice*, Potsdam, New York, pp. 1025–1031.
[164] Carter, J. E., Daley, C., Fuglem, M., Jordaan, I. J., Koinonen, A., Revill, C., Butler, T., Muggeridge, K., and Zou, B., 1995, "Maximum Bow Force for Arctic Shipping Pollution Prevention Regulations—Phase II," Ocean Engineering Research Center, Memorial University of Newfoundland, Canadian Coast Guard, Arctic Ship Safety, p. 247.
[165] Fuglem, M., and Jordaan, I. J., 1999, "Estimation of Maximum Bow Force for Arctic Vessels," *Proceedings of the International Association of Hydraulic Engineering and Research (IAHR) Symposium on Ice*, Potsdam, New York, pp. 947–955.
[166] Cowper, B., and Edgecomb, M., 1987, "The 1985 Global Ice Impact Tests on the USCG Polar Sea," Transport Canada Development Center, Report No. TP8496E.
[167] Edgecomb, M., St. John, J. W., Liljestrom, G., and Ritch, A., 1992, "Full Scale Measurement of Hull-Ice Impact Loads and Propulsion Machinery Response Onboard I/B Oden During the 1991 International Arctic Ocean Expedition," Canadian Coast Guard Northern, Report No. TP11252E.
[168] Jordaan, I. J., 1987, "Probabilistic Analysis of Environmental Data for Design of Fixed and Mobile Arctic Offshore Structures," Reliability and Risk Analysis in Civil Engineering, *Proceedings of the Fifth International Conference on Applications of Statistics and Probability in Soil and Structural Engineering (ICASP5)*, Vancouver, Vol. 2, pp. 1130–1137.
[169] Morsy, U. A., and Brown, T. G., 1993, "Modeling for Ice-Structure Interactions," *Proceedings of the 12th International Conference on Offshore Mechanics and Arctic Engineering, OMAE*, Arctic/Poar Technology, Glasgow, UK, Vol. 4, pp. 119–125.
[170] Brown, P. W., Jordaan, I. J., Nessim, M. A., and Haddara, M. M. R., 1996, "Optimization of Bow Plating for Icebreakers," J. Ship Res., **40**(1), pp. 70–78.
[171] Jordaan, I. J., 2001, "Mechanics of Ice-Structure Interaction," Eng. Fract. Mech., **68**, pp. 1923–1960.
[172] Jordaan, I. J., Fuglem, M., and Matskevitch, D. G., 1996, "Pressure-Area Relationships and the Calculation of Global Ice Forces," *Proceedings of the International Association of Hydraulic Engineering and Research (IAHR) Symposium on Ice*, Beijing China, Vol. 1, pp. 166–175.
[173] 1973, *Ice Navigation Qualities of Ships*, D. I. Kheisin and Y. N. Popov, eds., Cold Regions Research and Engineering Laboratory (CRREL), Hanover, NH, Draft Translation 417.
[174] Korri, P., and Varsta, P., 1979, "On the Ice Trial of a 14500 dwt Tanker on the Gulf of Bothnia," Society of Naval Architects in Finland (LARADI), Report No. NSTM-79.
[175] Vuorio, J., Riska, K., and Varsta, P., 1979, "Long-Term Measurements of Ice Pressure and Ice-Induced Stresses on the Icebreaker Sisu in Winter 1978," Winter Navigation Research Board, Report No. 28.
[176] Ghoneim, G. A. M., and Keinonen, A. J., 1983, "Full Scale Impact Tests on Cannar Kigoriak in Thick Ice," *Proceedings of the Seventh International Conference on Port and Ocean Engineering Under Arctic Conditions, POAC'83, VTT Symposium, 27*, Technical Research Center of Finland, Espoo, Finland, pp. 329–346.
[177] Daley, C. G., St. John, J. W., Seibold, F., and Bayly, I., 1984, "Analysis of Extreme Ice Loads Measured on USCGS Polar Sea," Soc. Nav. Archit. Mar. Eng., Trans., **92**, pp. 241–252.
[178] Jordaan, I. J., Nessim, M. A., Ghoneim, G. A., and Murray, M. A., 1987, "A Rational Approach to the Development of Probabilistic Design Criteria for Arctic Shipping," *Sixth International Offshore Mechanics and Arctic Engineering Symposium, OMAE'87*, Vol. 4, pp. 401–406.
[179] Jordaan, I. J., Maes, M. A., Brown, P. W., and Hermans, I. P., 1993, "Probabilistic Analysis of Local Ice Pressure," ASME J. Offshore Mech. Arct. Eng., **115**, pp. 83–89.
[180] Nessim, M. A., Cheung, M. S., and Jordaan, I. J., 1987, "Ice Action on Fixed Offshore Structures: A State-of-the-Art Review," Can. J. Civ. Eng., **14**(3), pp. 381–407.
[181] Varsta, P., 1983, "On the Mechanics of Ice Load on Ships in Level Ice in the Baltic Sea," Ph.D. thesis, Technical Research Center of Finland, Espoo, Finland.
[182] Varsta, P., 1984, "Determination of Ice Loads Semi-Empirically," *Ship Strength and Winter Navigation, Technical Research Center of Finland VTT Symposium 52*, Espoo, Finland.
[183] Riska, K., 1987, "On the Mechanics of the Ramming Interaction Between a Ship and a Massive Ice Floe," Doctor of Technology thesis, Technical Research Center of Finland, Espoo, Finland.
[184] Carter, J. E., Frederking, R. M. W., Jordaan, I. J., and Crocker, G., 1992, "Review and Verification of Proposals for the Arctic Shipping Pollution Pre-

vention Regulations," Ocean Engineering Research Center, Memorial University of Newfoundland, Canadian Coast Guard, Arctic Ship Safety.
[185] Fuglem, M., Jordaan, I. J., and Crocker, G., 1996, "Iceberg-Structure Interaction Probabilities for Design," Can. J. Civ. Eng., **23**(1), pp. 231–241.
[186] Fuglem, M., Muggeridge, K., and Jordaan, I. J., 1999, "Design Load Calculations for Iceberg Impacts," Int. J. Offshore Polar Eng., **9**(4), pp. 298–306.
[187] Jordaan, I. J., 2000, "Experience Using Probabilistic Methods in Problems of the Canadian Frontier," *Proceedings of the Eight Conference on Applications of Statistics and Probability*, R. E. Melchers and M. G. Stewart, eds., Belkman, pp. 1219–1226.
[188] Brown, P. W., Jordaan, I. J., and Croasdale, K. R., 2002, "Probabilistic Analysis of Ice Loads for the Confederation Bridge," Can. J. Civ. Eng., **28**(4), pp. 562–573.
[189] Kujala, P., 1994, "On the Statistics of Ice Loads on Ship Hull in the Baltic Sea," Ph.D. thesis, Acta Polytechnic Scandinavia, Mechanical Engineering, Helsinki.
[190] Kujala, P., 1996, "Semi-Empirical Evaluation of Long Term Ice Loads on a Ship Hull," Mar. Struct., **9**, pp. 849–871.
[191] Bea, R. G., 1993, "Evaluation of Uncertainties in Loadings on Offshore Structures Due to Extreme Environmental Conditions," ASME J. Offshore Mech. Arct. Eng., **115**(4), pp. 237–245.
[192] Croasdale, K. R., and Brown, T., 2000, "Ice Load Uncertainties: Progress in Their Resolution," *Proceedings of the International Offshore and Polar Engineering Conference*, Seattle, WA, Vol. 1, pp. 583–588.
[193] Wu, X., Wang, A. T., Heuer, C. E., Ralston, T. D., Davenport, G. F., and Toro, G., 2002, "A Reliability-Based Method for Determining Design Ice Loads on Offshore Structures," *Proceedings of the International Conference on Offshore Mechanics and Arctic Engineering, OMAE*, Oslo, Norway, Vol. 3, pp. 645–652.
[194] Hakala, M. K., 1980, "A Nonlinear Finite Element Analysis of an Ice-Strengthened Ship Shell Structure," Comput. Struct., **12**(4), pp. 541–547.
[195] Horrigmoe, G., and Andersen, R., 1994, "Nonlinear Finite Element Analysis of Ice-Structure Interaction at Varying Strain Rates," *Proceedings of the Fourth International Offshore and Polar Engineering Conference*, Vol. 2, pp. 521–525.
[196] Chiu, R., Heciski, E., and Hirsimaki, M., 1981, "Application of Plastic Analysis to US Coast Guard Icebreaker Shell Plating," Soc. Nav. Archit. Mar. Eng., Trans., **89**, pp. 249–274.
[197] Wiernicki, C., 1987, "Damage of Ship Plating Due to Ice Impact Loads," Mar. Struct., **24**, pp. 43–58.
[198] Daley, C. G., 2001, "Derivation of Plastic Framing Requirements for Polar Ships," Mar. Struct., **15**, pp. 543–559.
[199] IACS, 2001, "Unified Requirements for Polar Ships," PSI—Polar Ship Structures. Draft Requirements. International Association of Classification Societies.
[200] Daley, C. G., 2000, "Background Notes to Design Ice Loads—IAC Unified Requirements for Polar Ships," Prepared for IACS Ad-Hoc Group on Polar Class Ships and Transport, Canada, January.
[201] Daley, C. G., 2001, "Oblique Ice Collision Loads on Ships Based on Energy Methods," Ocean Engineering International, **5**(2), pp. 67–72.
[202] FMA, 2002, Finnish-Swedish Ice Class Rules, FMA Bulletin No. 13/1.10.2002, Finish Maritime Administration.
[203] FMA, 2003, Tentative Guidelines for Application of Direct Calculation Methods for Longitudinally Framed Hull Structure, Finish Maritime Administration.
[204] FMA, 2003, Background for the Tentative Guidelines for Application of Direct Calculation Methods for Longitudinally Framed Hull Structure, Finish Maritime Administration and Helsinki University of Technology.
[205] FMA, 2004, Guidelines for the Application of the Finnish-Swedish Ice Class Rules, Finnish Maritime Administration.
[206] ABS, 2004, Guidance Notes on Nonlinear Finite Element Analysis of Side Structures Subject to Ice Loads, American Bureau of Shipping (ABS) (www.eagle.org).
[207] ABS, 2005, Guidance Notes on Ice Class, American Bureau of Shipping (ABS) (www.eagle.org).
[208] Card, J., Haugland, B. K., and Pomeroy, V., 2004, "Developing the Next Generation of Classification Rules for Oil Tankers," Royal Institution of Naval Architects, pp. 128–140.
[209] ABS, 2003, Rules for Building and Classing Steel Barges, Rules Change Notice, 1, March 2005, American Bureau of Shipping (ABS) (www.eagle-.org).
[210] ABS, 2005, Rules for Building and Classing Steel Vessels, American Bureau of Shipping (www.eagle. org).
[211] Wang, G., Basu, R., Chavda, D., and Liu, S., 2004–2005, "Rationalizing of the Design of Ice Strengthened Structures" (www.eagle.org).
[212] Wang, G., Basu, R., and Chavda, D., 2005, "A Trend in Rationalizing Design of Ice Strengthening Side Structures," *International Congress of International Maritime Association of the Mediterranean (IMAM)*, Lisboa, Portugal, Sept. 26–30.
[213] Wang, G., Basu, R., Chavda, D., Liu, S., Lee, M., Suh, Y., and Han, Y., 2005, "Rationalizing of the Design of Side Structure of Ice Strengthened Tankers," *Proceedings of the 15th International Conference of Offshore and Polar Engineering (ISOPE 2005)*, Seoul, Korea.
[214] Wang, G., and Wiernicki, C. J., 2006, "Using Nonlinear Finite Element Method to Design Ship Structures for Ice Loads," Marine Technology, **43**(1), pp. 1–15.
[215] Wang, G., Liu, S., and Riska, K., 2006, "Recent Advances in Structural Design of Ice-Strengthened Vessels," *Proceedings of the Seventh International Conference and Exhibition on Performance of Ships and Structures in Ice*, Banff, Canada, July 16–19, Paper No. ICETECH06-127-RF.
[216] RS, 2006, Russian Maritime Register of Shipping, ID: 554.
[217] Kawasaki, T., Taguchi, Y., Kayo, Y., Fujishima, K., Yano, S., Nawata, T., and Kaminokado, S., 1987, "Study of Ice Forces for Offshore Structures," Mitsubishi Heavy Industries, Mitsubishi Technical Bulletin, January, No. 174, p. 26.
[218] Kawasaki, T., Tozawa, S., Kayo, Y., and Yano, S., 1994, "Industrial Research and Development of Ice Technology," *Proceedings of the Fourth International Offshore and Polar Engineering Conference*, Osaka, Japan, Vol. 2, pp. 503–508.
[219] Kato, K., Kamesaki, K., Akagawa, S., Takeuchi, T., Kawasaki, T., Nakazawa, N., and Kurokawa, A., 1999, "Study on Ice Loads Acting on Marine Structures: Interim Report of JOIA Project," *Proceedings of the Ninth International Offshore and Polar Engineering Conference*, Vol. 2, pp. 483–490.
[220] Saeki, H., Hiyayama, K., Kawasaki, T., Akagawa, S., Kato, K., Kamesaki, K., Saka, K., and Kurokawa, A., 1997, "JOIA Project of Study on Ice Load," *Proceedings of the Seventh International Offshore and Polar Engineering Conference*, Honolulu, HI, Vol. 2, pp. 349–355.
[221] Blenkarn, K. A., 1970, "Measurement and Analysis of Ice Forces on Cook Inlet Structures," *Proceedings of Offshore Technology Conference (OTC)*, Houston, TX, Vol. II, pp. 365–378.
[222] Määttänen, M., 1977, "Stability of Self-Excited Ice-Induced Structural Vibration," *Fourth International Conference on Port and Ocean Engineering Under Arctic Conditions*, Newfoundland, pp. 684–694.
[223] Määttänen, M., 1980, "Ice Force on Fixed, Flexible Structures," A State-of-the-Art Report by the Working Group on Ice Forces on Structures, International Association of Hydraulic Engineering and Research (IAHR), U.S. Army Cold Regions Research and Engineering Laboratory, Special Report No. 80-26, ADA 089674.
[224] Määttänen, M., 1981, "Ice Structure Dynamic Interaction: Ice Forces Versus Velocity, Ice-Induced Damping," *Proceedings of Quebec 1981 International Association of Hydraulic Research International Symposium on Ice Problems*, Laval University, QB, Canada, July 27–31, pp. 783–796.
[225] Määttänen, M., 1983, "Dynamic Ice-Structure Interaction During Continuous Crushing," U.S. Army Cold Regions Research and Engineering Laboratory, CREL Report No. 83-5.
[226] Neill, C., 1976, "Dynamic Ice Forces on Piers and Piles: An Assessment of Design Guidelines in the Light of Recent Research," Can. J. Civ. Eng., **3**(2), pp. 305–341.
[227] Peyton, H. R., 1966, *Sea Ice Strength*, Final Report to the Office of Naval Research, Geophysical Institute, University of Alaska Geophysical Institute, Report No. 182.
[228] Peyton, H. R., 1968, "Sea Ice Forces," National Research Council of Canada, Technical Memo 92.
[229] Peyton, H. R., 1968, "Ice and Marine Structures, Part 1: The Magnitude of Ice Forces Involved in Design," Ocean Industry, **3**(3), pp. 40–44.
[230] Eranti, E., Haynes, F. D., Määttänen, M., and Soong, T. T., 1981, "Dynamic Ice-Structure Interaction Analysis for Narrow Vertical Structures," *Proceedings of the Sixth International Conference on Port and Ocean Engineering Under Arctic Conditions*, Laval University, QB, Canada, July 27–31, pp. 472–479.
[231] Eranti, E., 1991, "General Theory of Dynamic Ice Structure Interaction With Applications," *Proceedings of the First International Offshore and Polar Engineering Conference*, Edinburgh, Scotland, pp. 489–498.
[232] Eranti, E., 1992, "Ice Forces in Dynamic Ice Structure Interaction," Int. J. Offshore Polar Eng., **2**(3), pp. 204–211.
[233] Matskevitch, D. G., 1995, "Static and Dynamic Analysis of the Ice-Structure Interaction Under the Slippage Boundary Conditions," *Proceedings of the 14th International Conference on Offshore Mechanics and Arctic Engineering—OMAE*, Copenhagen, Vol. 4, pp. 1–8.
[234] Yue, Q. Ji, Du, X. Z., Bi, X. J., and Zhang, X., 2004, "Dynamic Ice Loads During Interaction With Vertical Compliant Structures," (in Chinese) Chin. J. Eng. Mech., **21**(1), pp. 202–208.
[235] Peyton, H. R., 1968, "Ice and Marine Structures, Part 2: Sea Ice Properties," Ocean Industry, **3**(9), pp. 59–65.
[236] Peyton, H. R., 1968, "Ice and Marine Structures, Part 3: The Importance of Design Alternatives," Ocean Industry, **3**(12), pp. 51–58.
[237] Matlock, H., Dawkins, W. P., and Panak, J. J., 1971, "Analytical Model for Ice-Structure Interaction," J. Engrg. Mech. Div., **97**(EM4), pp. 1083–1092.
[238] Toyama, Y., Sensu, T., Minamami, M., and Yashima, N., 1983, "Model Tests on Ice-Induced Self-Excited Vibration of Cylindrical Structure," *Proceedings of the Seventh International Conference on Port and Ocean Engineering in Arctic Conditions*, Helsinki, Vol. II, pp. 834–844.
[239] Engelbrektson, A., 1997, "A Refined Ice/Structure Interaction Model Based on Observations in the Gulf of Bothnia," *Proceedings of Offshore Mechanics and Arctic Engineering Conference (OMAE)*, Yokohama, Japan, Vol. 4, pp. 373–376.
[240] Nordlund, O. P., Kärnä, T., and Järvinen, E., 1988, "Measurements of Ice-Induced Vibration of Channel Markers," *Proceedings of the Ninth Proceedings of the International Association of Hydraulic Engineering and Research (IAHR) Ice Symposium*, Sapporo, Vol. 2, pp. 637–548.
[241] Jefferies, M., and Wright, W. H., 1988, "Dynamic Response of Molikpaq to Ice-Structure Interaction," *Proceedings of the Conference on Offshore Mechanics and Arctic Engineering*, pp. 201–220.
[242] Tsuchiya, M., Kanie, S., and Ikejiri, K., Yoshida, A., and Saeki, H., 1985,

"An Experimental Study on Ice-Structure Interaction," *Proceedings 17th Offshore Technology Conference (OTC)*, Astrodomain, Houston, TX, Vol. 4, pp. 321–327.
[243] Xu, J., and Wang, L., 1986, "Ice Force Oscillator Model for Dynamic Ice-Structure Interaction Analysis," *Proceedings of the First International Conference on Ice Technology*, pp. 391–396.
[244] Wang, L., and Xu, J., 1991, "Description of Dynamic Ice-Structure Interaction and the Ice Force Oscillator Model," *Proceedings of the 11th International Conference on Port and Ocean Engineering Under Arctic Conditions, POAC*, St. John's, Newfoundland, Vol. 1, pp. 141–154.
[245] Shih, L. Y., 1991, "Analysis of Ice-Induced Vibrations on a Flexible Structure," Appl. Math. Model., **15**, pp. 632–638.
[246] Sodhi, D. S., 1988, "Ice-Induced Vibrations of Structures," *Proceedings of the Ninth International Association of Hydraulic Engineering and Research Symposium on Ice*, Sapporo, Japan, Vol. II, pp. 625–657.
[247] Sundararajan, C., and Reddy, D. V., 1973, "Stochastic Analysis of Ice-Structure Interaction," *Proceedings of the Second International Conference Port and Ocean Engineering Under Arctic Conditions (POAC)*, Rykjavik, Iceland, pp. 345–353.
[248] Sundararajan, C., and Reddy, D. V., 1977, "Probabilistic Analysis of Ice-Offshore Structure Interaction Using Enveloping Step Function Power Spectral Densities," Can. J. Civ. Eng., **4**(4), pp. 455–461.
[249] Reddy, D. V., and Cheema, P. S., 1974, "Response of an Offshore Structure to Random Ice Forces," *Proceedings of the IEEE International Conference on Engineering in the Ocean Environment*, Halifax, Vol. I, pp. 84–88.
[250] Reddy, D. V., Cheema, P. S., and Swamidas, A. S. J., 1975, "Ice Force Response Spectrum Modal Analysis of Offshore Towers," *Proceedings of the Third Port and Ocean Engineering Under Arctic Conditions (POAC)*, University of Alaska.
[251] Reddy, D. V., Cheema, P. S., Swamidas, A. S. J., and Haldar, A. A., 1975, "Stochastic Response of a Three-Dimensional Offshore Tower to Ice Force," *Proceedings of the International Association of Hydraulic Engineering and Research IAHR/AIRH Third Symposium on Ice Problems*, Hanover, NH, pp. 499–514.
[252] Swamidas, A. S. A., and Reddy, D. V., 1976, "Dynamic Ice Structure Interaction of Offshore Monopod by Hybridization of the Computer Programs EATSW and SAP-IV," *Proceedings of the First SAP-IV User's Conference*, Los Angeles, CA, pp. 1–33.
[253] Swamidas, A. S. A., Reddy, D. V., and Purcell, G., 1977, "Ice-Structure Interaction With Artificially Generated Force Records," J. Glaciol., **19**(81), pp. 265–283.
[254] Haldar, A. K., 1977, "Dynamic Response of a Framed Offshore Tower to Ice Force Considering Nonlinear Soil-Structure Interaction, M.Eng. thesis, Memorial University, Newfoundland, St. John's.
[255] Haldar, A. K., Swamidas, A. S., Reddy, D. V., and Arockiasamy, M., 1977, "Dynamic Ice-Water-Ice-Structure Interaction of Offshore Towers Including Nonlinear Soil Behavior," *Proceedings of the Ninth Annual Offshore Technology Conference (OTC)*, pp. 225–234.
[256] Afanasev, V. P., 1973, "Ice Pressure on Vertical Structures," NRC, Ottawa, Canada, Technical Translation 1708, pp. 1–6.
[257] Meng-Lan, D., 1993, *Low Temperature Fatigue and Damage of Offshore Fixed Platforms Under Random Ice Loads*, Ph.D. thesis, University of Petroleum, China.
[258] Chun-Tu, L., and Meng-Lau, D., 1996, "Experimental Investigation on Low-Temperature Fatigue Crack Propagation in Offshore Structural Steel A131 Under Random Sea Ice Loading," Eng. Fract. Mech., **53**(2), pp. 231–237.
[259] Sodhi, D. S., 1994, "Theoretical Model for Ice-Structure Interaction," *Proceedings of the 13th International Conference on Offshore Mechanics and Arctic Engineering—OMAE*, Houston, TX, Vol. 4, pp. 29–34.
[260] Sodhi, D. S., 2001, "Crushing Failure During Ice-Structure Interaction," Eng. Fract. Mech., **68**, pp. 1889–1921.
[261] Marcellus, R. W., Sander, M., Sinha, N. K., and Shah, V. K., 1990, "Theoretical Dynamic Ice Structure Interaction Model for Crushing With Extrusion," *Proceedings of the Ninth International Offshore Mechanics and Arctic Engineering Symposium*, Vol. 4, Arctic/Polar Technology, Houston, TX, pp. 95–101.
[262] Marcellus, R. W., 1991, "Dynamic Unloading: Is It the Missing Link in Ice Crushing and Ice-Structure Interaction Modelling?," *Proceedings of the 11th International Conference on Port and Ocean Engineering Under Arctic Conditions, POAC*, Vol. 1, pp. 109–125.
[263] Tuhkuri, J., and Riska, K., 1990, "Results From Tests on Extrusion of Crushed Ice," The Ship Laboratory, Helsinki University of Technology, Report No. M-89.
[264] Tuhkuri, J., 1994, "Analysis of Ice Fragmentation Process From Measured Particle Size Distributions of Crushed Ice," Cold Regions Sci. Technol., **23**(1), pp. 69–82.
[265] Nixon, W. A., Marcellus, R. W., and Weber, L. J., 1993, "Elastic Analysis of Stresses in Ice Structure Interactions," *Proceedings of the 12th International Conference on Offshore Mechanics and Arctic Engineering—OMAE*, Arctic/Polar Technology, Glasgow, UK, Vol. 4, pp. 83–88.
[266] Liu, Y., Wu, Y., Song, L., Shen, Z., and Duan, M., 2001, "A Dynamic Vibration Model for Ice-Structure Interaction," *Proceedings of the 20th International Conference on Offshore Mechanics and Arctic Engineering—OMAE*, Polar and Arctic Pipeline Technology, Rio de Janeiro, Brazil, Vol. 4, pp. 29–36.
[267] Määttänen, M., 1982, "Laboratory Tests for Dynamic Ice-Structure Interaction," Eng. Struct., **3**, pp. 111–116; also "On Conditions for the Rise of Self-Excited Ice-Induced Autonomous Oscillations in Slender Marine Pile Structures," Winter Nav. Board, Finland, Research Report No. 25.
[268] Kärnä, T., and Trunen, R., 1989, "Dynamic Response of Narrow Structures to Ice Crushing," Cold Regions Sci. Technol., **17**, pp. 173–187.
[269] Kärnä, T., 1992, "A Procedure for Dynamics Soil-Structure-Ice Interaction," *Proceeding Second International Offshore and Polar Energy Conference (ISOPE'92)*, San Francisco, CA, Vol. II, pp. 764–770.
[270] Kärnä, T., and Järvinen, E., 1994, "Dynamic Unloading Across the Face of a Wide Structure," *Proceedings of the 12th International Association of Hydraulic Engineering and Research on Ice Symposium (IAHR'94)*, Trondheim, Vol. 3, pp. 1018–1039.
[271] Takeuchi, T., and Saeki, H., 1995, "Indentation Pressure in Ice/Vertical Structure Interaction," Int. J. Offshore Polar Eng., **5**(4), pp. 279–285.
[272] Takeuchi, T., Sasaki, M., Akagawa, S., Kawamura, M., Sakai, M., Hamana, Y., Kurokawa, A., and Saeki, H., 1999, "Contact Ratio in Ice/Structure Interaction Based on Statistical Generation of Ice Failure Surface," *Proceedings of the Ninth International Offshore and Polar Engineering Conference*, Vol. 2, pp. 505–511.
[273] Hocking, G., Mustoe, G. C. W., and Williams, J. R., 1985, "Validation of the CICE Code for the Ice Ride-Up and Ice Ridge Cone Interaction," *ASCE Specialty Conference on Civil Engineering in the Arctic Offshore*, San Francisco, CA, pp. 962–970.
[274] Hocking, G., Williams, J. R., and Mustoe, G. C. W., 1985, "Dynamic Global Forces on Offshore Structure From Large Ice Flow Impacts," *ASCE Specialty Conference on Civil Engineering in the Arctic Offshore*, San Francisco, CA, pp. 202–219.
[275] Hocking, G., Mustoe, G. C. W., and Williams, J. R., 1987, "Dynamic Analysis for Generalized Three-Dimensional Contact and Fracturing for Multiple Bodies," *Proceedings of the International Conference on Numerical Methods in Engineering: Theory and Applications-NUMETA'87*, Swansea, UK, Balkema, The Netherlands.
[276] Williams, J. R., Mustoe, G. G. W., and Worgan, K., 1986, "Force Transfer and Behavior of Rubble Piles," *Proceedings of International Association of Hydraulic Engineering and Research Symposium on Ice*, Iowa City, IA, Vol. I, pp. 615–626.
[277] Vipulanandan, C., and Williams, A. N., 1989, "Effect of Interface Conditions on Dynamic Ice-Structure Interaction," ASME J. Offshore Mech. Arct. Eng., **111**(1), pp. 70–77.
[278] Mustoe, G. G. W., Williams, J. R., Hocking, G., and Worgan, K., 1987, "Penetration and Fracturing of Brittle Plates Under Dynamic Impact," *Proceedings of the International Conference on Numerical Methods in Engineering: Theory and Applications-NUMETA'87*, Swansea, UK, Balkema, The Netherlands.
[279] Selvadurai, A. P. S., and Sepehr, K., 1999, "Two-Dimensional Discrete Element Simulations of Ice-Structure Interaction," Int. J. Solids Struct., **36**, pp. 4919–4940.
[280] Bekker, A. R., and Rudetsk, V. A., 1994, "Initial Conditions of Ice-Structure Interaction Problems," *Proceedings of the ASME 13th International Conference on Offshore Mechanics and Arctic Engineering—OMAE*, Houston, TX, Vol. 4, pp. 89–91.
[281] Bekker, A. R., and Rudetsk, V. A., 1994, "About Initial Conditions of Ice-Structure Interaction Problems," *Proceedings of the Fourth International Offshore and Polar Engineering Conference*, Osaka, Japan, Vol. 2, pp. 514–516.
[282] Bekker, A. T., 1995, "Ice-Structure Dynamic Interaction: Failure Ice Model," *Proceedings of the 14th International Conference on Offshore Mechanics and Arctic Engineering—OMAE*, Copenhagen, Vol. 4, pp. 41–45.
[283] Bekker, A. T., Uvarova, T. E., and Chetyrbotsky, A. N., 1998, "Interactive Model of Ice-Structure Interaction," *Proceedings of the Eighth International Offshore and Polar Engineering Conference*, Montreal, Canada, Vol. 2, pp. 493–496.
[284] Bekker, A. T., Uvarova, T. E., Kim, S. D., Seliverstov, V. I., and Kharitonova, E. A., 2001, "Loading Regime of Ice-Structure Interaction," *Proceedings of the 11th International Offshore and Polar Engineering Conference*, Vol. 1, pp. 761–769.
[285] Bekker, A. T., Uvarova, T. E., and Kim, S. D., 2004, "Numerical Simulation of the Process of Interaction Between Drifting Ice Fields and Structure Support," *Proceedings of the Sixth ISOPE Pacific/Asia Offshore Mechanics Symposium*, Vladivostok, Russian Federation, pp. 123–128.
[286] Bekker, A. T., Uvarova, T. E., and Kim, S. D., 2004, "Model of Mechanical Ice-Structure Interaction for Sakhalin Offshore Conditions," *Proceedings of the 14th International Offshore and Polar Engineering Conference, Proceedings of the 14th International Offshore and Polar Engineering Conference—ISOPE*, Toulon, France, pp. 885–890.
[287] Makrygiannis, C., McKenna, R., Wright, B., Allyn, N., Sildnes, T., Jolles, W., Morland, M., and Grant, R., 2006, "The Development of Arctic Standard for Floating Production Systems," *Proceedings of the Seventh International Conference and Exhibition on Performance of Ships and Structures in Ice*, Banff, Canada, July 16–19, Paper No. ICETECH06-150-RF.
[288] Miura, F., and Wang, J., 1994, "Effect of Ice on Nonlinear Seismic Responses of an Off-Shore Structure Surrounded by Thick Ice Considering Dynamic Interaction With Water," (in Japanese) *Doboku Gakkai Rombun-Hokokushu/Proceedings of the Japan Society of Civil Engineers*, Vol. 483, pp. 117–125.
[289] Adachi, H., Yashima, N., Nakanishi, M., Sato, K., Takada, Y., and Okamoto, N., 1997, "Seismic Response of Offshore Platforms in Ice-Covered Seas (Part 1: Dynamic Ice—Structure Interaction)," *Proceedings of the 16th International Conference on Offshore Mechanics and Arctic Engineering—OMAE*, Arctic/Polar Technology, Yokohama, Japan, Vol. 4, pp. 301–306.

[290] Yamauchi, Y., and Kamesaki, K., 2000, "Experimental Study on Ice-Structure Interaction During Earthquakes," *Proceedings of the International Offshore and Polar Engineering Conference*, Seattle, WA, Vol. 1, pp. 569–576.
[291] Yamauchi, Y., and Kamesaki, K., 2001, "Experimental Study on Ice-Structure Interaction During Earthquakes," Int. J. Offshore Polar Eng., **11**(4), pp. 290–297.
[292] Yamauchi, Y., Kamesaki, K., and Hyodo, M., 2002, "Numerical Simulation on Ice-Structure Interaction During Earthquakes," *Proceedings of the 12th International Offshore and Polar Engineering Conference*, Kitakyushu, Japan, Vol. 12, pp. 802–807.
[293] Kheisin, D. E., and Cherepanov, N. W., 1973, "Change of Ice Structure in the Zone of Impact of a Solid Body Against the Ice Cover Surface," *Problems of the Arctic and Antarctic*, A. F. Treshnikov, ed., pp. 239–245 (trans. from Russian by National Science Foundation, Washington, DC, Division of Polar Programs, Report TT-77-52041, 1981, 175 pp.).
[294] Xiao, J., Jordaan, I. J., and Singh, S. K., 1992, "Pressure Melting and Friction in Ice-Structure Interaction," *Proceedings of the 11th International Association of Hydraulic Engineering and Research (IAHR) Symposium on Ice*, Banff AB, Vol. 3, pp. 1255–1268.
[295] Dempsey, J. P., Palmer, A. C., and Soghi, D. S., 2001, "High Pressure Zone Formation During Compressive Ice Failure," Eng. Fract. Mech., **68**, pp. 1961–1974.
[296] Danys, J. V., and Bercha, F. G., 1976, "Investigations of Ice Forces on a Conical Offshore Structure," Ocean Eng., **3**(5), pp. 299–308.
[297] Bercha, F. G., Danys, J. V., and Rokne, J. G., 1978, "Probabilistic Ice-Structure Interaction Theory," *ACS Symposium Series of the International Association of Hydraulic Research, Ice Problems*, Lulea, Sweden, Vol. 1, pp. 77–95.
[298] Bercha, F. G., Brown, T. G., and Cheung, M. S., 1985, "Local Pressure in Ice-Structure Interactions," *ASCE Civil Engineering in the Arctic Offshore, Proceedings of the Conference Arctic '85*, San Francisco, CA, pp. 1243–1251.
[299] Izumiyama, K., Kitagawa, H., Koyama, K., and Uto, S., 1991, "On the Interaction Between a Conical Structure and Ice Sheet," *Proceedings of the 11th International Conference on Port and Ocean Engineering Under Arctic Conditions, POAC*, St. John's, Newfoundland, Vol. 1, pp. 155–166.
[300] Riska, K., Baarman, L., and Muhonen, A., 1993, "Modeling of Ice Induced Vibration of Slender Offshore Structures," The Arctic Offshore Research Center, Helsinki University of Technology, Report No. M-172.
[301] Poplin, J. P., and Timco, G. W., 2003, "Ice Damage Zone Around Conical Structures: Implications for Evacuation," *Proceedings of the 17th International Conference on Port and Ocean Engineering Under Arctic Conditions-POAC'03*, Norwegian University of Science and Technology, Trondheim, Norway, Vol. 2, pp. 797–906.
[302] Barker, A., Timco, G., Gravesen, H., and Vølund, P., 2005, "Ice Loading on Danish Wind Turbines, Part I: Dynamic Model Tests," Cold Regions Sci. Technol., **41**, pp. 1–23.
[303] Gravesen, H., Vølund, P., Timco, G., and Barker, A., 2005, "Ice Loading on Danish Wind Turbines, Part 2: Analysis of Results," Cold Regions Sci. Technol., **41**, pp. 25–47.
[304] Daley, C. G., Tuhkuri, J., and Riska, K., 2000, "Discrete Chaotic Ice Failure Model Incorporating Extrusion Effects" (www.engr.mun.ca).
[305] Timco, G. W., Barker, A., and Durand, N., 2005, "Ice Rubble Fields Around Offshore Structures in the Beaufort Sea," National Research Council of Canada Report.
[306] Timco, G. W., Wright, B. D., Barker, A., and Poplin, J. P., 2006, "Ice Damage Zone Around the Molikpaq: Implications for Evacuation Systems," Cold Regions Sci. Technol., **44**, pp. 67–85.
[307] Kärnä, T., Jochmann, P., Maattanen, M., Evers, K. U., Kolari, K., Xiangjun, B., and Martonen, P., 2003, "Tests on Dynamic Ice-Structure Interaction," *Proceedings of the 22nd International Conference on Offshore Mechanics and Arctic Engineering—OMAE, Materials Technology Ocean Engineering Polar and Arctic Sciences and Technology Workshops*, Cancun, Mexico, June 8–13, Vol. 3, pp. 823–829.
[308] Choi, K., and Rim, C. W., 1996, "Numerical Technique in Calculation of Dynamic Interaction Forces Between Ice Floe and Arctic Offshore Structures," *Proceedings of the Sixth International Offshore and Polar Engineering Conference*, Los Angeles, CA, Vol. 2, pp. 304–310.
[309] Jin, D. P., and Hu, H. Y., 1998, "Ice-Induced Nonlinear Vibration of an Offshore Platform," J. Sound Vib., **214**(3), pp. 431–442.
[310] Engelbrektson, A., 1983, "Observations on a Resonance Vibrating Lighthouse Structure in Moving Ice," *Proceedings of the International Conference on Part and Ocean Engineering Under Arctic Conditions (POAC)*, Helsinke, Finland, Vol. 2, pp. 855–864.
[311] Salo, I., 1973, "Measuring Systems for Ice and Wind Loads on a Steel Lighthouse," *Proceedings of the International Conference on Port and Ocean Engineering Under Arctic Conditions-POAC'73*, Reykjavik, pp. 271–278.
[312] Määttänen, M., 1975, "Experience of Ice Forces Against a Steel Lighthouse Mounted on the Seabed and Proposed Construction Refinements," *Proceedings of the International Conference on Port and Ocean Engineering Under Arctic Conditions-POAC'75*, Fairbanks, Vol. 4, pp. 857–871.
[313] Schwarz, J., 2001, "Validation of Low Level Ice Forces on Coastal Structures," *Proceedings of the International Offshore Polar Engineering Conference (ISOPE)*, Stavanger, Norway, pp. 749–753.
[314] Brown, T., 2001, "Four Years of Ice Force Observations on the Confederation Bridge," *Proceedings of the 16th International Conference on Port and Ocean Engineering Under Arctic Conditions (POAC)*, Ottawa, Canada, Vol. 1, pp. 285–298.
[315] Bjerkås, M., 2006, "Wavelet Transforms and Ice Actions on Structures," Cold Regions Sci. Technol., **44**, pp. 159–169.
[316] Engelbrektson, A., 1977, "Dynamic Ice Loads on a Lighthouse," *Proceedings of the Port and Ocean Engineering Under Arctic Conditions*, Canada, pp. 654–663.
[317] Björk, B., 1981, "Ice-Induced Vibrations of Fixed Offshore Structures: Part 2, Experiences With Baltic Lighthouses," in Marine Structures and Ships in Ice, T. Carstens, ed., p. 100, Report No. 81–06/2.
[318] Luk, C. H., 1984, "In-Plane Structure Vibration Analysis by Two-Dimensional Elastic Wave Theory," ASME J. Energy Resour. Technol., **106**(2), pp. 160–168.
[319] Williams, A. N., and Vipulanandan, C., 1986, "Steady-State Ice-Structure Interaction Analysis," J. Eng. Mech., **112**(10), pp. 989–1006.
[320] Arockiasamy, M., El-Tahan, H., Swamidas, A. S. J., Russell, W. E., and Reddy, D. V., 1984, "Semi-Submersible Response to Transient Ice Forces," Ocean Eng., **11**(5), pp. 463–490.
[321] Chehayeb, F. S., Connor, J. J., and Sunder, S. S., 1986, "Numerical Modeling of Ice-Structure Interaction," *Proceedings of the First International Conference on Ice Technology*, Cambridge, MA, pp. 431–444.
[322] Suman, J. C., 1991, "Predicting Ice-Structure Interactive Forces," J. Cold Reg. Eng., **5**(2), pp. 69–76.
[323] Iyer, S. H., and Kivisild, H. R., 1993, "Analysis for Dynamic Ice Structure Interaction Involving Finite Difference Model and Damage Considerations," *Proceedings of the 12th International Conference on Offshore Mechanics and Arctic Engineering—OMAE*, Arctic/Polar Technology, Glasgow, UK, Vol. 4, pp. 199–206.
[324] Huovinen, S., 1993, "Abrasion of Concrete Structures by Ice," Cem. Concr. Res., **23**(1), pp. 69–82.
[325] Fiorio, B., Meyssonnier, M., and Boulon, M., 2002, "Experimental Study of the Friction of Ice Over Concrete Under Simplified Ice-Structure Interaction Conditions," Can. J. Civ. Eng., **9**, pp. 347–359.
[326] Fiorio, B., 2005, "Wear Characterization and Degradation Mechanism of a Concrete Surface Under Ice Friction," Constr. Build. Mater., **19**, pp. 366–375.
[327] Abul-Azm, A. G., and Williams, A. N., 1992, "Approximation of Interference Effects in Dynamic Ice-Structure Interactions," ASME J. Offshore Mech. Arct. Eng., **114**(4), pp. 299–309.
[328] Kärnä, T., and Trunen, R., 1990, "A Straightforward Technique for Analyzing Structural Response to Dynamic Ice Action," *Proceedings of the Ninth International Conference on Offshore Mechanics and Arctic Engineering (OMAE)*, Houston, TX, Vol. IV, pp. 135–142.
[329] Izumiyama, K., Irani, M. P., and Timco, G. W., 1994, "Influence of Compliance of Structure on Ice Load," *Proceedings of the 12th International Symposium on Ice*, Vol. 1, pp. 229–238.
[330] Izumiyama, K., and Uto, S., 1997, "Ice Loading on a Compliant Indenter," *Proceedings of the 14th International Conference on Port and Ocean Engineering in Arctic Conditions*, Yokohama, Vol. IV, pp. 431–436.
[331] Kärnä, T., Nyman, T., Vuorio, J., and Järvinen, E., 1993, "Results From Indentation Tests in Sea Ice," *Proceedings of the 12th International Conference on Offshore Mechanical and Arctic Engineering (MAE-93)*, Glasgow, Vol. IV, pp. 177–185.
[332] Sodhi, D. S., 1992, "Ice-Structure Interaction With Segmented Indenters," *Proceedings of the 11th International Association of Hydraulic Engineering and Research Symposium on Ice (IAHR-92)*, Banff, AB, Canada, Vol. 2, pp. 909–929.
[333] Sodhi, D. S., 1991, "Effective Pressure Interaction With Segmented Indenters," *Proceedings of the 11th International Association of Hydraulic Engineering and Research Symposium on Ice (IAHR-92)*, Banff, AB, Canada, Vol. 2, pp. 909–929.
[334] Fransson, L., 1993, "Ice Load on Structures, Ice Testing in Luleå Harbour," Cold Tech Report No. 1995:06.
[335] Korzhavin, K. N., 1962, "Action of Ice on Engineering Structures," U.S. Army Cold Regions Research and Engineering Laboratory, CRREL draft translation No. 260.
[336] Croasdale, K. R., and Kennedy, K. P., 1996, "Ice Loads Consensus Study Update," *Proceedings of the 15th International Conference on Offshore Mechanics and Arctic Engineering*, W. A. Nixon, ed., Arctic/Polar Technol, Vol. IV, pp. 115–118.
[337] Schninek, K. L., Blanchet, D., Croasdale, K. R., Matskevitch, D. G., and Bhat, S. U., 1994, "Comparisons of the Russian and Foreign Codes and Methods of Global Load Estimations," *Proceedings of the 15th International Conference on Offshore Mechanics and Arctic Engineering*, W. A. Nixon, ed., Arctic/Polar Technology, Vol. IV, pp. 75–82.
[338] Ashby, M. F., Palmer, A. C., Thouless, M., Goodman, D. J., Howard, M., Hallam, S. D., Murrell, S. A. E., Jones, N., Sanderson, T. J. O., and Ponter, A. R. S., 1986, "Non-Simultaneous Failure and Ice Loads on Arctic Structures," *Offshore Technology Conference (OTC)*, pp. 399–404.
[339] Vinogradov, O. G., Kentfield, J. A. C., and Vermeulen, P. J., 1979, "Ice-Breaking Mechanisms for Ice-Breakers and Offshore Structures," *Proceedings of the Fifth International Conference on Port and Ocean Engineering Under Arctic Trondheim*, Norway, pp. 1069–1079.
[340] Mueller, A., and Ettema, R., 1984, "Dynamic Response of an Ice-Breaker Hull to Ice Breaking," Iowa Institute of Hydraulic Research, Report No. 273, pp. 1–124.
[341] Uto, S., Shimoda, H., and Izumiyama, K., 1997, "Model-Ship Comparison of

Propulsive Performance of Icebreaker 'PM TESHIO' in Continuous Icebreaking Mode," *Proceedings of the 16th International Conference on Offshore Mechanics and Arctic Engineering*, Yokohama, Japan, Pt. 4, pp. 225–232.
[342] 2000, Standard Ship Model Tests, Ice Conditions and Analysis Methods at MASA-Yards Arctic Research Centre, Arctic Technology, MARC Report No. D-114.
[343] Sandvik, P. C., 1990, "Feasibility Study of an Oil Production Ship Concept for Arctic Conditions," *Proceedings of the International Conference on Development and Utilization of Technologies in Polar Regions*, Danish Hydraulic Institute, pp. 590–600.
[344] Jolles, W., Browne, R., and Keinonen, A., 1997, "Model Development of Vessel Approach and Mooring Operations at Arctic Loading Terminals," *Proceedings of the Offshore Mechanics and Arctic Engineering—OMAE'97 Conference*, Arctic/Polar Technology, Yakohama, Vol. IV, pp. 393–400.
[345] Løset, S., Kanestrøm, Ø, Pytte, T., Evers, K. U., Jochman, P., and Sandvick, P. C., 1997, "Model Tests in Ice of a Submerged Turret Loading (STL) Concept," *Proceedings of the Offshore Mechanics and Arctic Engineering—OMAE'97 Conference*, Arctic/Polar Technology, Yokohama, Vol. IV, pp. 191–200.
[346] Murray, J. J., and Spencer, D. S., 1996, "Preliminary Investigations Into Mooring Forces on a Semi-Submersible and a Turret Moored Tanker in Pack Ice: Current and Waves," *Proceedings of the Offshore Mechanics and Arctic Engineering—OMAE'96 Conference*, Arctic/Polar Technology, Florence, Italy.
[347] Løset, S., 1994, "Discrete Element Modeling of a Broken Ice Field, Part I: Model Development," Cold Regions Sci. Technol., **22**, pp. 339–347.
[348] Hansen, E. H., 1998, "A Discrete Element Model to Study Marginal Ice Zone Dynamics and the Behavior of Vessels Moored in Broken Ice," Department of Marine Hydrodynamics, Norwegian University of Science and Technology, Trondheim, Norway.
[349] Hansen, E. H., and Løset, S., 1999, "Modeling Floating Offshore Units Moored in Broken Ice: Model Description," Cold Regions Sci. Technol., **29**, pp. 97–106.
[350] Hansen, E. H., and Løset, S., 1999, "Modeling Floating Offshore Units Moored in Broken Ice: Comparing Simulations With Ice Tank Tests," Cold Regions Sci. Technol., **29**, pp. 107–119.
[351] Jebaraj, C., Swamidas, A. S. J., and Shih, L. Y., 1988, "Numerical Modelling of Ship/Ice Interaction," *Offshore and Arctic Operations Symposium*, Jan. 22–25, Houston, TX, Vol. 26, pp. 199–205.
[352] Jebaraj, C., Swamidas, A. S. J., Shih, L. Y., and Munaswamy, K., 1992, "Finite Element Analysis of Ship/Ice Interaction," Comput. Struct., **43**(2), pp 205–221.
[353] Noble, P. G., Tam, W. K., Menon, B., and Bayly, I. M., 1979, "Ice Forces and Accelerations on a Polar Class Icebreaker," *Proceedings of the Fifth International Conference on Port and Ocean Eng Under Arctic Conditions*, Trondheim, Norway, pp. 1003–1022.
[354] Daley, C. G., Phillips, L. D., and McCallum, J. S., 1986, "Dynamic Ship/Ice Impact: Results of Parametric Model Testing," *Proceedings of the First International Conference on Ice Technology*, Cambridge, MA, pp. 349–363.
[355] St. John, J. W., and Meyer, J. R., 1986, "Structural Design Methods for Surface Ships Operating at the Ice Edge," Nav. Eng. J., **98**(3), pp. 88–94.
[356] Phillips, L. D., and Tanaka, H., 1994, "Simulation of Ship-Ice Collision Dynamics: Ice Interface Modeling Considerations," *Marine, Offshore and Ice Technology*, Wessex Institute of Technology, Southampton, UK, pp. 295–302.
[357] Penney, W., and Parker, N., 1995, "Software Studies Ice-Going Ship Designs," Motor Ship, **75**(897), pp. 55–56.
[358] Ionov, B. P., and Belyakov, V. B., 1991, "Energetic Approach to the Modelling of Resistance of Icebreaking Craft Motion in Level Ice," *Proceedings of the 11th International Conference on Port and Ocean Engineering Under Arctic Conditions, POAC*, St. John's, Newfoundland, Canada, Vol. 2, pp. 666–684.
[359] Zuyev, V. A., Gramusov, E. M., and Ionov, B. P., 1991, "Power Approach to Investigation of Ice-Ship Interaction," *Proceedings of the 11th International Conference on Port and Ocean Engineering Under Arctic Conditions, POAC*, Vol. 2, pp. 728–745.
[360] Goldstein, R. V., and Osipenko, N. M., 1993, "Fracture Mechanics in Modeling of Icebreaking Capability of Ships," J. Cold Reg. Eng., **7**(2), pp. 33–43.
[361] Estrada, Jr., H., and Ward, S. R., 1968, "Forces Exerted by Ice on Ships," J. Ship Res., **12**(4), pp. 302–312.
[362] Enkvist, E., Varsta, P., and Riska, K., 1979, "Ship-Ice Interaction," *Proceedings of the Fifth POAC 79, International Conference on Port and Ocean Engineering Under Arctic Conditions*, Trondheim, Norway, pp. 977–1002.
[363] Sandvik, P. C., 1990, "Feasibility of Floating Production Concept for Arctic Conditions," ESARC Report No. 19, Task 89/02; SINTEF Report No. SF 604040.06.
[364] Løset, S., 1995, "Ice Loads on the STL Tanker," Department of Structural Engineering, The Norwegian Institute of Technology, Trondheim, Report No. R-9-95.
[365] Løset, S., Kanestrøm, Ø., and Pytte, T., 1998, "Model Tests of a Submerged Turret Loading Concept in Level Ice, Broken Ice, and Pressure Ridges," Cold Regions Sci. Technol., **27**, pp. 57–73.
[366] Luk, C. H., 1991, "A Three-Dimensional Plasticity and Momentum Model for Ship Resistance in Level Ice," ASME J. Offshore Mech. Arct. Eng., **113**(1), pp. 53–60.
[367] Peirce, T. H., 1979, "Arctic Marine Technology: A Review of Ship Resistance in Ice," Naval Architect, **4**, pp. 219–235.
[368] Haas, C., Rupp, K.-H., and Uuskallio, A., 1999, "Comparison of Along Track EM Ice Thickness Profiles With Ship Performance Data," *POAC'99 Proceedings of the 15th International Conference on Port and Ocean Engineering Under Arctic Conditions*, Espoo, Finland, Aug. 23–27, Helsinki University of Technology, pp. 343–353.
[369] Liu, C. T., and Duan, M. L., 1995, "Structural Mechanical Problems in Engineering Ice Mechanics," Chinese Journal of Mechanical Strength, **17**(3), pp. 7–20.
[370] Crowe, C. T., 1996, "Multi-Phase Multi-Component Flows," *Fundamentals of Fluid Dynamics*, Handbook of Fluid Dynamics and Fluid Machinery, J. A. Schutz, and A. E. Fuhs, eds., Wiley, New York, Vol. 1, Chap. 14, pp. 883–919.
[371] Blanchet, D., and DeFranco, S. J., 1996, "Global First-Year Ice Loads: Scale Effects and Non-Simultaneous Failure," *Proceedings of the International Association of Hydraulic Engineering and Research (IAHR) Ice Symposium*, Beijing, pp. 203–213.
[372] Løset, S., Shkhinek, K. N., and Uvarova, E., 1999, "Evaluation of Existing Ice Force Prediction Methods," LOLEIF Report No. 3, pp. 1–8.
[373] Løset, S., Shkhinek, K. N., and Uvarova, E., 1999, "An Overview of the Influence of Structure Width and Ice Thickness on the Global Ice Load," *Proceedings of the Port and Ocean Engineering Under Arctic Conditions (POAC)*, Finland, Vol. 1, pp. 425–434.
[374] Løset, S., Shkhinek, K. N., and Kärnä, T., 2003, "Global Ice Load Dependency on Structure Width and Ice Thickness," *Proceedings of the Port and Ocean Engineering Under Arctic Conditions (POAC)*, Trondheim, Vol. 2, pp. 857–868.
[375] Kärnä, T., and Qu, Y., 2003, "Peak Forces in Continuous Brittle Crushing," International Report on Measurements of Structures in ICE (STRICE)/NEST Deliverable, Finland, pp. 1–40.
[376] Bjerkås, M., 2004, "Global Design Ice Loads Dependence of Failure Mode," Int. J. Offshore Polar Eng., **14**(3), pp. 189–195.
[377] Blanchet, D., and Kennedy, K. P., 1996, "Global First-Year Ice Load Measurements in the Arctic," *Proceedings of the Conference on Offshore Mechanics and Arctic Engineering*, Italy, Vol. 4, pp. 103–113.
[378] Lever, J., Colbourne, B., and Mak, L., 1989, "Model Study of the Wave-Driven Impact of Ice Masses With Semi-Submersible Platform," *Proceedings of the Eighth International Offshore Mechanics and Arctic Engineering*, Vol. IV, pp. 393–403.
[379] Foschi, R., Isaacson, M., Allyn, N., and Yee, S., 1996, "Combined Wave-Iceberg Loading on Offshore Structures," Can. J. Civ. Eng., **23**, pp. 1099–1110.
[380] Cumming, D., and Georghiou, A., 1999, "Physical Model Experiments to Assess the Hydrodynamic Interaction Between Iceberg Models and a Floating Structure: Phase II," Institute of Ocean Technology, Report No. TR-1999-08.
[381] Isaacson, M., and McTaggart, K., 1990, "Influence of Hydrodynamic Effects in Iceberg Collisions," Can. J. Civ. Eng., **17**, pp. 329–337.
[382] Farell, C., 1971, "On the Flow About a Spheroid Near a Plane Wall," J. Ship Res., **15**, pp. 246–252.
[383] Grue, J., 1986, "Time-Periodic Wave Loading on a Submerged Circular Cylinder in a Current," J. Ship Res., **30**, pp. 153–158.
[384] Lewandowski, E. M., 1992, "Hydrodynamic Forces and Motions of a Cylinder Near a Vertical Wall," J. Ship Res., **36**, pp. 248–254.
[385] Gagnon, R., 2001, *Analysis of Physical Model Experiments to Assess the Hydrodynamic Interaction Between a Transiting Tanker: Phase II*, Institute for Ocean Technology, Report No. TR-200102.
[386] Gagnon, R., 2004, "Physical Model Experiments to Assess the Hydrodynamic Interaction Between Floating Glacial Ice Masses and a Transiting Tanker," ASME J. Offshore Mech. Arct. Eng., **126**, pp. 297–309.
[387] Buzuev, A., and Ryvlin, A. Y., 1961, "Calculation of the Resistance Encountered by an Icebreaker Moving Through Ice Cakes and Brash," Morskoi Flot, **21**(8), pp. 136–138.
[388] Kashtelyan, V. I., Posnjak, I. I., and Ryvlin, A. Y., 1968, "Ice Resistance to Motion of a Ship," Sudostrenis, Leningrad.
[389] Ettema, R., Stern, F., and Lazaro, J., 1987, "Dynamics of Continuous-Mode Icebraking by a Polar-Class Icebreaking Hull," Iowa Institute of Hydraulic Research, The University of Iowa, IIHR Report.
[390] Ashton, G. D., Den Hartog, S. L., and Hanamoto, B., 1972, "Icebreaking by Tow on the Mississippi River," U.S. Army Cold Regions and Engineering Laboratory, CRREL Special Report No. 192.
[391] Levine, G. H., Voelker, R. P., and Mentz, P. B., 1974, "Advances in the Development of Commercial Ice-Transiting Ships," *The Society of Naval Architects and Marine Engineers, Annual Meeting*, New York.
[392] Mellor, M., 1980, "Ship Resistance in Thick Brash Ice," Cold Regions Sci. Technol., **3**(4), pp. 305–321.
[393] Duthinh, D., 1992, "Pressure of Crushed Ice as Mohr-Coulomb Material Against Flat, Axisymmetric Indentor," J. Cold Reg. Eng., **6**(4), pp. 139–151.
[394] Greisman, P., 1981, "Brash Ice Behavior," U.S. Coast Guard Research and Development Center, Report No. CGRDC-9/81.
[395] Kitazawa, T., and Ettema, R., 1985, "Resistance to Ship-Ice Motion Through Brash Ice," Cold Regions Sci. Technol., **10**, pp. 219–234.
[396] Ettema, R., and Matsuishi, M., 1985, "Ice Loads and Motions Experienced by a Floating Moored Platform in Mushy Ice Rubble," Iowa Institute of Hydraulic Research, The University of Iowa, IIHR Report No. 295.
[397] Ettema, R., and Matsuishi, M., 1985, "The Dynamical Behavior of a Floating, Cable-Moored Platform Continuously Impacted by Ice Floes," Iowa In-

stitute of Hydraulic Research, The University of Iowa, IIHR Report No. 294.
[398] Ettema, R., Matsuishi, M., and Kitazawa, T., 1986, "Model Tests Ice-Rubble Size and Ship Resistance in Ice Rubble," Cold Regions Sci. Technol., **12**, pp. 229–243.
[399] Keinonen, A., 1979, "An Analytical Method for Calculating the Pure Resistance Encountered by Ships in the First Year Ice Ridges," Ship Hydrodynamics Laboratory, Helsinki University of Technology, Report No. 17.
[400] Rennie, R. P., and Turnbull, M. J., 1964, "Life of Ice Breaker: Her External Corrosion Problems in Icy Northumberland Strait," Materials Protection, **3**(4), pp. 50–52, 54; 57.
[401] Rennie, R. P., and Turnbull, M. J., 1966, "Cathodic Protection of Ships Operating in Ice," Materials Protection, **5**(4), pp. 44–45.
[402] Aromaa, J., Pehkonen, A., and Forsen, O., 2006, "Cathodic Protection of Ships in Brackish Water," J. Solid State Electrochem., **10**(9), pp. 681–688.
[403] Edwards, R. Y., Jr., 1976, "Methods for Predicting Forces Encountered by Propellers During Interactions With Ice," Int. Shipbuild. Prog., **23**(268), pp. 406–419.
[404] Kostilainen, V., 1986, "Problems in Physical Modeling of the Propulsion and Maneuvering of Ice Transiting Ships," *Proceedings of the First International Conference on Ice Technology*, Cambridge, MA, pp. 323–331.
[405] Yuen, C., and Lasca, N. P., 1989, "Fracturing of an Ice Sheet by Ship-Induced, Ice-Coupled Waves," Cold Regions Sci. Technol., **16**(1), pp. 75–82.
[406] Browne, R. P., Keinonen, A., and Semery, P., 1991, "Ice Loading on Open and Ducted Propellers," *Proceedings of the First International Offshore and Polar Engineering Conference*, Edinburgh, Scotland, pp. 562–570.
[407] Luznik, L., Walker, D., Bose, N., and Jones, S. J.,1995, "Effects of Ice Blockage Size and Proximity on Propeller Performance During Non-Contact Propeller-Ice Interaction," *Proceedings of the 14th International Conference on Offshore Mechanics and Arctic Engineering*, Copenhagen, Pt. 4, pp. 35–39.
[408] Morin, A., Caron, S., Van Neste, R., and Edgecombe, M. H., 1996, "Field Monitoring of the Ice Load of an Icebreaker Propeller Blade Using Fiber Optic Strain Gauges," Proc. SPIE, **2718**, pp. 427–438.
[409] Veitch, B., 1995, "Predictions of Ice Contact Forces on a Marine Screw Propeller During the Propeller-Ice Cutting Process," Acta Polytech. Scand., Mech. Eng. Ser., **118**, pp. 1–110.
[410] Veitch, B., 1997, "Predictions of Propeller Loads Due to Ice Contact," Int. Shipbuild. Prog., **44**(439), pp. 221–239.
[411] Jones, S. J., Soininen, H., Jussila, M., Koskinen, P., Newbury, S., and Browne, R., 1998, "Propeller-Ice Interaction," *Proceedings of 105th Annual Meeting of the Society of Naval Architects and Marine Engineers*, Ottawa, Canada, Vol. 105, pp. 399–425.
[412] Trägårdh, P., Lindell, P., and Sasaki, N., 2005, "Double Acting Tanker: Experiences From Model Tests and Sea Trials," Proc. Inst. Mech. Eng., Part M: Journal of Engineering for the Maritime Environment, **219**(3), pp. 109–119.
[413] Ryerson, C. C., and Gow, A. J., 2000, "Ship Superstructure Icing: Crystalline and Physical Properties," U.S. Army Corps of Engineering, Engineering Research Development Cent, Cold Regions Research and Engineering Laboratory, Technical Report No. ERDC/CRREL TR-00-11.
[414] Ryerson, C. C., and Gow, A. J., 2000 "Crystalline Structure and Physical Properties of Ship Superstructure Spray Ice," Philos. Trans. R. Soc. London, Ser. A, **358**, pp. 2847–2871.
[415] Overland, J. E., Pease, C. H., Preisendorfer, R. W., and Comiskey, A. L., 1986, "Prediction of Vessel Icing," J. Clim. Appl. Meteorol., **25**(12), pp. 1793–1806.
[416] Overland, J. E., 1990, "Prediction of Vessel Icing for Near Freezing Sea Temperatures," Weather and Forecasting, **5**(1), pp. 62–77.
[417] Hay, R. F. M., 1956, "Meteorological Aspects of the Loss of the Lorella and Roderigo," The Marine Observer, **26**, pp. 89–94.
[418] Blackmore, R. Z., and Lozowski, E. P., 1994, "A Heuristic Freezing Spay Model of Vessel Icing," Int. J. Offshore Polar Eng., **4**(2), pp. 119–126.
[419] Zakrzewski, W. P., Blackmore, R., and Lozowski, E. P., 1988, "Mapping Icing Rates on Sea-Going Ships," J. Meteorol. Soc. Jpn., **66**(5), pp. 661–675.
[420] Lozowski, E. P., Szilder, K., and Makkonen, L., 2000, "Computer Simulation of Marine Ice Accretion," Philos. Trans. R. Soc. London, Ser. A, **358**, pp. 2811–2845.
[421] Sarchin, T. H., and Goldberg, L. L., 1962, "Stability and Buoyancy Criteria for U.S. Navy Surface Ships," Soc. Nav. Archit. Mar. Eng., Trans., **70**, pp. 418–458.
[422] IMO, 2006, "Review of Intact Stability Code (Chapter 6: Icing Considerations)," International Maritime Organization, SLF Report No. 49/5 (http://www.sname.org/committees/tech_ops/044/49/49-5.pdf).
[423] Coles, W. D., Rollin, V. G., and Mulholland, D. R., 1950, "Icing-Protection Requirements for Reciprocating-Engine Induction System," NACA Report No. 982.
[424] VECTOR, 2002, "Induction System Icing," Civil Aviation Authority of New England.
[425] Farzaneh, M., 2000, "Ice Accretions on High-Voltage Conductors and Insulators and Related Phenomena," Philos. Trans. R. Soc. London, Ser. A, **358**(1776), pp. 2971–3005.
[426] Makkonen, L., 2000, "Models for the Growth of Rime, Glaze, Icicles and Wet Snow on Structures," Philos. Trans. R. Soc. London, Ser. A, **358**, pp. 2913–2939.
[427] Ackly, S., 1985, "Sea Spray Icing: A Review of Current Models," *Proceedings of the 1985 U.S. Navy Symposium on Arctic/Cold Weather Operations of Surface Ships*, Deputy Chief of Naval Operations for Surface Warfare, Washington, D.C.
[428] Chung, K. K., and Lozowski, E. P., 1998, "A Three-Dimensional Time Dependent Icing Model for a Stern Trawler," J. Ship Res., **42**(4), pp. 266–273.
[429] Chung, K. K., Lozowski, W. P., Zakrewski, R., and Thompson, T., 1998, "Spraying Experiments With a Model Stern Trawler," J. Ship Res., **42**(4), pp. 260–265.
[430] Francescutto, A., Serra, A., and Scarpa, S., 2001, "A Critical Analysis of Weather Criterion for Intact Stability of Large Passenger Vessels," *Proceedings of the International Conference on Offshore Mechanics and Arctic Engineering—OMAE*, Vol. 1, pp. 829–836.
[431] Spyrou, K., 2002, "A Basis for Developing a Rational Alternative to the Weather Criterion: Problems and Capabilities," *Sixth International Ship Stability Workshop Proceedings*, Oct. 13–16.
[432] USCG, 2004, *A Best Practices Guide to Vessel Stability: Guiding Fishermen Safely Into the Future*, 2nd ed., U.S. Department of Homeland Security, Washington, DC (http://www.uscg.mil/hq/gm/cfvs/Stability%20Book%202nd%20Ed%202004.pdf).
[433] Thompson, J. M. T., 1997, "Designing Ships Against Capsize in Beam Seas: Recent Advances and New Insights," Appl. Mech. Rev., **50**, pp. 307–324.
[434] Nayfeh, A. H., and Balachandran, B., 1995, *Applied Nonlinear Dynamics*, Wiley, New York.
[435] Arnold, L., Chueshov, I., and Ochs, G., 2004, "Stability and Capsizing of Ships in Random Sea—a Survey," Nonlinear Dyn., **36**, pp. 135–179.
[436] Surendran, S., Lee, S. K., Reddy, J. V. R., and Lee, G., 2005, "Nonlinear Roll Dynamics of a Ro-Ro Ship in Waves," Ocean Eng., **32**, pp. 1818–1828.
[437] Bulian, G., 2005, "Nonlinear Parametric Rolling in Regular Waves—a General Procedure for the Analytical Approximation of the GZ Curve and Its Use in Time Domain Simulations," Ocean Eng., **32**, pp. 309–330.
[438] Falzarano, J., and Troesch, A., 1990, "Application of Modern Geometric Methods for Dynamical Systems to the Problem of Vessel Capsizing With Water-On-Deck," *Fourth International Conference on the Stability of Ships and Ocean Vehicles*, Naples, Italy, pp. 565–572.
[439] Esparza, I., and Falzarano, J., 1993, "Nonlinear Rolling Motion and Capsizing of a Statically Biased Vessel Under the Effect of External and Parametric Wave Excitation," *14th ASME Biennial Conference on Vibrations and Noise*, pp. 111–122.
[440] Lansbury, A. N., Thompson, J. M. T., and Stewart, H. B., 1992, "Basin Erosion in the Twin-Well Duffing Oscillator: Two Distinct Bifurcations Scenarios," Int. J. Bifurcation Chaos Appl. Sci. Eng., **2**, pp. 505–532.
[441] Thompson, J. M. T., 1989, "Loss of Engineering Integrity Due to the Erosion of Absolute and Transient Basin Boundaries," *Proceedings of the IUTAM Symposium on Nonlinear Dynamics in Engineering Systems*, Stuttgart, Aug. 21–25, Springer, Berlin.
[442] Thompson, J. M. T., 1989, "Chaotic Phenomena Triggering the Escape From a Potential Well," Proc. R. Soc. London, Ser. A, **421**, pp. 195–225.
[443] Thompson, J. M. T., and McRobie, F. A., 1993, "Intermediate Bifurcations and Global Dynamics of Driven Oscillators," *First European Nonlinear Oscillations Conference*, Hamburg, E. Kreuzer and G. Schmidt, eds., Academie-Verlag, Berlin, pp. 107–128.
[444] Thompson, J. M. T., Rainy, R. C. T., and Soliman, M. S., 1992, "Mechanics of Ship Capsize Under Direct and Parametric Wave Excitation," Philos. Trans. R. Soc. London, Ser. A, **338**, pp. 471–490.
[445] Lin, H., and Yim, S. C. S., 1995, "Chaotic Roll Motion and Capsize of Ships Under Periodic Excitation With Random Noise," Appl. Ocean. Res., **17**, pp. 185–204.
[446] Scolan, Y. M., 2001, "Analysis of Direct and Parametric Excitation With the Melnikov Method and the Technique of Basin Erosion," *Fifth International Workshop Stability and Operational Safety of Ships*, University of Trieste, Sept. 12 and 13.
[447] Falzarano, J., Shaw, S., and Troesch, A., 1992, "Application of Global Methods for Analyzing Dynamical Systems to Ship Rolling Motion and Capsizing," Int. J. Bifurcation Chaos Appl. Sci. Eng., **2**(1), pp. 101–115.
[448] Falzarano, J., 1990, "Predicting Complicated Dynamics Leading to Vessel Capsizing," Ph.D. thesis Department of Naval Architecture and Marine Engineering, University of Michigan.
[449] Kubicek, M., and Marek, M., 1983, *Computational Methods in Bifurcation Theory and Dissipative Structures*, Springer-Verlag, New York.
[450] Parker, T. S., and Chua, L. O., 1987, "Chaos: A Tutorial for Engineers," Proc. IEEE, **75**(8), pp. 982–1008.
[451] Falzarano, J., Vishnubhotla, S., and Juckett, S., 2005, "Combined Steady State and Transient Analysis of a Patrol Vessel as Affected by Varying Amounts of Damping and Periodic and Random Wave Excitation" *The 24th International Conference on Offshore Mechanics and Arctic Engineering*, Halkidiki, Greece, CD 5.
[452] Falzarano, J., Esparza, I., and Taz Ul Mulk, M., 1995, "A Combined Steady-State and Transient Approach to Study Large Amplitude Ship Rolling Motion and Capsizing," J. Ship Res., **39**(2), pp. 213–224.
[453] Meyerhoff, W. K., and Schlachter, G., 1980, "An Approach for the Determination of Hull-Girder Loads in a Seaway Including Hydrodynamic Impacts," Ocean Eng., **7**(2), pp. 305–326.
[454] Froude, W. F., 1863, "Remarks on Mr. Scott Russell's Paper on Rolling," Transactions of the Institute of Naval Research, **4**, pp. 232–275.
[455] Paulling, J. R., and Rosenberg, R. M., 1959, "On Unstable Ship Motions Resulting From Nonlinear Coupling," J. Ship Res., **2**, pp. 36–46.
[456] Price, W. G., and Bishop, R. E. D., 1974, *Probabilistic Theory of Ship Dynamics*, Chapman and Hall, London.
[457] Lloyd, A. R. J. M., 1989, *Seakeeping: Ship Behavior in Rough Weather*, Ellis Howood, Chichester, UK.

[458] Price, W. G., 1975, "A Stability Analysis of the Roll Motion of a Ship in an Irregular Seaway," Int. Shipbuild. Prog., **22**, pp. 103–112.
[459] Haddara, M. R., 1975, "A Study of Stability of the Mean and Variance of Rolling Motion in Random Waves," *Proceedings of the International Conference on Stability of Ships and Ocean Vehicles*, University of Strathclyde, Glasgow.
[460] Muhuri, P. K., 1980, "A Study of the Stability of the Rolling Motion of a Ship in an Irregular Seaway," Int. Shipbuild. Prog., **27**, pp. 139–142.
[461] Roberts, J. B., 1982, "A Stochastic Theory for Nonlinear Ship Rolling in Irregular Seas," J. Ship Res., **26**(4), pp. 229–245.
[462] Roberts, J. B., 1982, "Effect of Parametric Excitation on Ship Rolling Motion," J. Ship Res., **26**(4), pp. 246–253.
[463] Roberts, J. B., and Dacunha, N. C., 1985, "Roll Motion of a Ship in Random Beam Waves: Comparison Between Theory and Experiment," J. Ship Res., **29**, pp. 112–126.
[464] Huang, X., Gu, X., and Bao, W., 1994, "The Probability Distribution of Rolling Amplitude of a Ship in High Waves," *Fifth International Conference on Stability of Ships and Ocean Vehicles*, Melbourne, FL.
[465] Roberts, J. B., 1972, "System Response to Random Impulses," J. Sound Vib., **24**, pp. 23–34.
[466] Iwankiewicz, R., and Nielsen, S. R. K., 1992, "Dynamic Response of Nonlinear Systems to Poisson Distributed Random Impulses," J. Sound Vib., **156**(3), pp. 407–423.
[467] Iwankiewicz, R., and Nielsen, S. R. K., 1992, "Dynamic Response of Hysteretic Systems to Poisson Distributed Pulse Trains," Probab. Eng. Mech., **7**, pp. 135–148.
[468] Köylüoğlu, H. U., Nielsen, S. R. K., and Iwankiewicz, R., 1994, "Reliability of Nonlinear Oscillators Subject to Poisson Driven Impulses," J. Sound Vib., **176**(1), pp. 19–33.
[469] Köylüoğlu, H. U., Nielsen, S. R. K., and Iwankiewicz, R., 1995, "Response and Reliability of Poisson-Driven Systems by Path Integration," J. Eng. Mech., **121**(1), pp. 117–130.
[470] Di Paola, M., and Vasta, M., 1997, "Stochastic Integro-Differential and Differential Equations of Nonlinear Systems Excited by Parametric Poisson Pulses," Int. J. Non-Linear Mech., **32**(5), pp. 855–862.
[471] Di Paola, M., and Pirrotta, A., 1999, "Nonlinear Systems Under Impulsive Parametric Input," Int. J. Non-Linear Mech., **34**, pp. 843–851.
[472] Proppe, C., 2003, "Exact Stationary Probability Density Functions for Nonlinear Systems Under Poisson White Noise Excitation," Int. J. Non-Linear Mech., **38**, pp. 557–564.
[473] Gagnon, R., Jones, S. J., Frederking, R., Spencer, P. A., and Masterson, D. M., 2001, "Large-Scale Hull Loading of Sea Ice, Lake Ice, and Ice in Tuktoyaktuk Harbour," ASME J. Offshore Mech. Arct. Eng., **123**, pp. 159–169.
[474] Gagnon, R., Jones, S. J., Frederking, R., Spencer, P. A., and Masterson, D. M., 1999, "Large-Scale Hull Loading of Ice in Tuktoyaktuk Harbour," *18th International Conference on Offshore Mechanics and Arctic Engineering*, St. John's, Newfoundland, ASME Paper No. OMAE99/P&A-119 (CD-ROM).
[475] Karr, D. G., Troesch, A. W., and Wingate, W. C., 1992, "Nonlinear Dynamic Response of a Simple Ice-Structure Interaction Model," *Proceedings of the 11th International Offshore Mechanics and Arctic Engineering Symposium, Arctic/Polar Technology*, Calgary, AB, Canada, Vol. 4, pp. 231–237.
[476] Karr, D. G., Troesch, A. W., and Wingate, W. C., 1993, "Nonlinear Dynamic Response of a Simple Ice-Structure Interaction Model," ASME J. Offshore Mech. Arct. Eng., **115**(4), pp. 246–252.
[477] Troesch, A. W., Karr, D. G., and Beier, K. P., 1992, "Global Contact Dynamics of an Ice-Structure Interaction Model," Int. J. Bifurcation Chaos Appl. Sci. Eng., **2**(3), pp. 607–620.
[478] Falzarano, J., and Zhang, F., 1993, "Multiple Degree-Of-Freedom Global Analysis of Transient Ship Rolling Motion," *ASME Winter Annual Meeting, Nonlinear Dynamics of Marine Vehicles*, J. M. Falzarano and F. Papoulias, eds., Vol. DSC 51, pp. 57–72.
[479] Senjanović, I., Ciprić, G., and Parunov, J., 2000, "Survival Analysis of Fishing Vessels Rolling in Rough Seas," Philos. Trans. R. Soc. London, Ser. A, **358**, pp. 1943–1965.
[480] Spanos, P. T., and Chen, T., 1980, "Response of a Dynamic System to Flow-Induced Load," Int. J. Non-Linear Mech., **15**, pp. 115–126.
[481] Dalzell, J., 1978, "A Note on the Form of Ship Roll Damping," J. Ship Res., **22**(3), pp. 178–185.
[482] Bruce, R., 1985, "Quasi-Static Response of Jacket Platform Subject to Nonlinear Wave Loading," *Proceedings of the 14th Conference on the Behavior of Offshore Structures*, Elsevier, Amsterdam, pp. 899–905.
[483] Jiang, C., Troesch, A. W., and Shaw, S. W., 2000, "Capsize Criteria for Ship Models With Memory-Dependent Hydrodynamics and Random Excitation," Philos. Trans. R. Soc. London, Ser. A, **358**, pp. 1761–1791.
[484] Senjanović, I., Parunov, J., and Ciprić, G., 1997, "Safety Analysis of Ship Rolling in Rough Sea," Chaos, Solitons Fractals, **8**(4), pp. 659–680.
[485] Hsieh, S. R., Troesch, A. W., and Shaw, S. W., 1994, "A Nonlinear Probabilistic Method for Predicting Vessel Capsizing in Random Beam Seas," Proc. R. Soc. London, Ser. A, **446**, pp. 1–17.
[486] Schauer, T., Romberg, B., Jiang, C., and Troesch, A. W., 1995, "Risk Assessment of Small Fishing Vessel Trap Net Operations," Marine Technology, **32**(2), pp. 231–243.
[487] Belenk, V. L., Weems, K. M., Lin, W. M., and Pauling, J. R., 2003, "Probabilistic Analysis of Roll Parametric Resonance in Head Seas," *Proceedings of STAB'03 Eighth International Conference on Stability of Ships and Ocean Vehicles*, Madrid, Spain.
[488] Bulian, G., Francescutto, A., and Lugni, C., 2003, "On the Nonlinear Modeling of Parametric Rolling in Regular and Irregular Waves," *Proceedings of STAB'03 Eighth International Conference on Stability of Ships and Ocean Vehicles*, Madrid, Spain.
[489] Shin, Y. S., Belenky, V. L., Pauling, J. R., Weems, K. M., Lin, W. M., McTaggart, K., Spyrou, K. J., Treakle, T. W., Leyadou, M., Hutchinson, B. L., Falzarano, J., Chen, H., and Letizia, L., 2004, "Criteria for Parametric Roll of Large Containerships in Longitudinal Seas," Trans. Soc. Naval Arch. Marine Eng. (SNAME), Washington, DC, pp. 14–47.
[490] Leavdou, M., and Palazzi, L., 2003, "Assessment of Operational Risk of Parametric Roll," WorldMaritimeConferenceand2003SocietyofNavalArchitectsandMarineEngineers(SNAME)AnnualMeeting' San Francisco [Soc. Nav. Archit. Mar. Eng., Trans., **111**, pp. 517–531].
[491] Moshchuk, N. K., Ibrahim, R. A., Khasminskii, R. Z., and Chow, P. L., 1995, "Asymptotic Expansion of Ship Capsizing in Random Sea Waves, Part I: First-Order Approximation," Int. J. Non-Linear Mech., **30**(5), pp. 727–740.
[492] Pontryagin, L. S., Andonov, A. A., and Vitt, A. A., 1933, "On Statistical Consideration of Dynamical Systems," Journal of Experimental and Theoretical Physics, **3**(3), pp. 165–172.
[493] Cai, G. Q., and Lin, Y. K., 1994, "On Statistics of First-Passage Failure," ASME J. Appl. Mech., **61**, pp. 93–99.
[494] Cai, G. Q., Yu, J. S., and Lin, Y. K., 1994, "Ship Rolling in Random Sea," in *Stochastic Dynamics and Reliability of Nonlinear Ocean Systems*, R. A. Ibrahim and Y. K. Lin, eds., ASME WAM GE Vol. 77.
[495] Moshchuk, N. K., Khasminskii, R. Z., Ibrahim, R. A., and Chow, P., 1995, "Asymptotic Expansion of Ship Capsizing in Random Sea Waves, Part II: Second-Order Approximation," Int. J. Non-Linear Mech., **30**(5), pp. 741–757.
[496] Feller, W., 1954, "Diffusion Processes in One-Dimension," Trans. Am. Math. Soc., **77**(1), pp. 1–31.
[497] Khasminskii, R., 1963, "The Averaging Principle for Parabolic and Elliptic Differential Equations and Markov Processes With Small Diffusion," Theor. Probab. Appl., **8**, pp. 121–140.
[498] Khasminskii, R., 1966, "A Limit Theorem for the Solution of Differential Equations With Random Right-Hand Sides," Theor. Probab. Appl., **11**, pp. 390–406.
[499] Ariaratnam, S. T., and Pi, H. N., 1973, "On the First-Passage Time for Envelope Crossing for a Linear Oscillator," Int. J. Control, **18**, pp. 89–96.
[500] Khasminskii, R., 1963, "On Diffusion Processes With a Small Parameter," Izv. USSR Academy of Sciences and Mathematics, **27**, pp. 1281–1300.
[501] Roberts, G. N., Sutton, R., Zirilli, A., and Tiano, A., 2003, "Intelligent Ship Autopilots: A Historical Perspective," Mechatronics, **13**(10), pp. 1091–1103.
[502] Monk, K., 1987, "A Warship Roll Criteria," Trans. RINA, London, UK.
[503] Crossland, P., 2003, "The Effect of Roll-Stabilization Controllers on Warship Operational Performance," Control Eng. Pract., **11**, pp. 423–431.
[504] Treakle, T. W., III, Mook, D. T., Liapis, S. I., and Nayfeh, A. H., 2000, "A Time-Domain Method to Evaluate the Use of Moving Weights to Reduce the Roll Motion of a Ship," Ocean Eng., **27**, pp. 1321–1343.
[505] Abdel Gawad, A. F., Ragab, S. A., Nayfeh, A. H., and Mook, D. T., 2001, "Roll Stabilization by Anti-Roll Passive Tanks," Ocean Eng., **28**, pp. 457–469.
[506] Vasta, J., Giddings, A. J., Taplin, A., and Stilwell, J. J., 1961, "Roll Stabilization by Means of Passive Tanks," Soc. Nav. Archit. Mar. Eng., Trans., **69**, pp. 411–460.
[507] Stigter, C., 1966, "The Performance of U-Tanks as a Passive Anti-Rolling Device," Trans. RINA, **ISP-13**(144), pp. 249–275.
[508] Bell, J., and Walker, W. P., 1966, "Activated and Passive Controlled Fluid Tank System for Ship Stabilization," Soc. Nav. Archit. Mar. Eng., Trans., **74**, pp. 150–193.
[509] Vugts, I. R. J. H., 1969, "A Comparative Study on Four Different Passive Roll Damping Tanks—Part II," Int. Shipbuild. Prog., **16**, pp. 212–223.
[510] Lewison, B. A., 1975, "Optimum Design of Passive Roll Stabilizer Tanks," Trans. RINA, **1**, pp. 31–45.
[511] Samoilescu, G., and Radu, S., 2002, "Stabilisers and Stabilising Systems on Ships," Constantin Brâncusi University, *University's Day, Eighth International Conference* (http://www.utgjiu.ro/conf/8th/S5/03.pdf)
[512] Webster, W. C., 1967, "Analysis of the Control of Activated Anti-Roll Tanks," *Proceedings of the Annual Meeting of the Society of Naval Architects and Marine Engineers*, New York, NY, pp. 296–325.
[513] Kawazoe, T., Nishikido, S., and Wada, Y., 1992, "Effect of Fin Area and Control Methods on Reduction of Roll Motion With Fin Stabilizers," Bulletin of the Marine Engineering Society in Japan, **28**(4), pp. 25–32, trans.
[514] Katebi, M. R., Hickey, N. A., and Grimble, M. J., 2000, "Evaluation of Fin Roll Stabilizer Controller Design," *Manoeuvering and Control of Marine Craft 2000 (MCMC 2000), Fifth International Federation of Automatic Control (IFAC) Conference Proceedings*, Aalborg, Denmark, pp. 69–74.
[515] Roberts, G. N., Sharif, M. T., Sutton, R., and Agarwal, A., 1997, "Robust Control Methodology Applied to the Design of a Combined Steering/Stabilized System for Warship," IEE Proc.: Control Theory Appl., **144**(2), pp. 128–136.
[516] Andrew, R. N., Loader, P. R., and Penn, V. E., 1984, "The Assessment of Ship Seakeeping Performance in Likely to Be Encountered Wind and Wave Conditions," *Proceedings of the Royal Institution of Naval Architects International Symposium on Wave and Wind Climate Worldwide*, London.
[517] Hint, J. A., 1991, *Automation in Merchant Ships*, 4th ed., LTD, London.
[518] Cowley, J. B., and Lambert, T. H., 1972, "The Use of the Rudder as a Roll Stabilizer," *Proceedings of the Third Ship Control Systems Symposium*, Bath, Vol. C.

[519] Lloyd, A. R. J. M., 1975, "Roll Stabilization by Rudder," *Proceedings of the Fourth Ship Control Systems Symposium*, The Hague, Vol. 2, pp. 214–241.
[520] Carley, J. B., 1975, "Feasibility Study of Steering and Stabilizing by Rudder," *Proceedings of the Fourth Ship Control Systems Symposium*, The Hague, Vol. 2, pp. 172–193.
[521] Van Amerongen, P. G. M., and Piffers, J. B. M., 1987, "Rudder Roll Stabilization—Controller Design," *Proceedings of Eighth Ship Control Systems Symposium*, The Hague, Vol. 2, pp. 120–142.
[522] Baitis, A. E., and Schmidt, L. V., 1989, "Ship Roll Stabilization in the U.S. Navy," Nav. Eng. J., **101**(3), pp. 43–53.
[523] Van Der Klugt, P. G. M., 1990, "ASSA: The RRS Autopilot for the Dutch M-Class Frigates," *Proceedings of the Ninth Ship Control Systems Symposium*, Bethesda, Vol. 2, pp. 265–275.
[524] Frahm, H., 1911, "Results of Trials of the Anti-Rolling Tanks at Sea," Trans. RINA, **53**, pp. 183–197.
[525] Den Hartog, J. P., 1985, *Mechanical Vibrations*, Dover, New York.
[526] Yang, Y., Zhou, C., and Jia, X., 2002, "Robust Adaptive Fuzzy Control and Its Application to Ship Roll Stabilization," Inf. Sci. (N.Y.), **142**, pp. 177–194.
[527] Sutton, R., Roberts, G. N., and Dearden, S. R., 1989, "Design Study of a Fuzzy Controller for Ship Roll Stabilization," Electronics and Communication Engineering Journal, **1**(4), pp. 159–166.
[528] Roberts, G. N., and Towill, D. R., 1987, "Integrated Control of Warship Maneuvering," *Proceedings of the Eighth Ship Control Symposium*, The Hague, pp. 356–368.
[529] Hill, W. A., Creelman, G., and Mischke, L., 1992, "Control Strategy for an Icebreaker Propulsion System," IEEE Trans. Ind. Appl., **28**(4), pp. 887–892.

Raouf A. Ibrahim *is a Professor of Mechanical Engineering at Wayne State University. He received his BSc and MSc in Aeronautical Engineering in 1963 and 1969, respectively, from Cairo University (Egypt). He received his Ph.D. in Mechanical Engineering from the University of Edinburgh in 1974 and continued as a postdoctoral Fellow for two years. From 1963 through 1971, he worked as a research engineer at the Aerospace Research Center of the rockets industry in Egypt. From 1976 through 1979, he was appointed as a Senior Research Specialist at Sakr Factory in Cairo and as an Adjunct Assistant Professor at Cairo University. In 1979, he moved to United States and worked at Shaker Research Corporation, in Ballston Lake, N.Y.; then, in 1980, he joined Texas Tech University as Assistant, Associate, and then full Professor. While at Texas Tech, he was a recipient of the Outstanding Professor Award in Teaching in 1982, two Halliburton Awards of Excellence in 1983 and 1986, and Texas Tech Presidential Award in Research 1987. In 1987, he joined Wayne State University and continued his research activities in nonlinear random vibration, liquid sloshing dynamics, friction-induced vibration, and flutter of aeroelastic structures. In 1994, he was named the Arthur Carr Professor of Engineering; in 1995, he was awarded the Board of Governors Outstanding Professor Award; and in 2006, he was honored with a WSU Faculty Recognition Award. He has published more than ninety papers in refereed journals and two research monographs entitled Parametric Random Vibration (Wiley, 1985) and Liquid Sloshing Dynamics: Theory and Applications (Cambridge University Press, 2005). He is a Fellow of ASME and the International Center of Vibro-Impact Systems.*

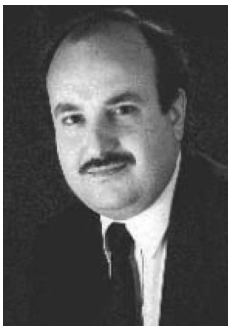

Nabil G. Chalhoub *received BS and MS degrees in mechanical engineering from Wayne State University in 1980 and 1981, respectively, and a Ph.D. degree in mechanical engineering from The University of Michigan, in 1986. Dr. Chalhoub joined the University of Nevada-Reno in 1986 as an Assistant Professor. Since 1989, he has been with the Mechanical Engineering Department at Wayne State University where he served as an Assistant Professor, Associate Professor, and currently as a Professor. His research interests include fuzzy controllers, fuzzy-sliding controllers, nonlinear robust observers, active control of flexible structures, robotics, engine friction, modeling of combustion in diesel engines, and automatic ship steering systems. He is currently an Associate Editor for the Journal of Vibration and Control.*

Dr. Jeffrey M. Falzarano *is a Fellow of ASME and the Society of Naval Architects and Marine Engineers. He graduated with a Ph.D. in Naval Architecture and Marine Engineering from the University of Michigan in 1990. He is currently a Professor of Naval Architecture and Marine Engineering at the University of New Orleans' School of Naval Architecture and Marine Engineering. He is also Associate Department Chair and Tow Tank Director. His research interests include nonlinear and stochastic ship and floating offshore platform dynamics, system identification of hydrodynamic forces, computational fluid dynamics, multibody dynamics, and analytical and experimental study of wave body interaction. He has taught and developed courses in dynamics of ships (seakeeping and maneuvering) and floating offshore structures, marine structures, hydrodynamics, offshore engineering, and probabilistic marine dynamics. He has visited and worked at a variety of universities (Vienna Technical University and Technical University of Lisbon), government research laboratories (Naval Surface Warfare Center, Carderock, and NFESC), and commercial companies (American Bureau of Shipping) during his* 25 year *career. He started his professional career working for the US Coast Guard, designing icebreakers and developing ice related technology. Since that time he worked in a wide variety of research, teaching, and consulting positions.*